Zentralanstalt für Meteorologie und Geodynamik
ZAMG
Bereich DMM - Abteilung Geophysik
Archeo Prospections®

Geophysical archaeological prospection at Tveiten (Gnr. 21 bnr. 1), Horten, Vestfold 2012

Report
September 25, 2012

Survey
Erich Nau, Roland Filzwieser, Lars Gustavsen,
Christer Tonning, Manuel Gabler, Petra Schneidhofer
Viktor Jansa

Data processing and visualization
Alois Hinterleitner, Erich Nau

Geophysical analysis
Alois Hinterleitner

Archaeological Interpretation
Erich Nau, Lars Gustavsen

Report
Erich Nau, Lars Gustavsen, Immo Trinks

Archeo Prospections®
Central Institute for Meteorology and Geodynamics
Hohe Warte 38
A-1190 Vienna
Austria

Phone: +43 1 36 0 26 2501
+43 1 36 0 26 2506
Fax: +43 1 3 68 6621
E-mail: archeoprospections@zamg.ac.at

in cooperation with
Ludwig Boltzmann Institute for Archaeological Prospection & Virtual Archaeology
Hohe Warte 38
A-1190 Vienna
Austria

Phone: +43 1 36026 3001
+43 664 60277 40304

Contents

Aims of the survey

In May 2012 geophysical archaeological prospection surveys were conducted by *Archeo Prospections*® in collaboration with NIKU and the archaeology team of Vestfold County administration in Horten municipality, Vestfold County, Norway. The surveys were initiated as part of archaeological evaluations carried out by archaeologists from Vestfold County Administration.

The aim of the survey was to investigate the areas in the vicinity of Tveiten farm using large-scale, high-resolution ground penetrating radar (GPR) and magnetic archaeological prospection. The area in question is currently undergoing redevelopment in order to extend parts of a nearby school, and the geophysical surveys were conducted in order to map and document possible prehistoric graves, traces of buildings or settlements and other man-made structures of archaeological interest prior to further planning decisions (Fig.1).

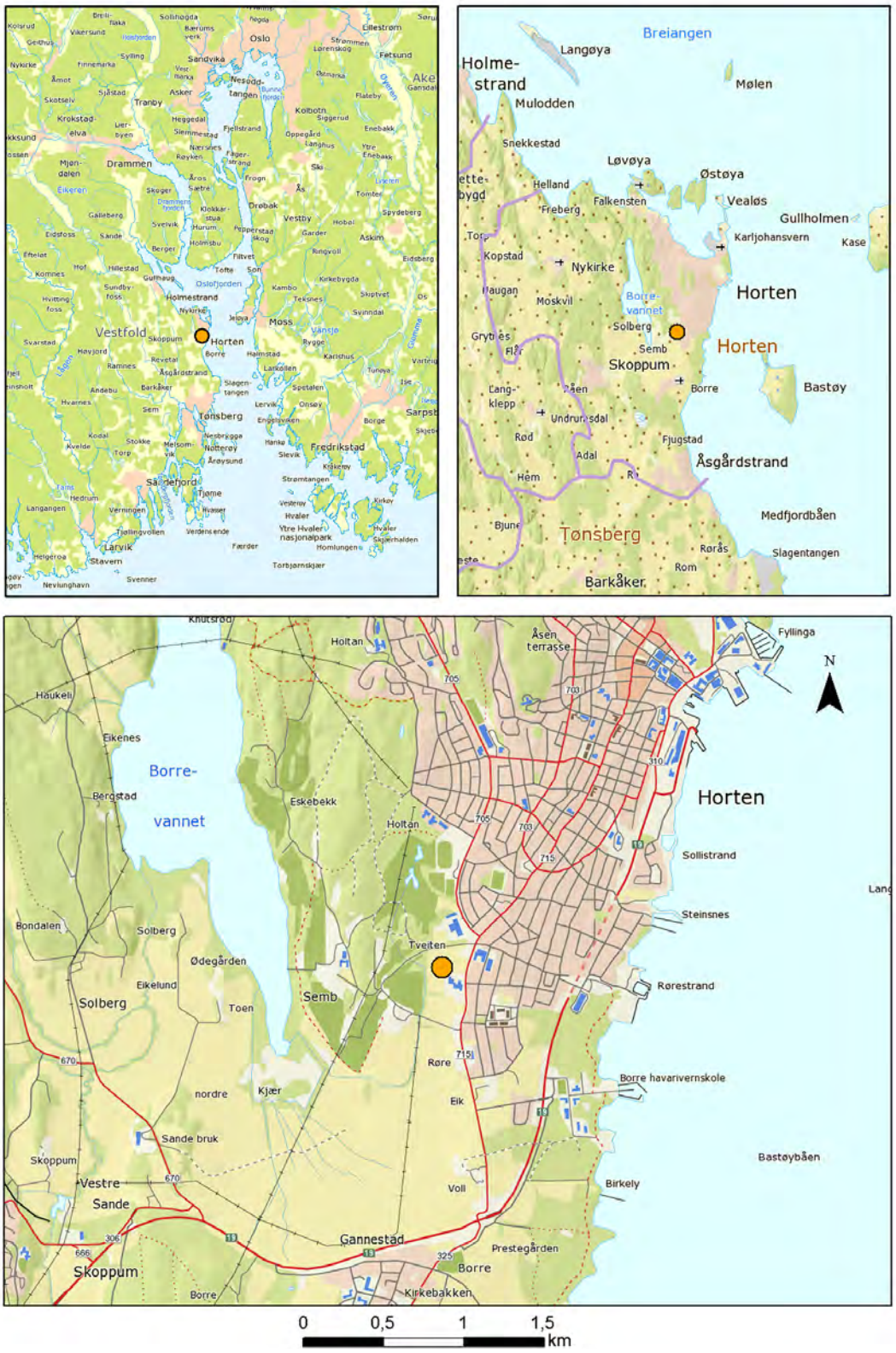

Figure 1: *Maps of Vestfold at different scales showing the location of the survey area.*

Survey site description

The survey area is situated in Horten municipality, Vestfold County and comprises a circa 4.5 ha open field belonging to the farm Tveiten (Gnr. 21 bnr. 1), located on the immediate south-western outskirts of Horten town. The site lies some 1 km to the east of lake Borrevannet and approximately 1.8 km north of Borre church. Sloping gently from east to west (circa 35 - 31 m AMSL) the site is bounded by a tarmacked road and industrial buildings to the north, a tarmacked road to the east (Fv 715, Borreveien), a fenced-off school yard, trees and hedges to the south, and a stream flanked by trees and shrubs to the west.

Geologically, the Horten area belongs to the so-called Oslo rift, a graben formed during a geologic rifting event in Permian time. The parent material of the prevalent soil consists of magmatic materials, mainly rhomb porphyry (latite) with some basalt intrusions. This material is overlain by relatively thick marine beach deposits containing silt and clay, although sandy beach deposits occur as well. A prominent feature of the Vestfold landscape is the so-called *Ra* moraine: a terminal moraine from the Younger Dryas (12,800 - 11,500 BP), which follows the coastline through the county before reaching the sea near Mølen at its southern tip. The well-drained properties of the *Ra* moraine has for millennia formed the basis for communication through the landscape and functioned as a natural border, exemplified by the alignments of farm boundaries and road networks on and around the *Ra*. Within the survey area the moraine can be observed as a slightly raised terrain formation to the east, from which the site slopes. Within the survey area the deposits consist of endogleyic arenosols characterized by sand and silty sand with a relatively high content of gravel and stones of varying sizes (10–90 cm). A large part of the marine deposits formed a ravine landscape, which has been flattened in the last decades to form a gently rolling landscape. A report from an archaeological evaluation carried out in the area in 1996 indicates that the topsoil varies in thickness between 25 and 40 cm, whilst the underlying soil horizon consists of reddish brown sand with a high stone and gravel content.

The archaeology in the immediate surroundings of the survey area is relatively poorly understood, although chance finds, rudimentary excavations and modern evaluations suggest that the potential for archaeological remains is high. Chance finds have been recovered from Tveiten farm as well as from neighbouring Røren farm to the south. These include several flint artefacts (e.g. ID 22219 and ID 61830) as well as fragments from two swords dated to the Late Iron Age (ID 23352 and ID 31122). As these finds have come to light through modern agricultural activities, however, they cannot be assigned to specific sites or features. In addition to the finds, several burial mounds are believed to have existed in the area, and traces of some can still be seen today. Within the survey area a circular burial mound (ID 42078) was excavated and completely removed sometime between 1910 and 1920. Although no finds were seemingly recovered from this mound, its approximate location is known. In the forest immediately to the west of the survey area, a circular burial mound can still be

observed. This mound, which appears to have been constructed using soil and fairly large stones measures approximately 15 m in diameters with a height of circa 1.5 m (ID 12356). It has never been investigated archaeologically, but it does appear to have been disturbed in modern times. A mound cemetery consisting of at least eight burial mounds is situated some 360 m to the west of the survey area (ID 32072), and a further mound cemetery is believed to have existed in an area to the east of the main road. The latter area was redeveloped sometime during the mid-1900s, without being investigated by archaeologists, and the size and character of the cemetery is therefore unknown. During the 1996 evaluations the local farmer informed the archaeologists that two more mounds had existed some 75–100 m to the north-west of the present school buildings. A slightly raised area could be observed at the location of one of these, but the site was never investigated by excavation. The trenches excavated in conjunction with this evaluation were concentrated to areas now forming the northwestern part of the school and school yard. Six possible postholes, thought to be part of a longhouse, were uncovered, as well as a concentration of charcoal and fire-cracked rocks, interpreted as the remnants of a cooking-pit or hearth. Again, the local farmer informed the archaeologists that concentrations of charcoal are occasionally brought to the surface in different places of the field during ploughing, especially in the area of the slight dip west of the school. The presence of cooking-pits in the area was also confirmed in 2004, in connection with evaluation excavations north of the survey area. Here, at least two cooking-pits were recorded (ID 89183), although it is not known whether these features were individual cooking-pits or formed part of a larger group. The presence of charcoal concentrations in the topsoil in and around the field may be an indication of this.

Figure 2: *High-resolution GPR prospection in Horten / Granly skole using the MALÅ Imaging Radar Array.*

Figure 3: Aerial image of the field and the limits of the actually surveyed area.

Chosen methodology

Over the past years geophysical prospection methods have developed to become an indispensable set of tools in archaeology and enjoy increasing popularity [14, 7]. From the numerous available methods, in particular magnetic prospection [9, 1], earth resistance [6] and GPR measurements[2, 8] have proven to be of particular use for archaeological applications. These methods permit the detection and mapping of buried man-made structures by measurement of the physical properties of the subsurface. In the case of archaeological prospection applications, dedicated measurement configurations are used for the spatial, gridded sampling with dense sample spacing for the investigation of several hectares of area in a short period of time. The data analysis and visualisation is conducted using specially developed processing algorithms and software [14, 9].

The potential of the methods used is primarily determined by the contrast of the physical properties of the soil in comparison to the present archaeological structures. From experience, under suitable conditions the magnetic prospection method is able to detect a diverse range of structures of archaeological interest (for example pits, postholes, trenches, hearths, furnaces, walls, track ways, palisade trenches). Arrays of optically pumped Cesium magnetometers as well as of Fluxgate type gradiometer instruments represent the most efficient, professional archaeological prospection tools today.

GPR prospection can be used to detect stratigraphic interfaces, trenches, pits and post holes, masoned architecture and stone structures (e.g. walls, hearths, stone lining in post holes) as well as modern utilities in three dimensions, down to depths of 2 m in many types of soil. The GPR method can be adversely affected by high soil humidity and soils rich in clay, or in dry climates where the topsoil can be rich in minerals due to evaporation. While traditional GPR measurements are conducted using single antenna systems, with coverage rates of some 2,500 square metres per day at 25 cm crossline spacing, modern motorized surveying systems permit a considerably increased spacial coverage at very dense profile spacing. For example, the novel MALÅ Imaging Radar Array - MIRA - offers daily coverage rates of 20,000 square metres with 8 cm sample spacing in both inline and crossline directions.

Both in the case of magnetic and GPR measurements, a preliminary data analysis is possible on site for quality control and further planning of the survey. For detailed data analysis, powerful computer and special processing software are used. The visualised data of the individual measurements are combined in the form of georeferenced images that are interpreted archaeologically including all available information in the framework of a Geographical Information System (GIS) by experienced experts.

Figure 4: *Archaeological prospection measurements in Horten / Granly skole with the motorized magnetometer system.*

Figure 5: *The 16 channel 400 MHz MALÅ Imaging Radar Array (MIRA).*

Basic principles of magnetometer prospection measurements

Data acquisition

Magnetic prospection is based on the highly sensitive measurement of the total intensity of the earth's magnetic field [9, 1]. The measurement unit used is nanotesla (nT). Individual measurement values are recorded in a regular grid with 50 cm cross-line and 12.5 cm in-line spacing using a magnetometer system. While in the past commonly manually operated magnetometer systems have been used, recently introduced motorized magnetometer systems permit much increased coverage rates at the same, or even denser spatial sampling (25 cm × 12.5 cm).

The use of sensor arrays consisting of up to 10 Förster Fluxgate type gradiometer probes, or up to 12 Cesium sensors, using automatic data positioning and navigation based on Realtime-Kinematic Global Positioning Systems (RTK-GPS) and software based data logging on ruggedized field computers permits the coverage of considerable areas (10–20 hectares) per day. While Cesium sensors offer a measurement resolution of as little as 0.005 nT, Fluxgate sensors provide data with 0.1 nT resolution. In addition to the sensitivity of the professional geophysical instrumentation used, the spatial sampling density is of great importance for the detection of small or weakly expressed archaeological structures (e.g. postholes).

The successful discovery and investigation of archaeological structures using magnetic prospection is based on the exactly positioned high-resolution measurement of minute magnetic anomalies in the much larger local earth's magnetic field. The small deviations in this field, of normally between 0.1 nT and 100 nT amplitude, are caused by different magnetisations of the subsurface and its contained structures. The soil's magnetisability (magnetic susceptibility) depends mainly on the contained iron oxides (in particular magnetite, maghemite and haematite), all of which are ferro-magnetic, with haematite being weakly magnetic compared to the two others.

The uppermost soil layers possess in general an increased magnetic susceptibility relative to deeper soil layers. This fact is known as the so called Le Borgne effect. Two mechanisms can be drawn on in order to explain this effect. Both comprise the conversion of the weakly magnetic haematite to magnetically stronger maghemite through reduction to magnetite and subsequent oxidation. Firstly, this process can occur through fermentation processes during the decomposition of organic matter. Secondly, this process can occur through heating by fire, in any form of burning. Fires additionally increase the magnetic susceptibility since material rich in clay, when heated above the so called Curie temperature, after undisturbed cooling in the earth's magnetic field retains a thermoremanent magnetisation.

Ferri-magentic iron composites, above all magnetite with very small grain sizes, have been observed in relation to archaeological structures [3]. These iron composites possess exceptionally high magnetic susceptibilities. It is assumed that they are remains of magnetotactic bacteriae, which make use of the orientation of the earth's magnetic field through magnetic crystals (magnetosomes) built into their cell for orientation purposes, and which take part in organic transformation processes [5, 4]. These very small but highly magnetic particles can be of importance for the prospection of wooden remains in case of palisades or individual posts.

A phenomenon, which is of significance for the magnetic detection of trenches and pits, is the viscose remanent magnetisation. It relies on the ability of small grains containing a singular magnetic domain, to spontaneously reorient themselves in the direction of the earth's magnetic field under absorption of thermal energy.

Magnetically prospectable structures comprise all kinds of pits with more or less organic filling, trenches filled with surface material, fire places, hearths and furnaces, which appear as anomalies with increased (i.e. positive) magnetization. Negative anomalies can be caused for example by roads, walls and basements. The strength of an anomaly is not only dependent on the magnetisation of a structure, but as well on the contrast in magnetisation between the structure and the surrounding soil.

Data processing and analysis

The magnetic prospection data measured with the motorized Förster gradiometer system is stored in form of XML, human readable data files containing GPS position information, magnetic and time stamp data as well as information on the survey, the instrumentation and settings used. The data format and data logging software was developed by the LBI ArchPro. For processing and visualization the data is loaded by the special software APMAG, which was developed over the past 17 years by Archeo Prospections®.

The measured magnetic data collected along approximately regularly spaced tracks is subsequently automatically gridded and interpolated into 12.5 cm bins using the GPS position information and line-shift correction filters. Advanced, specially developed data processing algorithms for data correction (line-shift and sub-grid balancing; displacement corrections; spike removal; noise reduction; data interpolation; bandpass filter; removal of the disturbing effect of the motorized survey vehicle) are applied and sets of optimized, georeferenced greyscale data images are generated [11]. The data can be exported for use in other commercial software packages.

The resulting data images are analysed and archaeologically interpreted [10] together with all available additional geospatial data and information within the framework of a Geographical Information System (ArcGIS 10). The final products are interpretation maps depicting structures of archaeological interest as well as other relevant features. These interpretation images and maps should be seen as guides how to read the data. In general the data contains a considerably larger amount of information than it is possible to represent in an interpretation map. Therefore the original data images should always be consulted together with the interpretation maps.

Basic principles of ground penetrating radar measurements

Ground penetrating radar (GPR) is currently the most modern, and potentially the most efficient geophysical archaeological prospection method. The GPR method is based on the reflection of electromagnetic waves in the subsurface. An electromagnetic pulse with maximum amplitude of a certain frequency (in general between 100 MHz and 1000 MHz) is emitted into the subsurface using a transmitter antenna. This pulse is travelling through the ground with a velocity dependent on the traversed material, and it is reflected from individual objects or interfaces with differing physical properties (i.e. dielectric permittivity, electric conductivity).

The part of the emitted signal that is returning to the surface is recorded with a receiver antenna and digitized. Changes in signal amplitude and frequency carry information about the composition of the subsurface (soil humidity, porosity, clay content) and contained structures. The travel-time of the signal is proportional to the distance of reflecting objects or interfaces.

It is mainly the dielectric permittivity of the medium, its electric conductivity, the radiation characteristics of the antennae used, and the frequency content of the emitted GPR pulse that govern its propagation in the subsurface (maximum signal penetration depth, vertical and horizontal resolution).

The contrast of the dielectric permittivity of two media determines the amount of energy reflected from objects or at layer interfaces. In the upper soil layers strong reflection coefficients are caused by changes in the substrate, by strong inhomogeneities due to varying soils humidity, and by contained anthropogenic objects or structures (e.g. utilities, foundation walls). Table 1 lists approximate values of the relative dielectric permittivity ϵ_r, the electric conductivity σ and the GPR signal velocity v for several common materials.

The absorption of the electromagnetic energy transmitted into the ground depends on the transversed medium (material dependent absorbtion loss). The reduction in signal amplitude of the transmitted energy pulse depends mainly on the electrical conductivity of the medium and the travelled distance, with the conductivity being the determining factor for the actual penetration depth of the electromagnetic pulse. By comparing amplitudes it is possible to differentiate areas according to their absorption properties.

GPR antennae emitting a low frequency signal (e.g. 100–200 MHz) permit a greater depth of investigation at reduced resolution, due to the longer wavelength of the signal. High-frequency signals (e.g. 800–1000 MHz) offer greatest resolution, but only limited signal penetration (< 1 m). GPR antennae commonly used for archaeological prospection operate with signals centred around 400 or 500 MHz, offering investigation depths of 1.5 – 3 m and sufficient resolution.

Material	ϵ_r	σ **[mS/m]**	v **[m/ns]**
Air	1	0	0.30
Sweet water	81	1 – 300	0.03
Salt water	81	4000	0.03
Dry sand	3 – 5	0.5 – 1.5	0.13 – 0.17
Wet sand	20 – 30	5 – 20	0.05 – 0.17
Dry clay	10 – 50	20 – 200	0.08 – 0.17
Wet clay	2 – 30	10 – 100	0.05 – 0.07
Peat	20 – 40	100 – 300	0.04 – 0.06
Granite	4 – 6	0.3 – 2	0.11 – 0.16
Limestone	4 – 8	0.1 – 2	0.1 – 0.14
Sandstone	4 – 12	1 – 10	0.08 – 0.13

Table 1: *Approximate values of the relative dielectric permittivity ϵ_r, the electric conductivity σ and the GPR signal velocity v for several common materials.*

Data acquisition

Individual GPR sections are recorded by moving a set of transmitter and receiver antennae along straight lines, called GPR profiles. GPR measurements are conducted with a dense in-line sampling of typically 2 – 5 cm along the profiles. Traditional manual GPR surveys using a single or up to three antennae mounted in a cart that is pushed by the operator, or towed in a sledge behind the surveyor, utilize a distance wheel, a.k.a. odometer, emitting trigger pulses, for exact in-line data positioning. For crossline positioning marker lines of 30–50 m length are placed between fibre glass tape measures on the ground. By measuring a large number of densely spaced GPR profiles (e.g. crossline profile spacing of 25 cm) it is possible to generate a virtual three-dimensional GPR data volume. In general the GPR system is moved in zig-zag mode along parallel lines over an rectangular survey area. The corner points of the survey area, which provide a local coordinate system, are georeferenced using a totalstation and fix-points with known global coordinates in the vicinity of the survey area, or a RTK-GPS.

Modern multichannel GPR systems, such as the 16-channel 400 MHz MALÅ Imaging Radar Array (MIRA), or the Sensors & Software SPIDAR system, permit efficient use of multiple, closely spaced GPR antennae, multiplying the efficiency of the fieldwork and permitting measurements with much increased spatial sampling density. By operating these systems with motorized survey vehicles it is possible to cover in case of the MIRA system (Fig. 2, 5) over two hectares per day with eight centimetre both in-line as well as cross-line measurement spacing. Power supply, data logging and navigation systems are installed on the survey vehicles, e.g. small tractors or quad bikes. In case of motorized GPR surveys positioning is generally conducted using exact RTK-GPS or robotic total stations.

GPR surveys require smooth surfaces free of obstacles (rocks, trees, high vegetation). Grass covered areas should be mowed prior to a survey. It is in general not meaningful to conduct GPR surveys in forested areas, on ploughed fields, on wet soils or in areas with strongly varying topography.

Data processing and analysis

In general, GPR data are substantial and contain a large amount of information. The visualisation of GPR data is commonly realized in form of greyscale images showing the amplitudes of the recorded signals as a function of space and time.

Within the individual GPR sections, representing vertical cuts through the subsurface, typical reflection and diffraction patterns of the signals can be observed that are generally very difficult to interpret. Laymen and archaeologists without special training will be unable to derive an archaeological interpretation from vertical GPR sections. Often comments and explanatory line drawings are inserted into such GPR section presentations. However, the use and visualisation in form of vertical GPR sections is today rather uncommon in geophysical archaeological prospection and outdated, with exception of special applications.

The individual GPR sections collected manually or with motorized survey systems are merged after the fieldwork in the computer using specially developed software solutions. Through interpolation a virtual three-dimensional data volume is generated. If the velocity of the GPR signal in the subsurface is known or estimated (a value commonly used is a constant velocity for the entire subsurface of 10 cm/ns; however, variations between 5 and 15 cm/ns can be encountered), it is possible to convert the vertical axis of the data volume from time to depth.

This digital block of data can be cut into horizontal slices, so called GPR time-slices or GPR depth-slices. Slices of different thickness can be computed, e.g. 5 cm, 10 cm, 20 cm, 30 cm, 40 cm and 50 cm thick slices, averaging variable amounts of information contained in the data volume.

Using these slices it is possible to map and image archaeological structures that occur at approximately the same depth, considerably facilitating their archaeological interpretation since the spatial context becomes clear to the observer. By scrolling through a stack of thin GPR depth- or time-slices in form of a quick succession of images or an animation, it becomes possible to understand the spatial extent of structures contained in the data. While the relative depth of structures using the GPR method is correctly imaged, it should be kept in mind that the absolute depth of the structures can vary due to the lack of knowledge of the exact GPR signal velocity distribution in the imaged volume. Selective velocity analyses can be conducted when reflection hyperbolae are observed in the GPR profile data, or when a dedicated common-mid-point survey and moveout analysis is performed.

Common data processing steps applied to the data prior to 3D volume generation include trace interpolation, band-pass frequency filtering, spike removal, dewow filter, average-trace-removal, amplitude gain correction, amplitude balancing and Hilbert transformation. In special cases it can be useful to utilize volume rendering in order to visualise certain anomalies or structures contained in the data. All generated data images are georeferenced for use and subsequent archaeological interpretation in GIS.

Fieldwork and data analysis

Magnetic survey

Description of magnetic prospection fieldwork

The magnetic survey was carried out on the 4th of May 2012 using a motorized magnetometer array pulled by a Yamaha ATV. A 10 channel EasternAtlas® digitizer and 8 Fluxgate sensors (Förster Ferex CON650) with 25 cm cross-line spacing were mounted on a non-magnetic trailer (Fig.4). A constant measuring frequency of 50 Hz was used leading to an in-line sample spacing of 10 - 13 cm depending on the actual driving speed. An Altus RTK GPS with CPOS subscription and 5 Hz update rate was used for positioning. Data were recorded on a rugged field computer (Panasonic CF19) using the acquisition software LoggerVIS, which also provides a navigation solution and thus allows for full coverage across the survey area. A total of 39.500 m^2 were surveyed within 4 hours resulting in 2.4 million single magnetic measurements and about 250.000 position values recorded in XML format and used for further processing.

Description of magnetic data processing

A first processing of the magnetic data was carried out immediately after the survey in order to control for accuracy and sufficient coverage. Further processing steps and visualization of the dataset were conducted using APMAG - a software especially developed for archaeological purposes by ArchaeoProspections®. The irregular grid of actually measured lines was re-sampled to a regular grid of 10 cm. Various automatic and semi-automatic processing algorithms were applied (line-shift and sub-grid balancing; displacement corrections; spike removal; noise reduction; data interpolation; bandpass filter; removal of the disturbing effect of the motorized survey vehicle) and optimized greyscale images with different magnetic value ranges were produced (Fig. 16). A wallis filter was applied to depress geological influence and enhance image contrast (Fig. 17). By using the GPS position information all images were automatically georeferenced in the coordinate system UTM 32N.

The resulting images were embedded in a Geographical Information System (ArcGIS 10) together with all other available georeferenced data (GPR images, aerial photographs, maps). Analysis, archaeological interpretation and map preparation was conducted within the framework of ArcGIS.

Ground penetrating radar survey

Description of GPR fieldwork

The GPR survey was carried out on the 13th of May. As the surface had finally dried up after a longer period of rain survey conditions were sufficiently good. A 16 channel MALÅ Imaging Radar Array (MIRA) mounted on the front hydraulics of a Kubota minitractor was used for the GPR survey (Fig.2, 5). 8 cm cross-line spacing between the channels created a 132 cm wide swath of 16 single GPR sections for each driven line. Each channel was recording 50 single measurements per second leading to an in-line trace spacing of 3-4 cm depending on the actual driving speed. The resulting minimum spatial resolution for this survey amounts to $8x4$ cm. A rugged field computer (Panasonic CF19) equipped with the software products MIRAsoft and LoggerVIS was used for data acquisition, measurement control and navigation. The centimetre accuracy for positioning was provided by a Leica RTK GPS system using a base and rover configuration. A total area of 40.200 m^2 was surveyed within 6.5 hours resulting in 3.800 GPR sections composed of 9.9 million recorded single GPR traces. Each of these traces is averaged out of 4 actually measured traces (4 stacks).

Description of GPR data processing

As the velocity of the GPR signal is dependent on the material and the moisture of the soil (Table 1) the actual velocity needs to be analysed and considered during the further processing to ensure a correct conversion from GPR travel times to depth. The analysis of reflection hyperbolas [2] was carried out on the Tveiten / Horten dataset. This method allows the quick analysis of several reflection hyperbolas in single GPR sections spread all over the survey area and determines the variety of GPR velocities in different depth and different regions of the survey area. The GPR velocity in Tveiten / Horten spreads from $0.07m/ns$ to $0.09m/ns$ For the further processing of the dataset an average velocity of $0.08m/ns$ was used for the time to depth conversion. Therefore it has to be considered that the absolute depth of the structures displayed in the result images is not absolutely exact. Variations in absolute depth of +/- 20% are possible in the whole dataset. The further processing and visualization steps were carried out using the software APRADAR, developed by ArchaeoProspections®. A 3D data block was created using the individual GPR sections, this data block was cut into horizontal slices (GPR depth-slices). Slices of different thickness (5 cm, 10 cm , 20 cm, 30 cm, 40 cm and 50 cm) were computed, theses slices are displayed as greyscale images. Various common GPR processing steps (trace interpolation; band-pass frequency filtering; spike removal; dewow filter; average-trace-removal; amplitude gain correction; amplitude balancing and Hilbert transformation) have been applied with different settings before the 3D data block was generated, leading to different result images (see attached DVD). Archaeological structures might be clearly visible in one of the datasets whereas they could be almost invisible on another one, therefore all resulting images need to be analysed and used for the interpretation. Various animated sequences (see attached DVD) of depth-slices either of the whole dataset or a selected depthrange were created and used to understand and interpret the data.

The resulting images were embedded into a ArcGIS project, the data analysis, archaeological interpretation and map creation was carried out in the framework of the GIS.

Archaeological interpretation and results

Magnetic data interpretation (Fig. 6, 7)

The magnetic images are mainly characterized by large areas with strong magnetic anomalies and a rather calm background which shows only limited magnetic variation (Fig.16). These magnetic anomalies consist of strong dipole anomalies in a chaotic pattern with positive magnetic anomalies along their sides. One of these areas in the northern part shows a distinct orientation from North-West to South-East whereas the orientation of the southern areas is not as pronounced. Magnetic data processed using a Wallis filter show these structures even better, as this specific filter levels larger anomalies in the background with anomalies remaining visible only if smaller than the filtering-window of 10 m (Fig. 17). Due to their large size and their chaotic pattern these magnetic anomalies are most likely of geological origin.

Alongside the western limits of the survey area a strong magnetic anomaly stretching in North-South direction is visible over a length of 260 m. Its straight direction and strong magnetic values are most likely caused by a modern iron pipe. Another strong anomaly caused by an iron pipe is stretching from the North-Eastern corner of the field towards its center, visible over a length of about 40 m.

Several other linear structures appear across the entire survey area as thin positive magnetic anomalies. Linear structures like these usually represent subsurface pipes or lines. The use of drainage pipes is very common in the Vestfold area. These pipes are either made from clay tiles or corrugated plastic tubes. The thermoremanent magnetisation of burnt clay is likely to be causing the linear structures visible in the magnetic data at Horten.

Single dipole anomalies are visible all across the prospected area. Such anomalies are often caused by modern iron objects buried in the topsoil, although some might be of archaeological interest. Due to the geological background in the Horten area, however, single boulders of igneous rock or granite might represent another explanation for these strong dipole anomalies. As there is no distinct pattern visible, a more detailed interpretation is not possible yet.

The remaining background displays as homogeneous, but flittering texture (Fig. 6). Only in the north-eastern corner, a weak stripy pattern indicates a former field system or ploughmarks. Single positive anomalies all across the survey area might be interpreted as both archaeological or geological features.

The integrated archaeological interpretation of GPR and magnetic data allows a better understanding and explanation of the observed magnetic anomalies (see p.33).

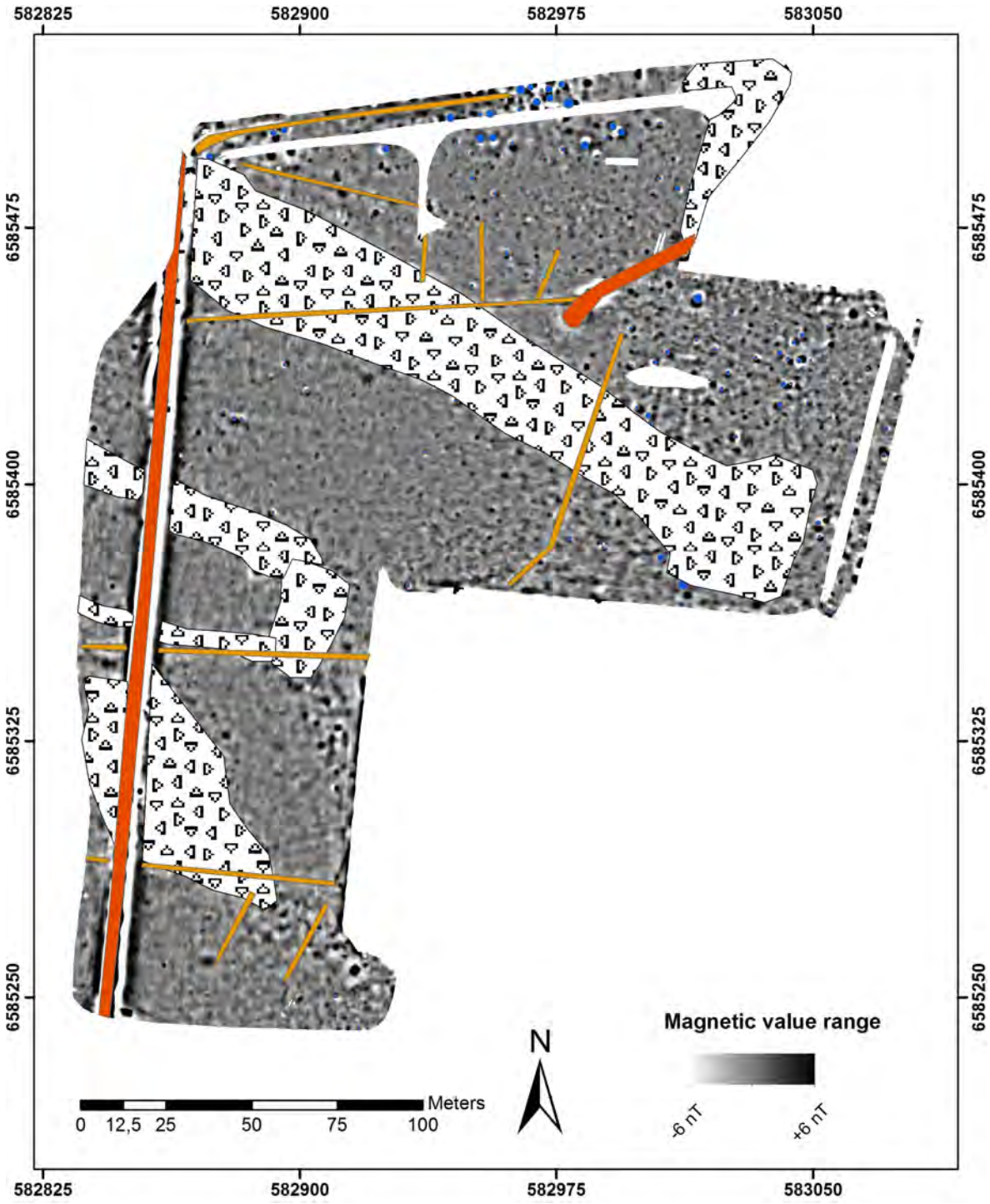

Figure 6: Greyscale image of the magnetic prospection data overlayed by the archaeological interpretation.

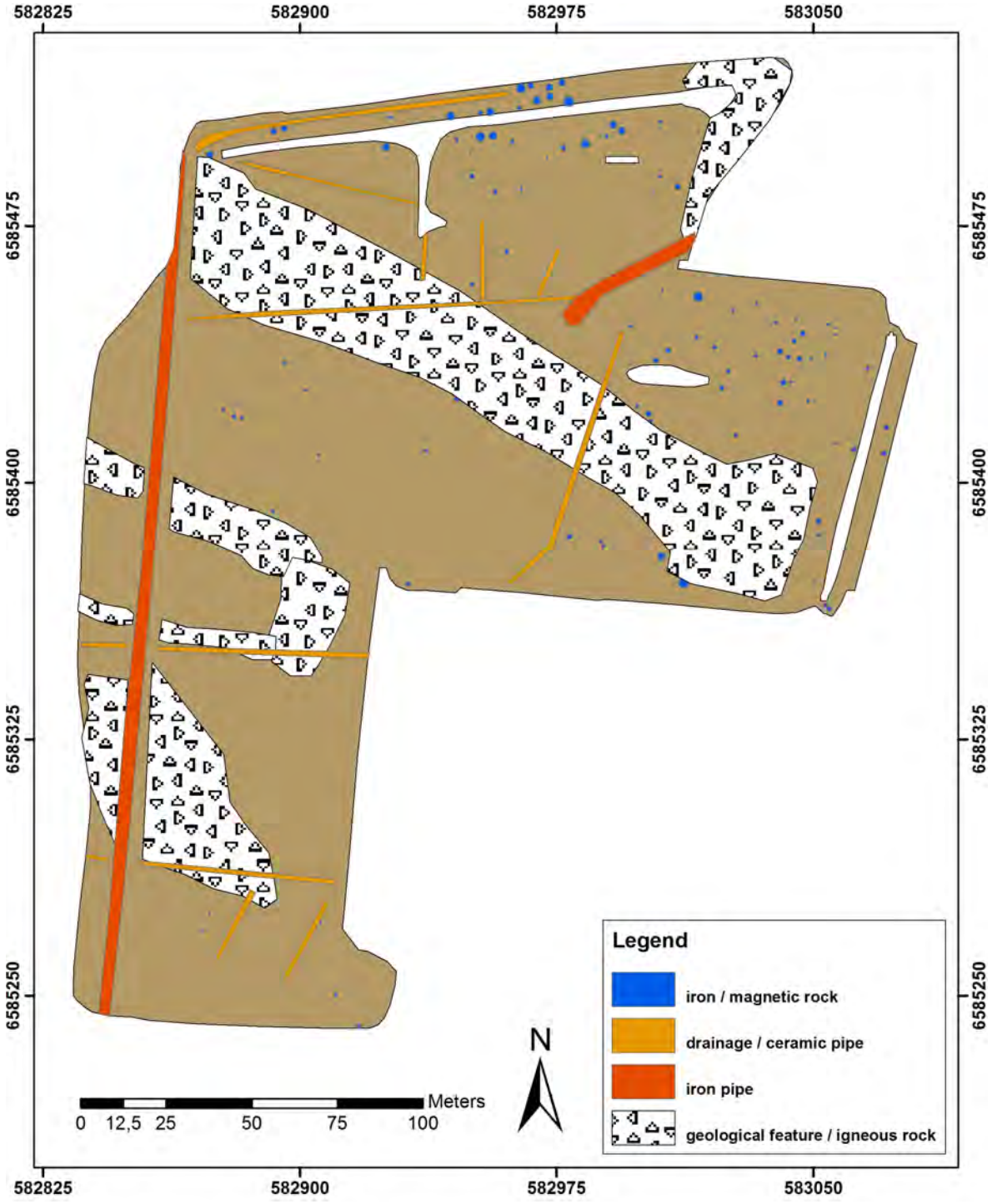

Figure 7: Archaeological interpretation of the magnetic prospection data.

GPR data interpretation

Depthrange 0 - 30 cm

The surveyed field was flattened by the farmer just a few days before the conduction of the GPR survey. The tractor wheels compressed the surface of the field. These tracks are also visible in the top most (0 - 15 cm) GPR depth-slices (Fig. 18 - 20). Beside the tractor tracks, the topmost 30 cm appear to be very homogeneous. This can easily be explained by the agricultural usage of the field. First heterogeneities can be observed at a depth of 25 - 30 cm (Fig. 23), which fits well with the typical depth of the ploughing layer.

Modern features - Drainage pipes (Fig. 8, 9)

A large number of straight linear features can be observed all across the prospected area with a cluster towards the western limits of the field (Fig. 8). The linear structures appear already at a depth of 40 - 150 cm, but the major proportion occurs within a depth range from 80 - 120 cm (Fig. 9). Most of these features have a two-way appearance. When first visible in the upper depth-slices, they are absorbing the GPR signal and are displayed white or light grey in the greyscale images. In the lower slices, they switch to reflective properties. These structures can be interpreted as being caused by pipes or lines. The pipe itself is causing a reflection of the GPR signal, the backfill of the assembly-ditch or a protective lining in the ditch is absorbing the signal in the upper zones. Only a smaller number of the linear structures, mainly very thin ones, are visible as only reflective. This interpretation is further supported by of their dimensions and spatial patterning. Within this feature type, larger, isolated and smaller, but obviously organized features can be distinguished.
Alongside the western limits of the area, two rather wide (1 - 1.4 m, parallel ditches are visible running in north-south direction. Other similar-dimensioned structures appear at the eastern edge parallel to the road and at the southern edge running in east-west direction. There seems to be no link with the majority of the linear features. Another, up to 5 m wide ditch can be observed in the north-eastern corner of the survey area. These larger, isolated features are most likely modern water-pipes. Some of these pipes could be detected by magnetometry displaying(Fig. 16, 7) strong dipole anomalies and most likely are made of iron, the others consist of a non-magnetic material like plastic. A circular structure, with a diameter of about 2.5 m, in the central area is connected to several of these pipes. It could be produced by an upright standing concrete tube and be used as some kind of a well.
The majority of linear structures shows much smaller dimensions between 20 cm and 70 cm width. Most of these run in an approximate east-west direction towards the adjacent creek. In-between these parallel features, a number of shorter structures run from north-east to south-west or south-east to north-west. Overall, they form a herringbone-pattern in some zones of the field - the typical appearance of an agricultural drainage system.

Depthrange 30 - 60 cm (Fig. 11)

Within this depth range, the first features of archaeological interest appear. In the north-eastern corner of the prospected area, a strongly reflective, rectangular structure oriented in north-south direction can be observed. With total dimensions of 30 m x 9 m, the reflective structure itself is thereby up to 2 m wide. Its northern extent remains unknown due to the limits of the survey area. In the south-eastern and south-western corner of the structure it

shows about 1 m wide extensions over a length of about 5 m. In the inner areas less reflective structures can be observed. The most likely interpretation of this feature would be a wall, respectively the foundations of a wall. The reduced reflection inside a possible foundation might indicate debris deposits. This is further supported by aerial photography taken in 1972 showing a greenhouse at the same spot.

Towards the northern limits of the survey area, several absorbing structures have been recorded. Structures as these are usually caused by processes involving the removal of earth material followed by its replacement with different type of sediments. Most of the observed features are circular with a diameter between 0.6 m and 4 m and seem to appear within a depth range between 0.3 and 0.5 m. Two types can be differentiated. Small features (up to a diameter of 1 m) are interpreted as postholes; Features with diameters from 1 m are understood as pits. The excavation of several cooking-pits just north of the survey area might justify a similar interpretation for the newly recorded pits. In contrast to the circular structures mentioned above, four structures display a rectangular shape of up to 7.5 m in length and 4 m in width together with an orientation from North-west to South-east. Their observation within a depth range between 0.35 m and 0.6 m indicates a preserved depth of 0.2 m to 0.35 m. The shape and depth strongly points towards the remains of pithouses. Inside these pithouses, several smaller, either reflective or absorbing features can be observed and are interpreted as stones, postholes and debris deposit inside the houses.

Another cluster of altogether seven as pits interpreted circular structures are located in the center of the survey area between two ridges of bedrock. (Fig. 14). Diameters move around 1 and 2 m, the preserved depth ranges between 0.2 m and 0.3 m. Adjacent to these pits, a couple of smaller features with a diameter of up to 1 m can be observed, which are interpreted as the remains of postholes.

Between the center of the survey area and a larger cluster of features in the northern part, a small number of features can be observed, which also can be interpreted as pits.

Depthrange 60 - 100 cm (Fig. 12)

The distribution of archaeological features within this depth range is similar to that in upper depth ranges. In the north-eastern corner of the survey area, the possible remains of a greenhouse are still visible, but now show a strict rectangular shape without the extensions observed in upper depth ranges. This depth range possibly displays the original shape of the greenhouse, whereas the extensions might be remains of walls added at a later time. The greenhouse remains visible to a depth of 0.95 m.

Just a few meters west of the greenhouse, a small group of pits and postholes can be located. Due to fewer contrast, these structures display a much weaker appearance than the pits in the northern area. Any interpretation therefore must be considered with care.

The large group of pits in the northern area can still be observed in this depthrange. Some of the pits have already been visible in the upper depthrange, but these appear now with a much smaller diameter displaying a conical shape of the pits. Especially towards the eastern limits of the group several new pits become visible. These new pits usually show a smaller diameter, up to 2.5, than the pits in the upper layers. At least 15 smaller features, interpreted as remains postholes, are visible in the area around the pits, but the clear shape of building structures can not be observed, even when the postholes observed in different depthranges are combined (Fig. 14).

A large circular structure, with a diameter of almost 7 m is located towards the south-

eastern corner of the survey area, appearing at a depth of 0.9 m and continuing to deeper zones. Due to its circular shape and absorbing properties, the interpretation as pit is possible. Its large diameter, however, makes this interpretation questionable.

Depthrange 100 - 150 cm (Fig. 13)

Only few archaeologically relevant features can be observed within this depth range. The northern part of the survey area even appears to be almost empty of archaeological features.

The large cluster of pits and postholes in the northern area disappears almost entirely. Only one of the pits remains visible down to a depth of 1.2 m.

The large circular structure located towards the south-eastern corner - visible first at 0.9 m - can be observed further down to a depth of 1.45 m. Its diameter shrinks from almost 7 m at 0.9 m to 3 m at 1.45 m depth. The properties thereby change from absorbing in the upper zones to highly reflective in the lower zones. Based on these observations, the structure can be interpreted as shallow pit with a layer of stones at the bottom and finer material - possibly clay - at its top. Do to its location along the flanks of a bedrock-ridge (Fig. 14), a geological explanation for this feature cannot be entirely excluded.

In the south-western corner of the survey area, a large circular band (around 20 m in diameter) with a width of 0.5 to 1 m shows absorbing properties. The structure is poorly visible within the depth ranges of 1.2 m to 1.4 m and seems to be partly destroyed by modern pipes. Inside the structure, different zones of varying electric properties - either absorbing or reflective - can be observed.

Based on its shape, this feature is interpreted as a extensively destroyed grave-mound surrounded by the remains of a ditch. The heterogeneity observable within the mound could be indicate the existence of a burial chamber. This is, however, not clearly visible in the data and any interpretation therefore must be taken with care. Some meters to the East of the grave-mound, several almost rectangular structures can be observed. Due to their properties displayed in the GPR data, they are interpreted as objects cut into the subsurface and therefore interpreted as pits. The small distance to the grave-mound might also indicate the remains of further burials. Compared to the larger cluster of pits in the northern area, these pits appear much weaker in the GPR data set leading to a limited interpretation.

About 75 m north of the grave-mound, a semi-circular structure with a reconstructed diameter of 12 m and two smaller circular structures approximately 1.5 m in diameter could be detected. These structures could favour an interpretation as a second grave-mound displaying the remains of a ditch and burial chamber.

Depthrange 150 - 200 cm

The conducted GPR survey achieved a depth penetration of about 2 m. The depth slices, however, showed no archaeologically relevant features below 1.5 m.

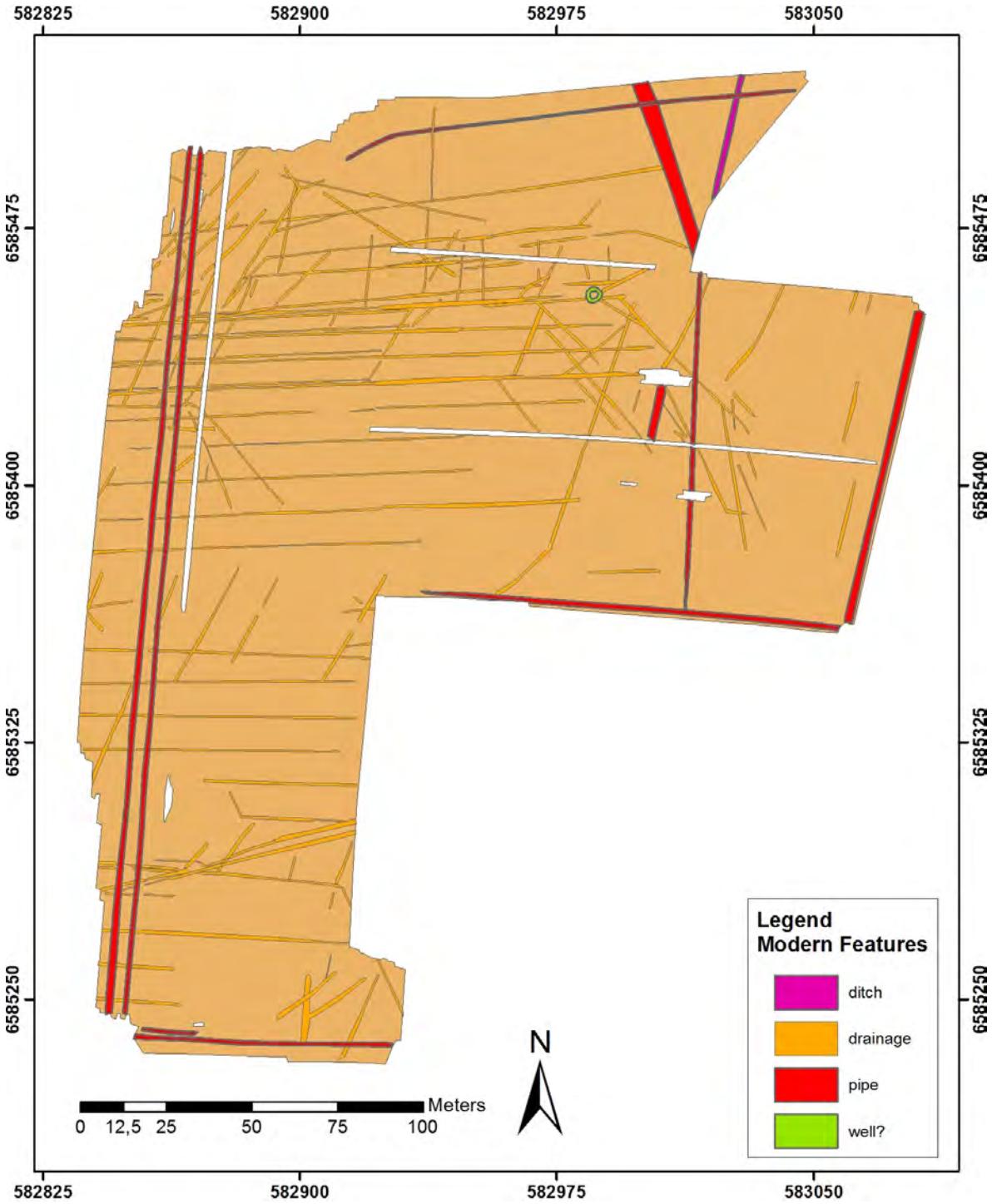

Figure 8: Interpretation of GPR data: Modern features.

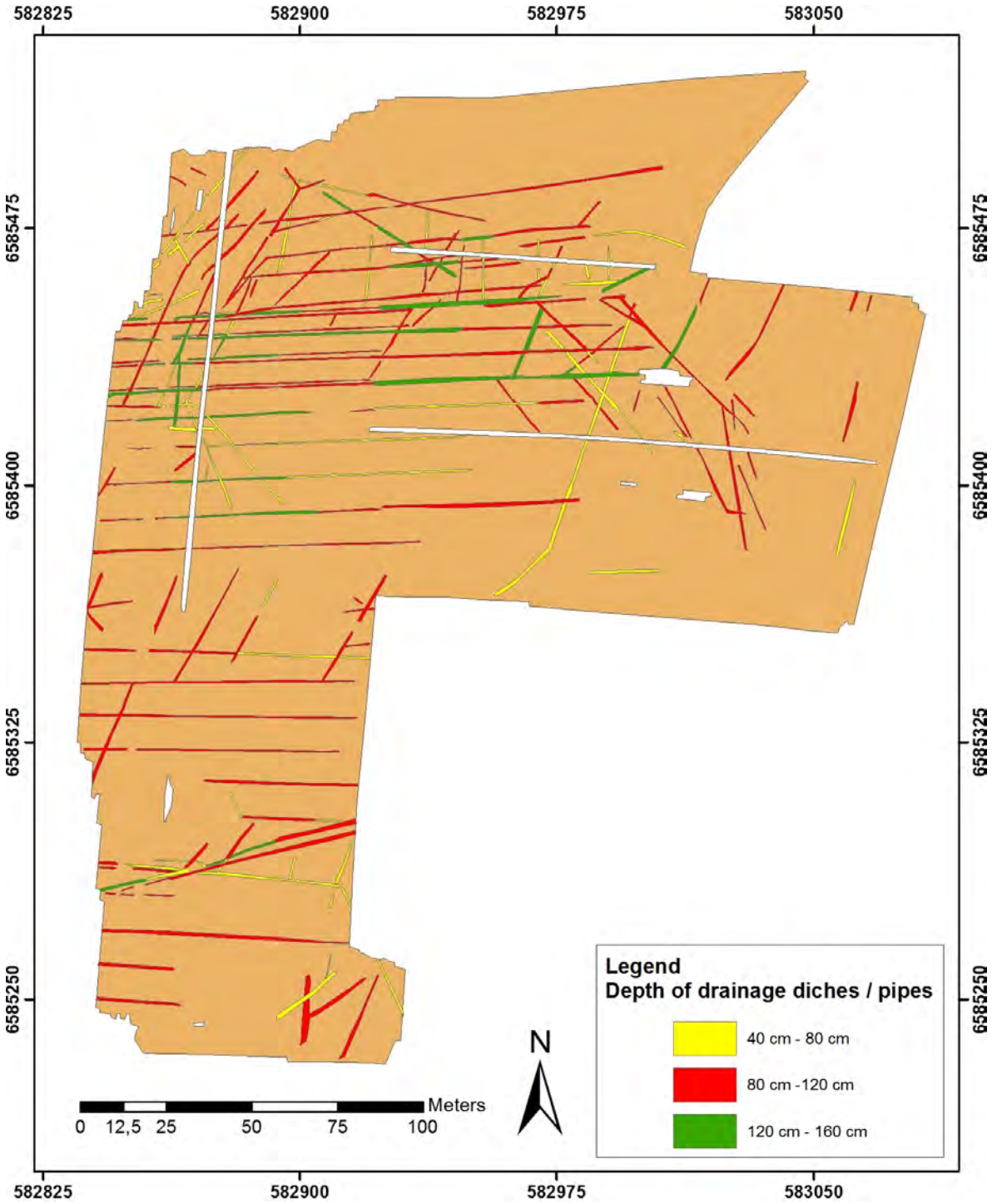

Figure 9: Interpretation of GPR data: Drainage ditches and pipes at different depths.

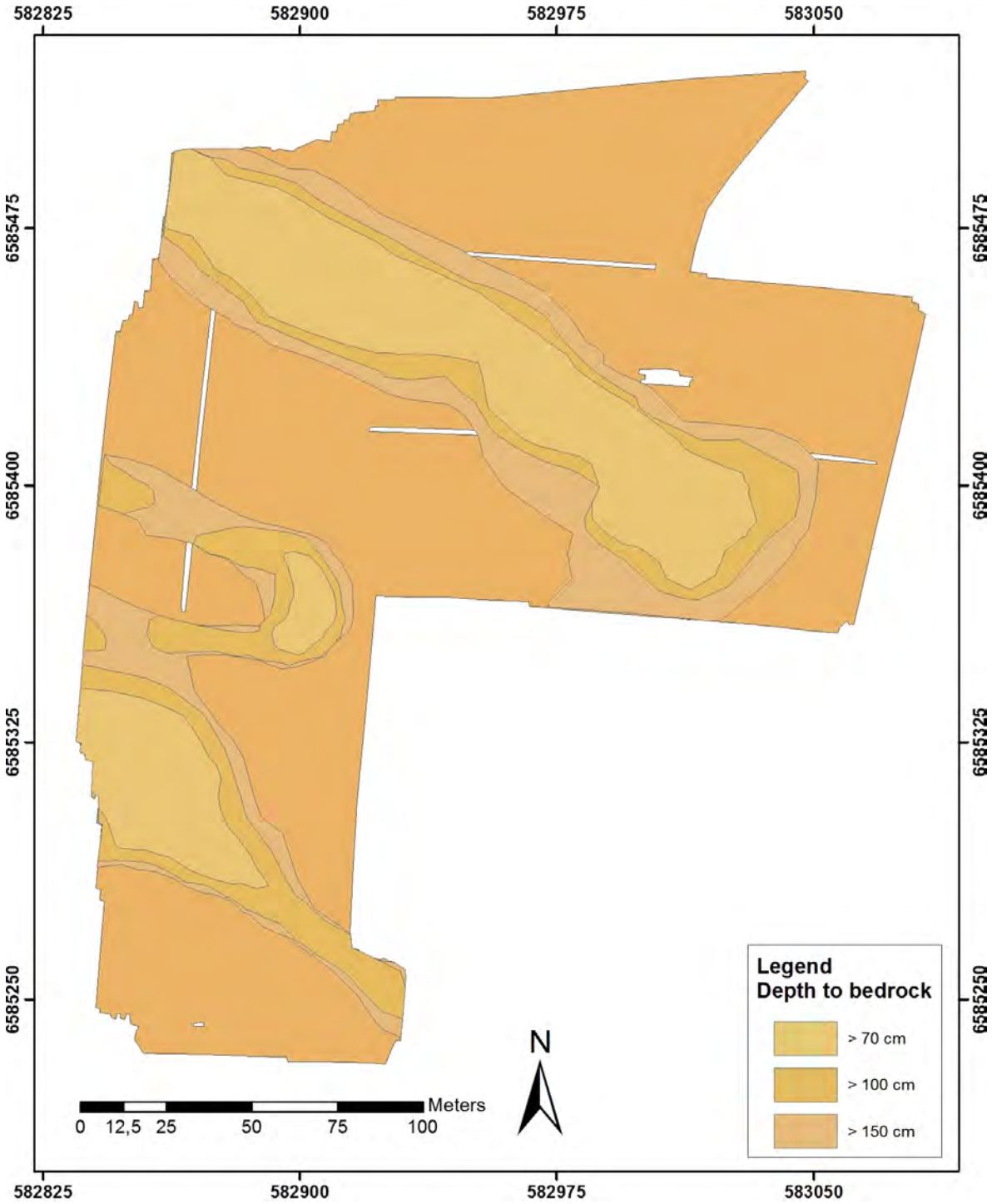

Figure 10: Interpretation of GPR data: Depth to bedrock.

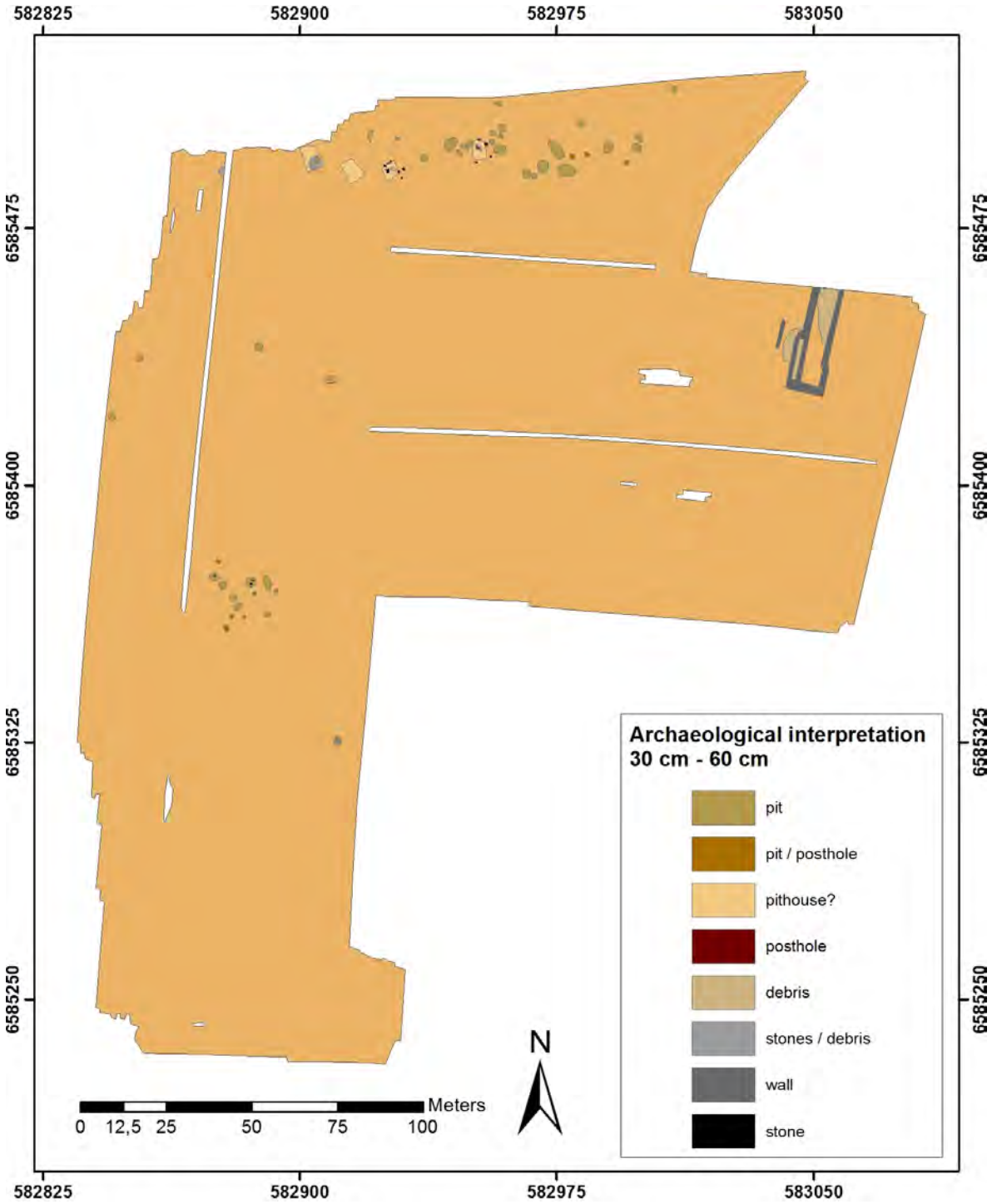

Figure 11: Archaeological interpretation of depthrange 30 cm - 60 cm.

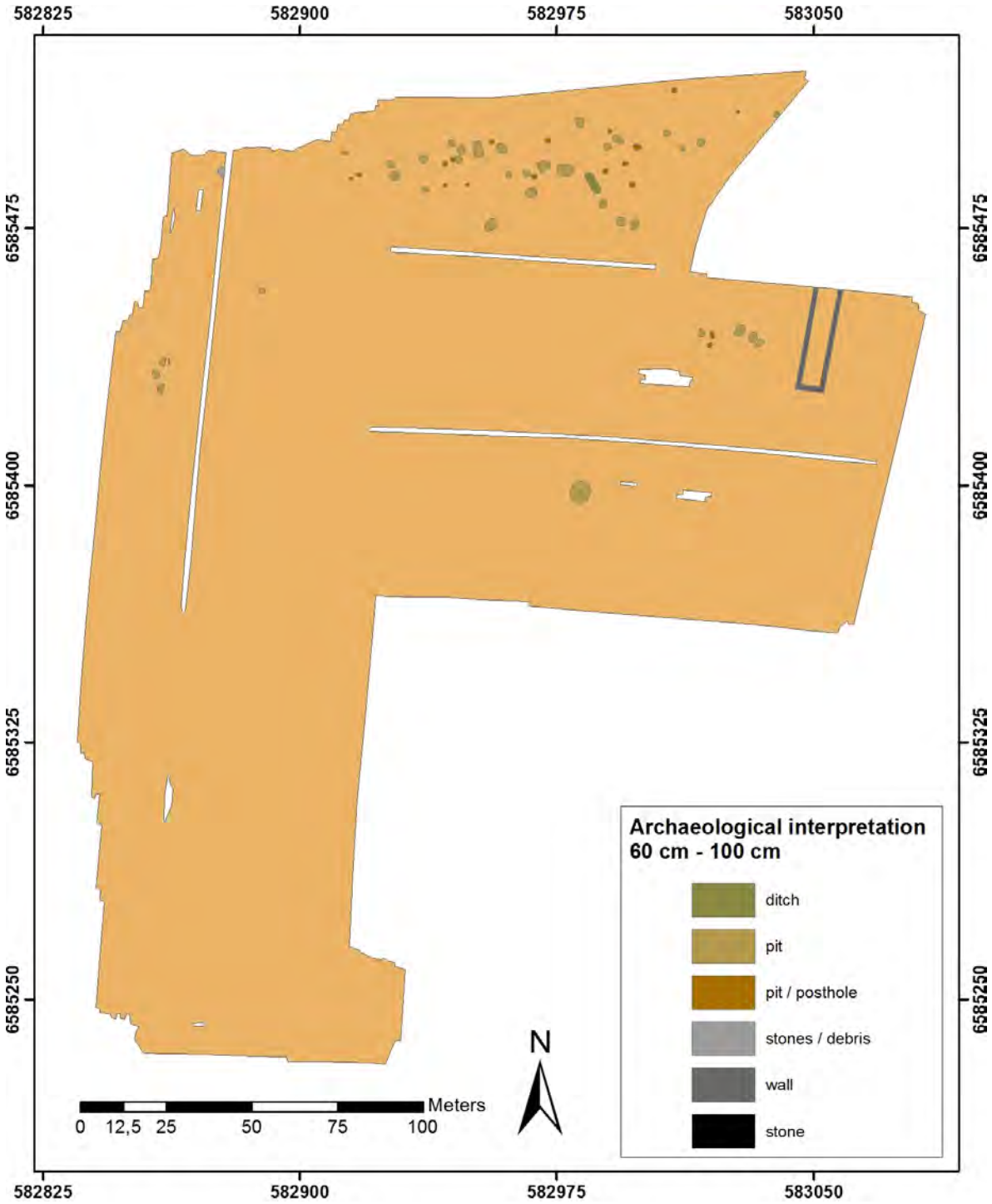

Figure 12: Archaeological interpretation of depthrange 60 cm - 100 cm.

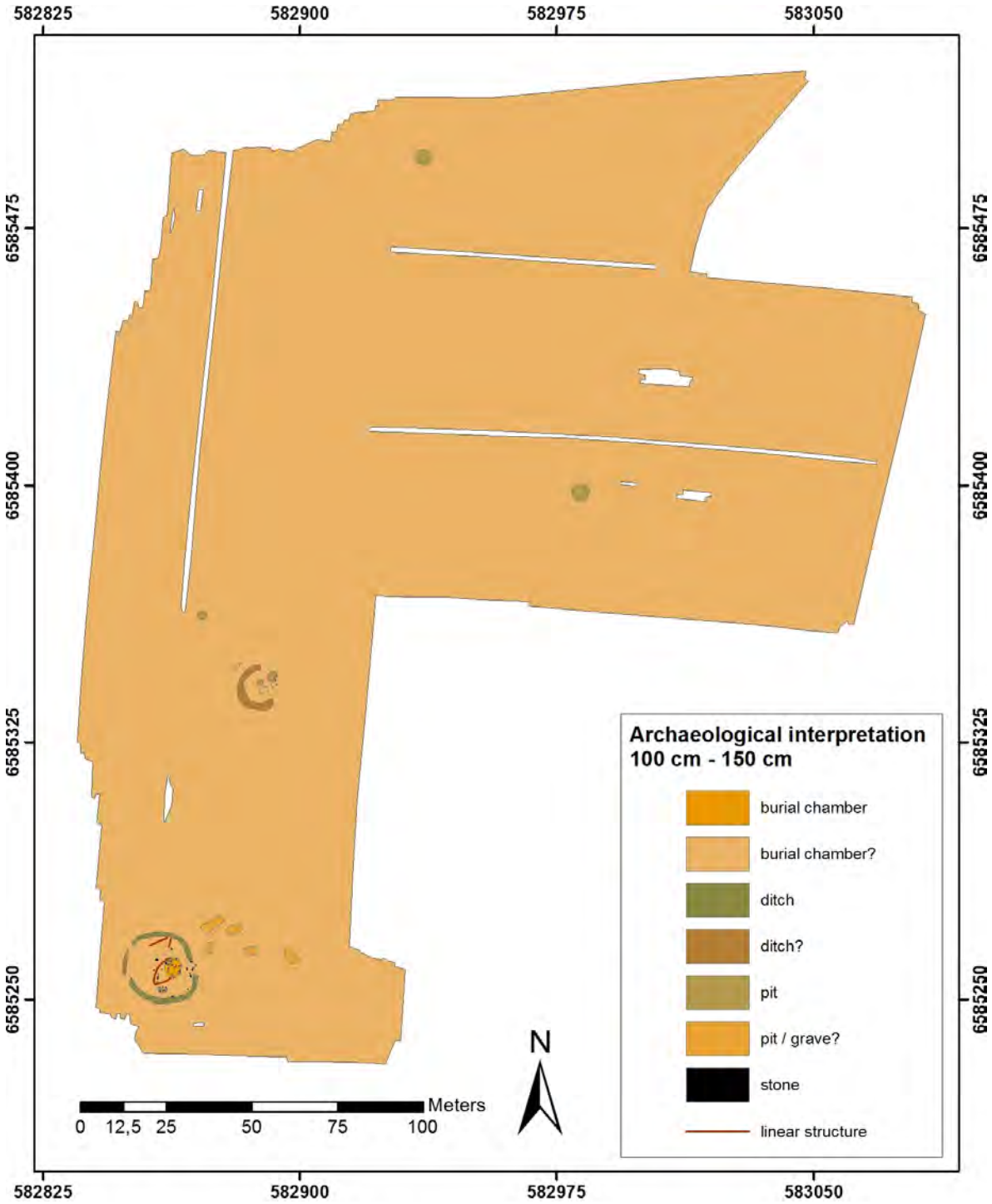

Figure 13: Archaeological interpretation of depthrange 60 cm - 150 cm.

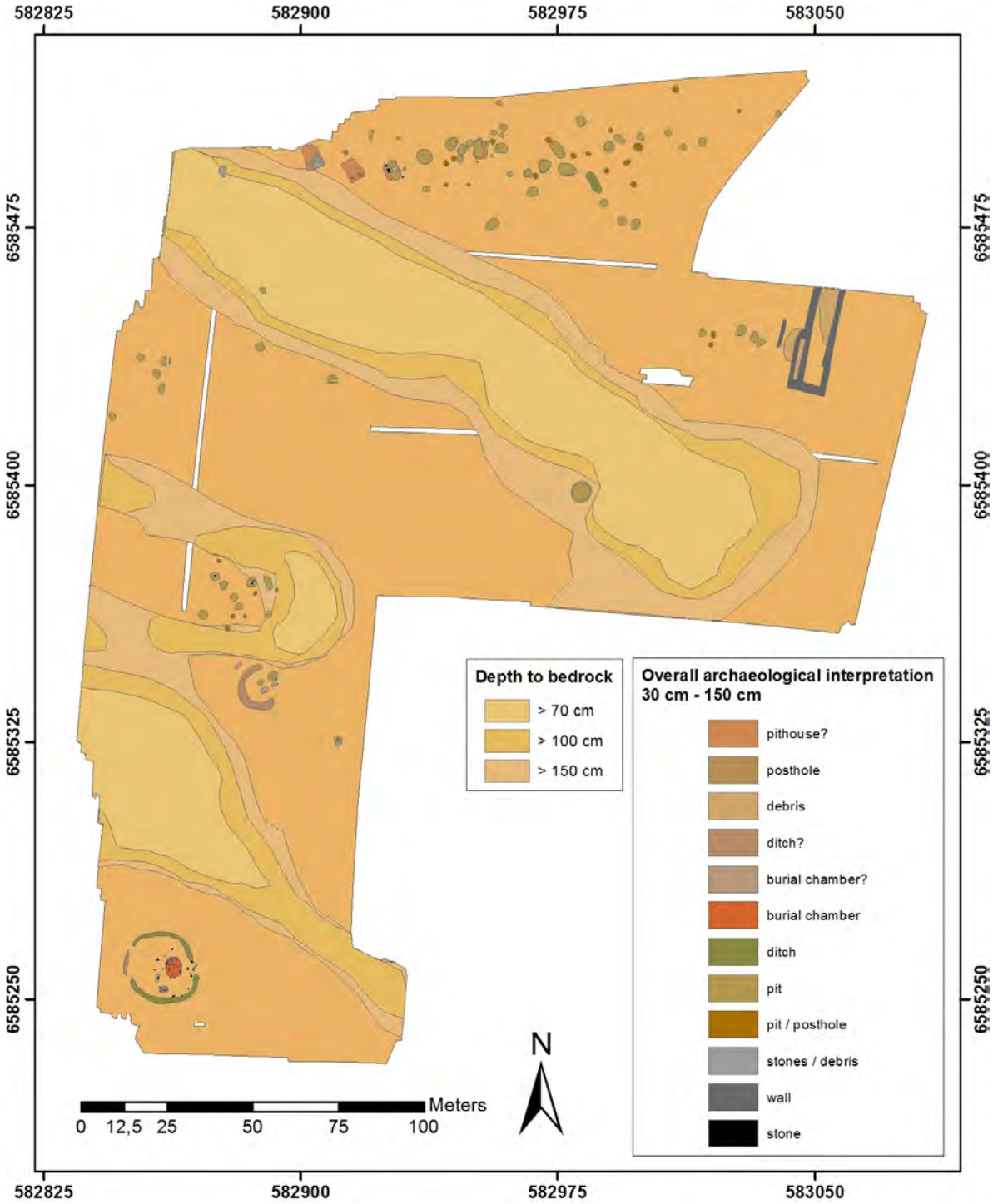

Figure 14: Archaeological interpretation of the complete depthrange.

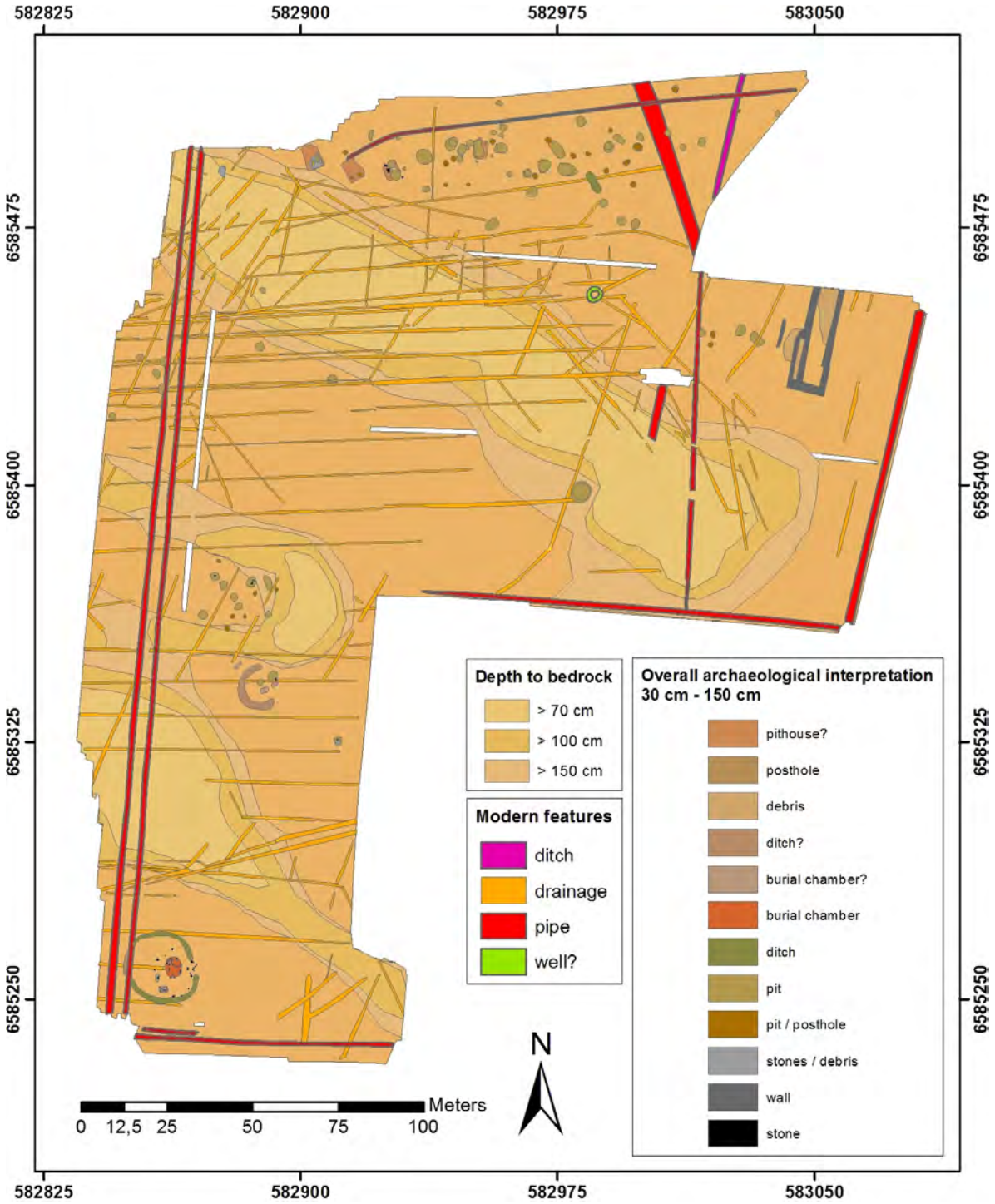

Figure 15: All archaeological, geological and modern features.

Conclusion

The geophysical surveys carried out at Tveiten have successfully detected subsurface features of archaeological, geological and modern character.

The magnetic data is characterised by a number of large, clearly defined geological features, which appear to traverse the site from approximately South-east to North-west. The composition of these anomalies remains unknown, although the geological make-up of the Horten area together with the physical properties recorded during the prospection suggests some form of mixed igneous material.

The Horten area saw a glacial retreat from East to West, as opposed to other areas in Vestfold where glaciers retreated from South to North. This becomes evident in the North-South orientated end moraine forming the foundation of the main road next to the site. During glacial retreat, coarse, heterogeneous material - eroded earlier during glacial advance - was deposited parallel to the retreat direction. These sediment bodies, or moraines appear as linear features in the landscape, situated roughly perpendicular to the end moraine. The extensive geological features observed at Horton, therefore, might represent interlobate or medial morains deposited during the last glacial period. Interestingly, the geological anomalies seen in the magnetic data, appear somewhat different in the GPR data and could as well be caused by ridges of bedrock consisting of magnetic material like rhomb porphyry, which is common in this area.

Modern features such as drainage ditches and pipes perforate the entire survey area and appear in both datasets. Additionally, the data have revealed the remains of a former greenhouse in the North-eastern part of the site, and a possible well in the central area. Despite these modern disturbances, a number of archaeological features could be detected within the prospected area.

If the rectangular, absorbing anomalies in the northern part of the survey area are indeed house structures, they represent a somewhat poorly understood feature type in the Norwegian archaeological context. Although these features are relatively common in the rest of Europe and also in southern Scandinavia, they have so far occurred infrequently in the archaeological record in Norway. In the southern part of the country, only a few pit-houses have been recognized, the most notable of which were excavated near Oddernes in Krisitansand municipality, Vest-Agder in the mid-1970s. Here, a total of 16 pit-houses were excavated at sites near Oddernes church and Kongsgård [12, 13]. Generally speaking, the Oddernes and Kongsgård pit-houses appear to be somewhat smaller than the features observed at Horten, although one of the Kongsgård features measured up to 9 x 5 m. Dated to the late pre-Roman Iron Age, the pit-houses were sub-rectangular in shape with rounded corners, and measuring between 0.3 1.2 m in depth. Upon excavation, some of the houses revealed internal features, such as postholes and hearths. Based on similar structures elsewhere in Europe, it is thought the pit-houses represent small workshops or buildings used for dwelling or storage.

In the southern part of the survey area, a circular anomaly interpreted as remains of a ploughed out burial mound could be observed in the GPR dataset. Its location roughly corresponds to a mound excavated and recorded in the early 20th century. It is therefore most likely that the observed anomalies represent the preserved remains of this mound. Interestingly, the mound only appears at a depth of c. 120 cm - 140 cm, at a considerably greater depth than the other archaeological features within the survey area. None of the upper depth slices displays traces of these structures. The building material of the mound and material covering it can only be determined to a limited extend using geophysical prospection. The

data, however, suggest that the mound has at some point been subject to either geological or anthropogenic processes. Although the survey area is situated close to a small stream, it is unlikely that this part of the site has been covered by a considerable amount of alluvial material. A more likely scenario is that the remains of the grave mound have been covered by soil in the process of levelling the area for more efficient farming.

Apart from few anomalies interpreted as pits, the central part of the survey area appears to be void of archaeological features. Archaeological geophysical prospection highly relies on the measurable contrast of physical properties of the underlying soils and sediments. If the environmental settings do not allow for a sufficient contrast, archaeological features are simply not detectable. The apparent absence of archaeological features in the central area may therefore either represent a reality or reflect specific sedimentological settings of the subsurface.

Bibliography

[1] A. Aspinall, C. Gaffney, and A. Schmidt. *Magnetometry for Archaeologists*. AltaMira Press, 2009.

[2] L. B. Conyers. *Ground-Penetrating Radar for Archaeology*. AltaMira Press, Walnut Creek, CA, 2004.

[3] J. W. E. Fassbinder. *Die magnetischen Eigenschaften und die Genese ferrimagnetischer Minerale in Böden im Hinblick auf die magnetische Prospektion archäologischer Bodendenkmäler*. Buch am Erlbach, 1994.

[4] J. W. E. Fassbinder and H. Stanjek. Occurrence of bacterial magnetite in soils from archaeological sites. *Archaeologia Polona*, 31:117–128, 1993.

[5] J. W. E. Fassbinder, H. Stanjek, and H. Vali. Occurence of magnetic bacteria in soil. *Nature*, 343:161–163, 1990.

[6] C. Gaffney. Detecting trends in the prediction of the buried past: a review of geophysical techniques in archaeology. *Archaeometry*, 50:313–336, 2008.

[7] C.F. Gaffney and J. Gater. *Revealing the buried past: geophysics for archaeologists*. Tempus., 2003.

[8] J. Leckebusch. Ground-penetrating Radar: A Modern Three-dimensional Prospection Method. *Archaeological Prospection*, 10:213–240, 2003.

[9] W. Neubauer. *Magnetische Prospektion in der Archäologie*. Verlag der Österreichischen Akademie der Wissenschaften, Wien., 2001.

[10] W. Neubauer. GIS in Archaeology - the Interface between Prospection and Excavation. *Archaeological Prospection*, 11:159–166, 2004.

[11] W. Neubauer, A. Eder-Hinterleitner, P. Melichar, and R. Steiner. Improvements in high resolution archaeological magnetometry. *Prospezioni Archeologiche*, 11:113–134, 2001.

[12] P. Rolfsen. Hustufter, grophus og groper fra eldre jernalder ved oddernes kirke, vest-agder. *Universitetets Oldsaksamling Årbok*, pages 65–82, 1972-1974.

[13] P. Rolfsen. *Porten til Europa*, chapter Gård - Tettsted - Kaupang - By, pages 33–51. 1992.

[14] I. Scollar, A. Tabbagh, A. Hesse, and I. Herzog. *Archaeological Prospecting And Remote Sensing*. Cambridge University Press, 1990.

Appendix

Magnetic data images

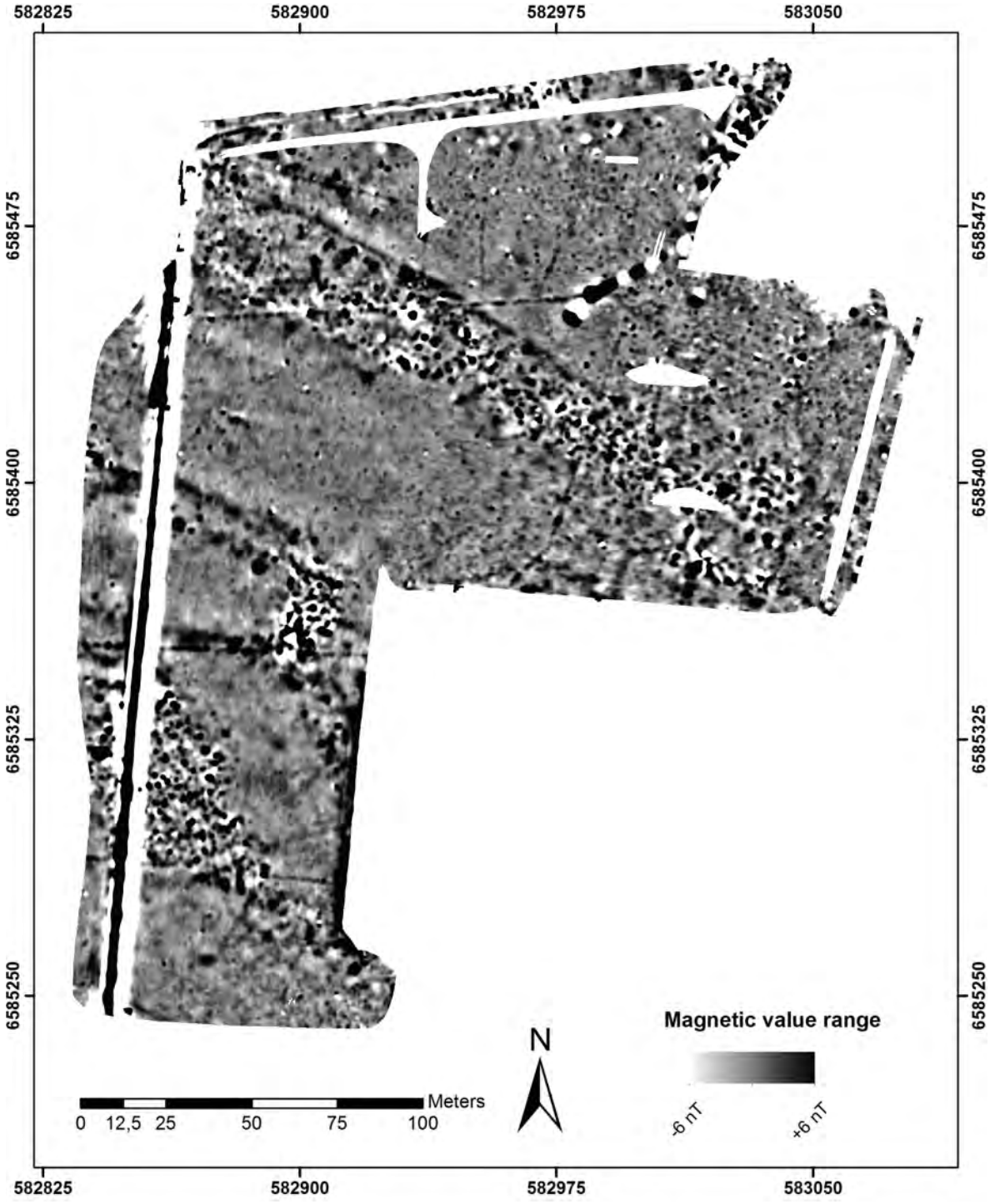

Figure 16: Greyscale image of the magnetic prospection data.

Figure 17: Greyscale image of the magnetic prospection data using a Wallis filter with 5m window size.

MIRA GPR depth-slices

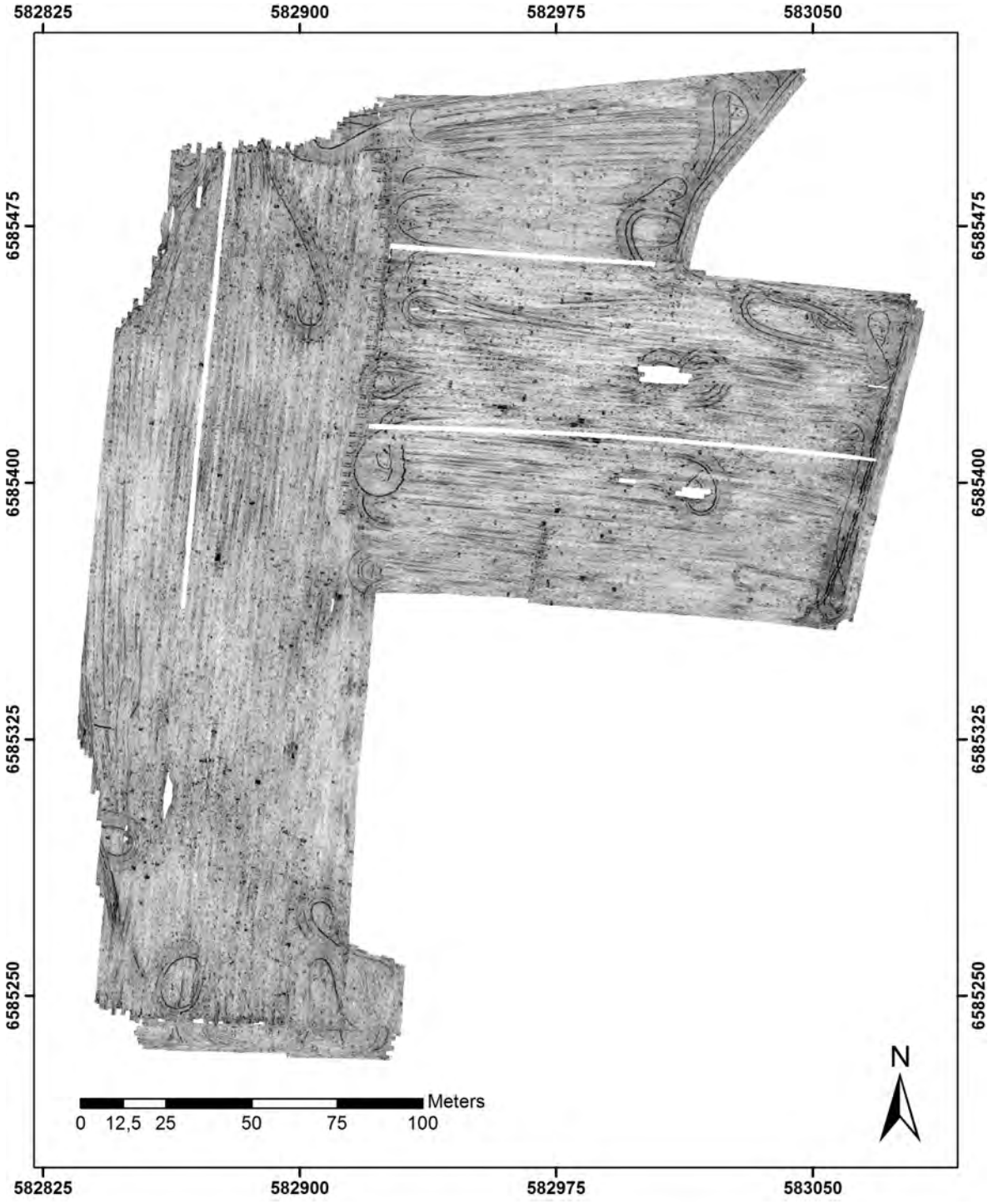

Figure 18: MIRA GPR depth-slice, circa 0 - 5 cm depth.

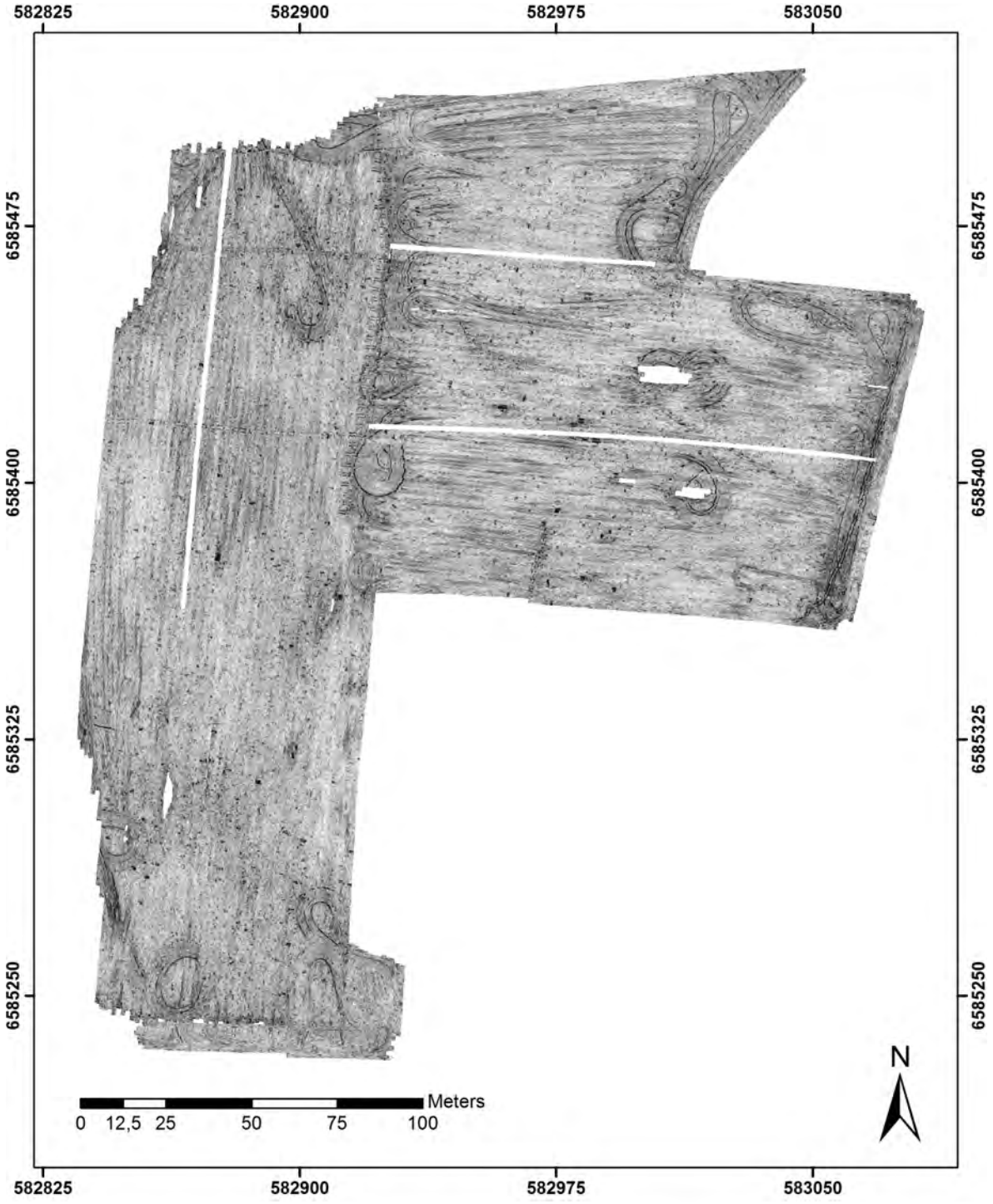

Figure 19: MIRA GPR depth-slice, circa 5 - 10 cm depth.

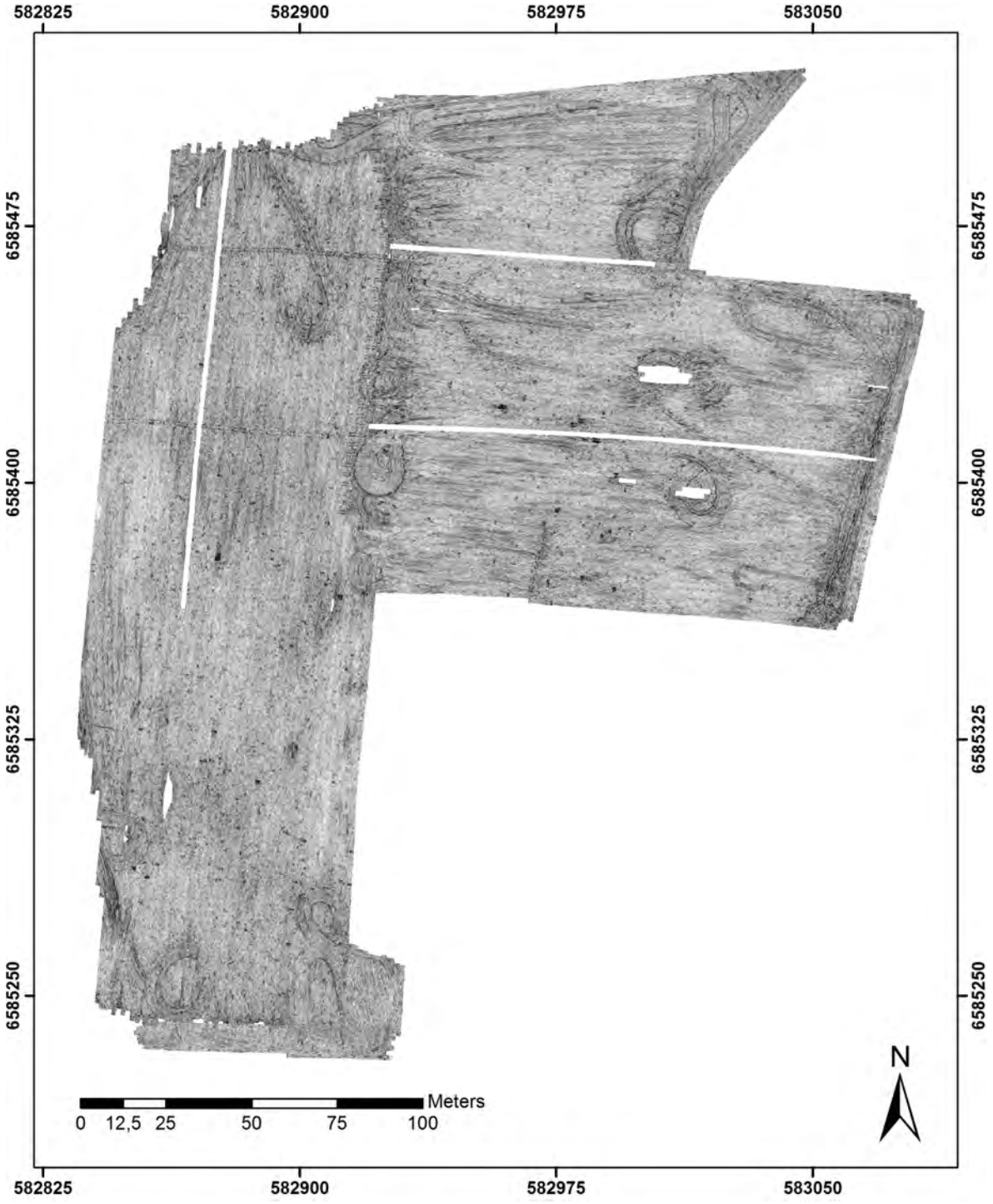

Figure 20: MIRA GPR depth-slice, circa 10 - 15 cm depth.

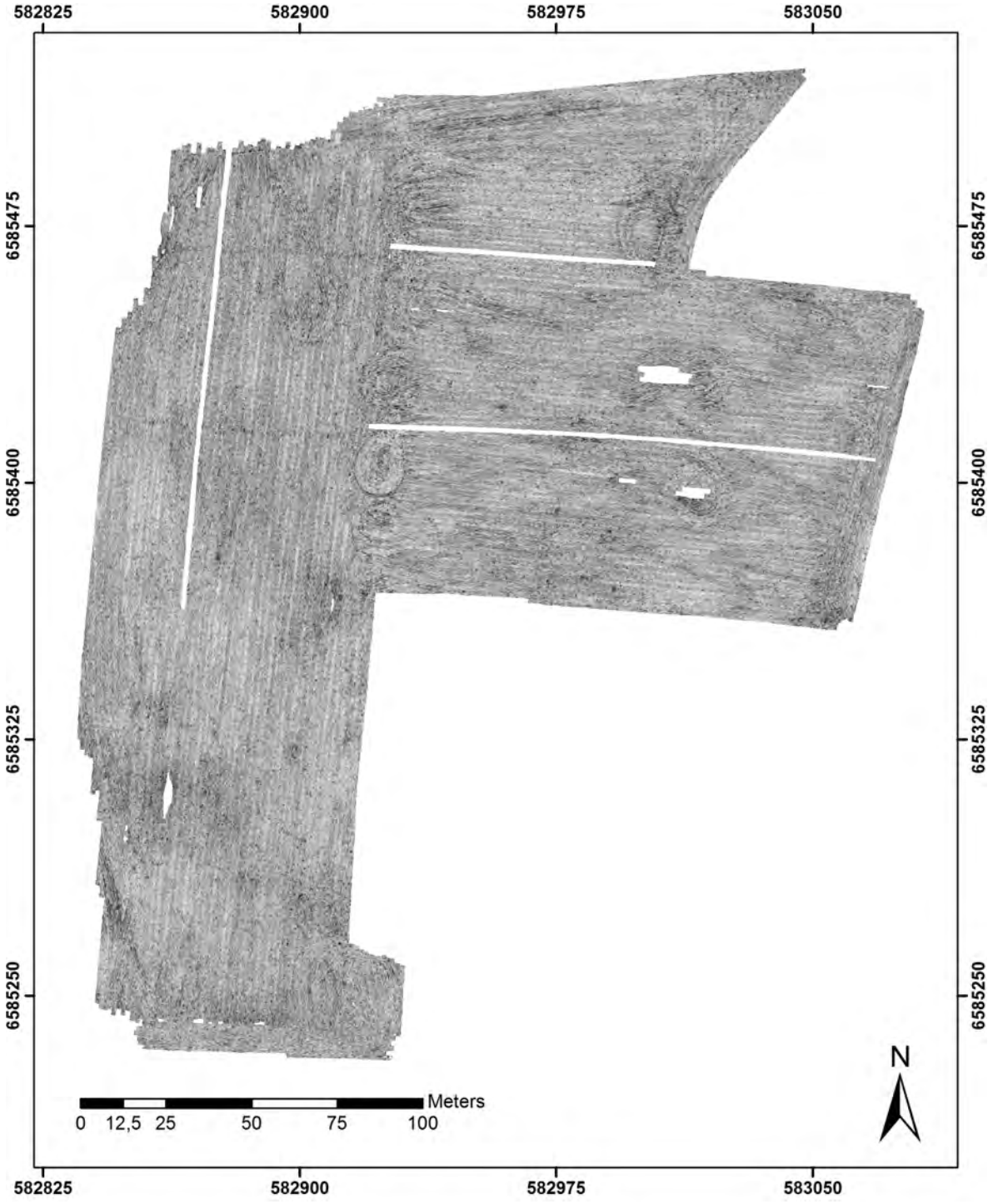

Figure 21: MIRA GPR depth-slice, circa 15 - 20 cm depth.

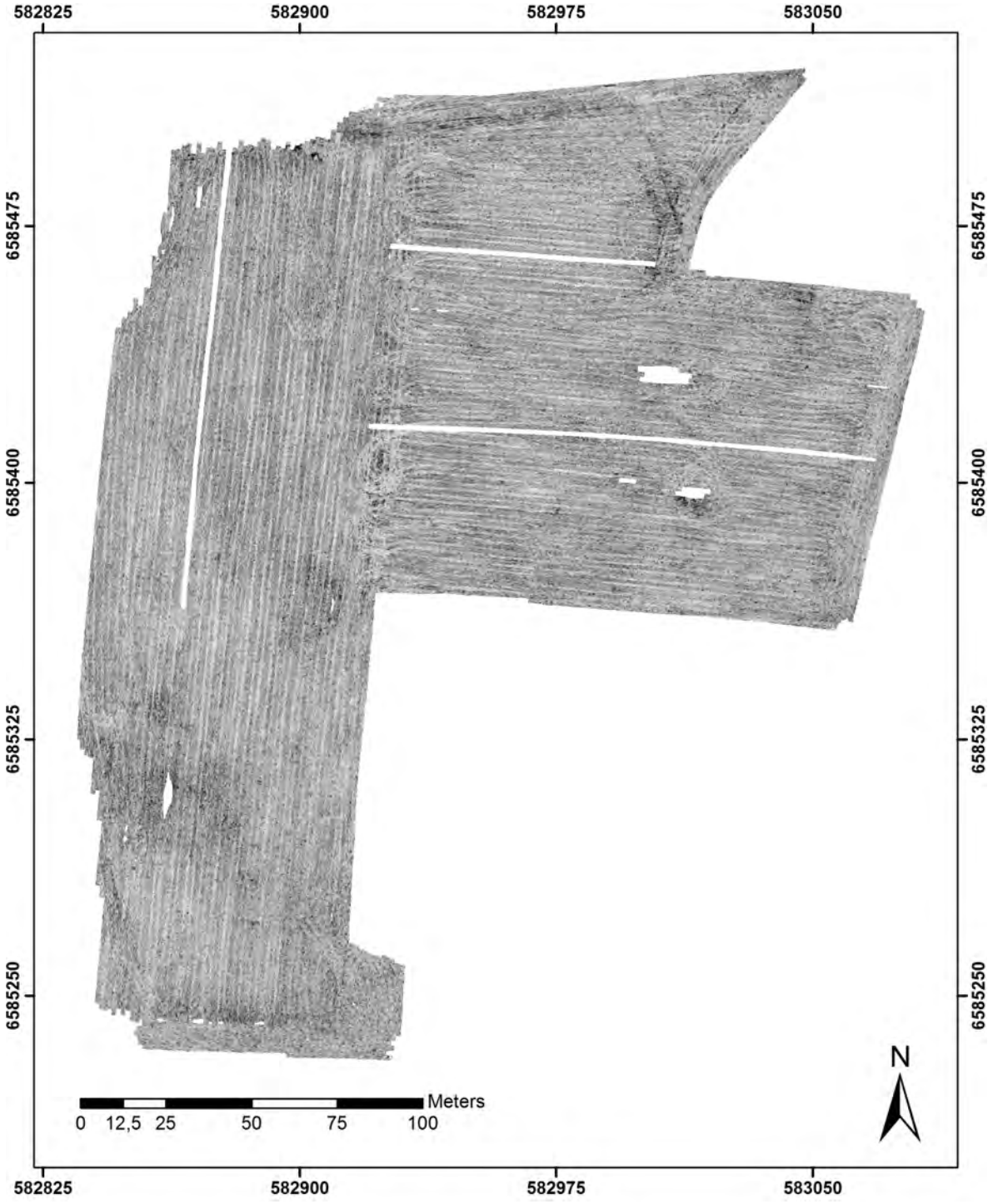

Figure 22: MIRA GPR depth-slice, circa 20 - 25 cm depth.

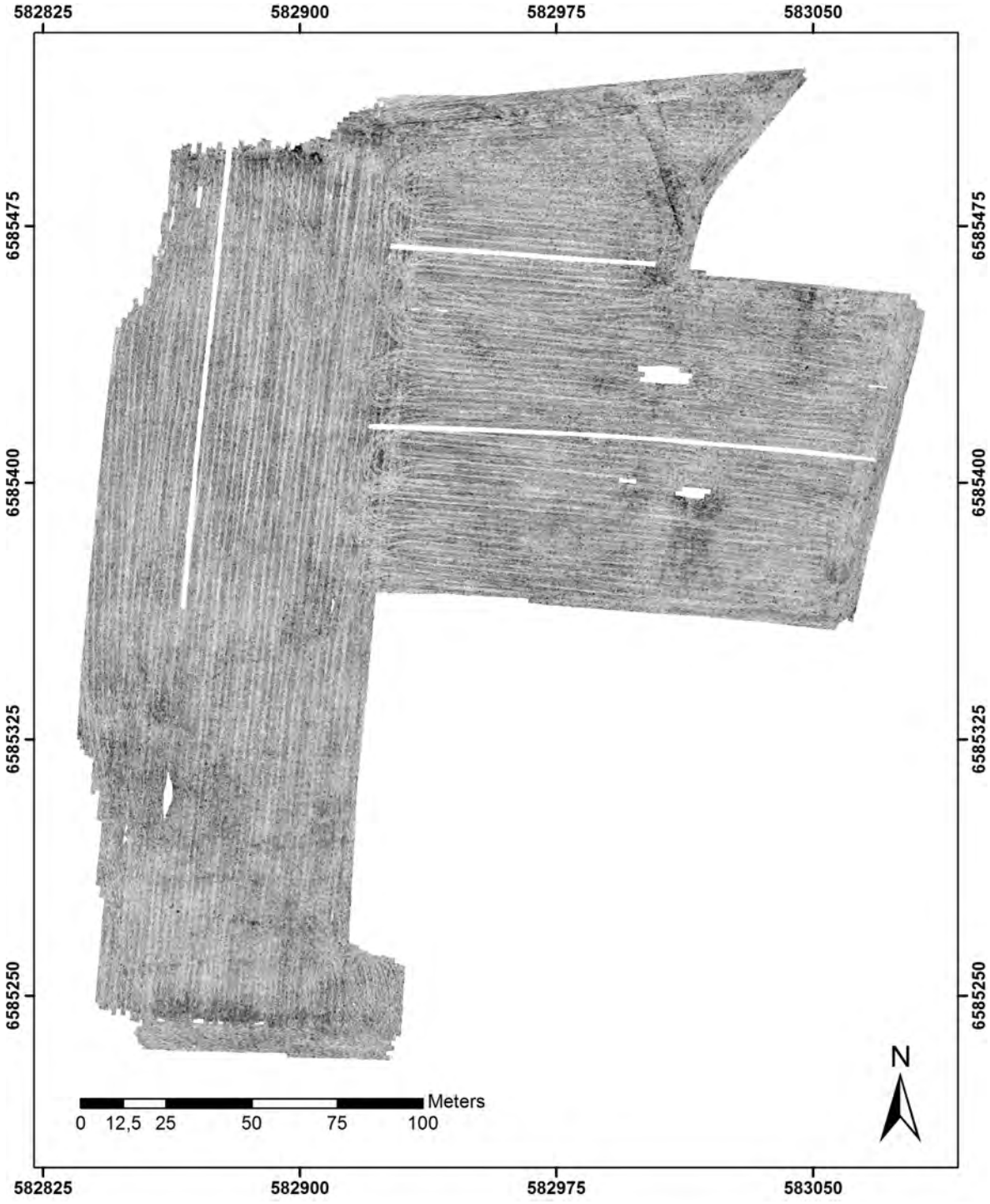

Figure 23: MIRA GPR depth-slice, circa 25 - 30 cm depth.

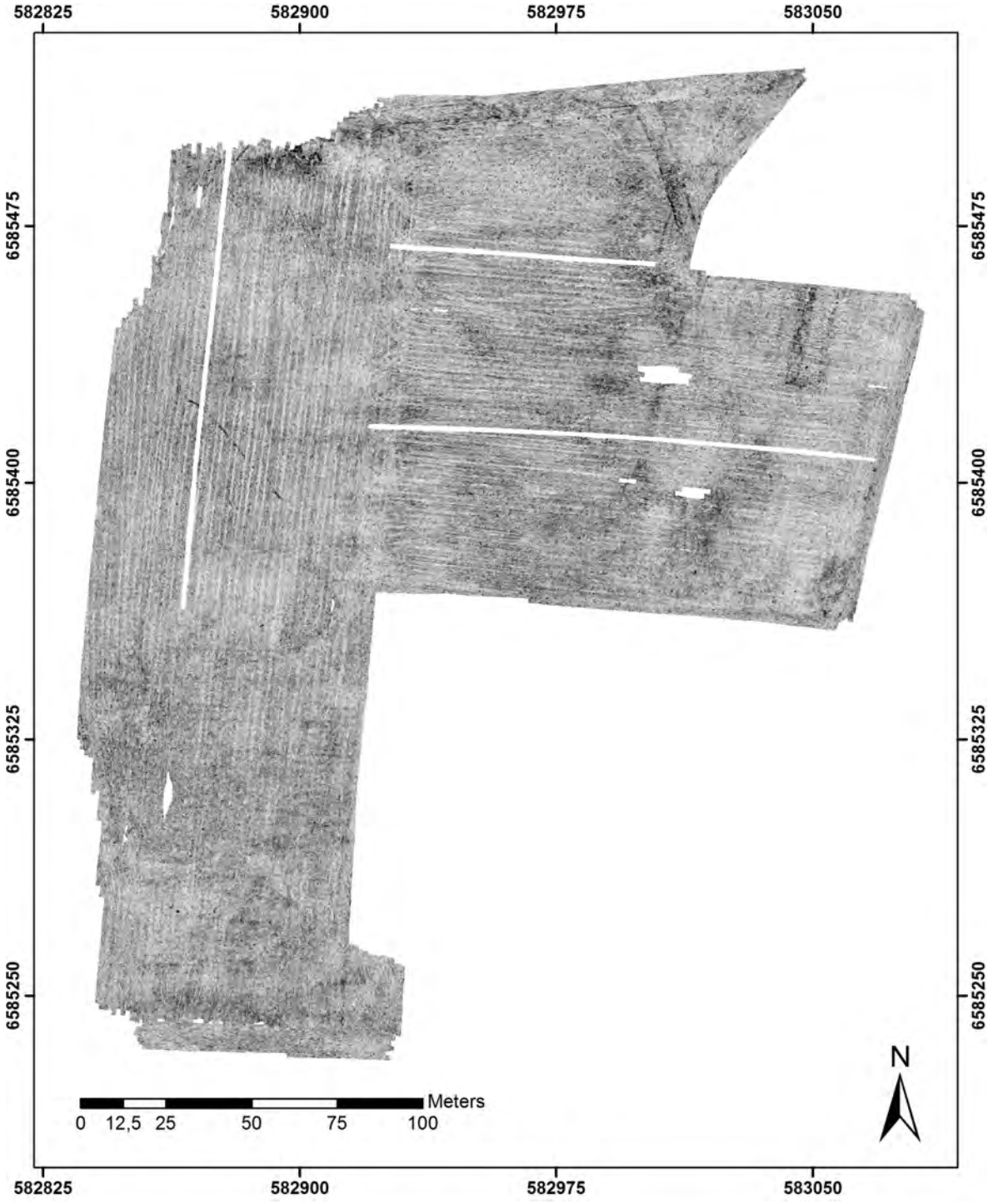

Figure 24: MIRA GPR depth-slice, circa 30 - 35 cm depth.

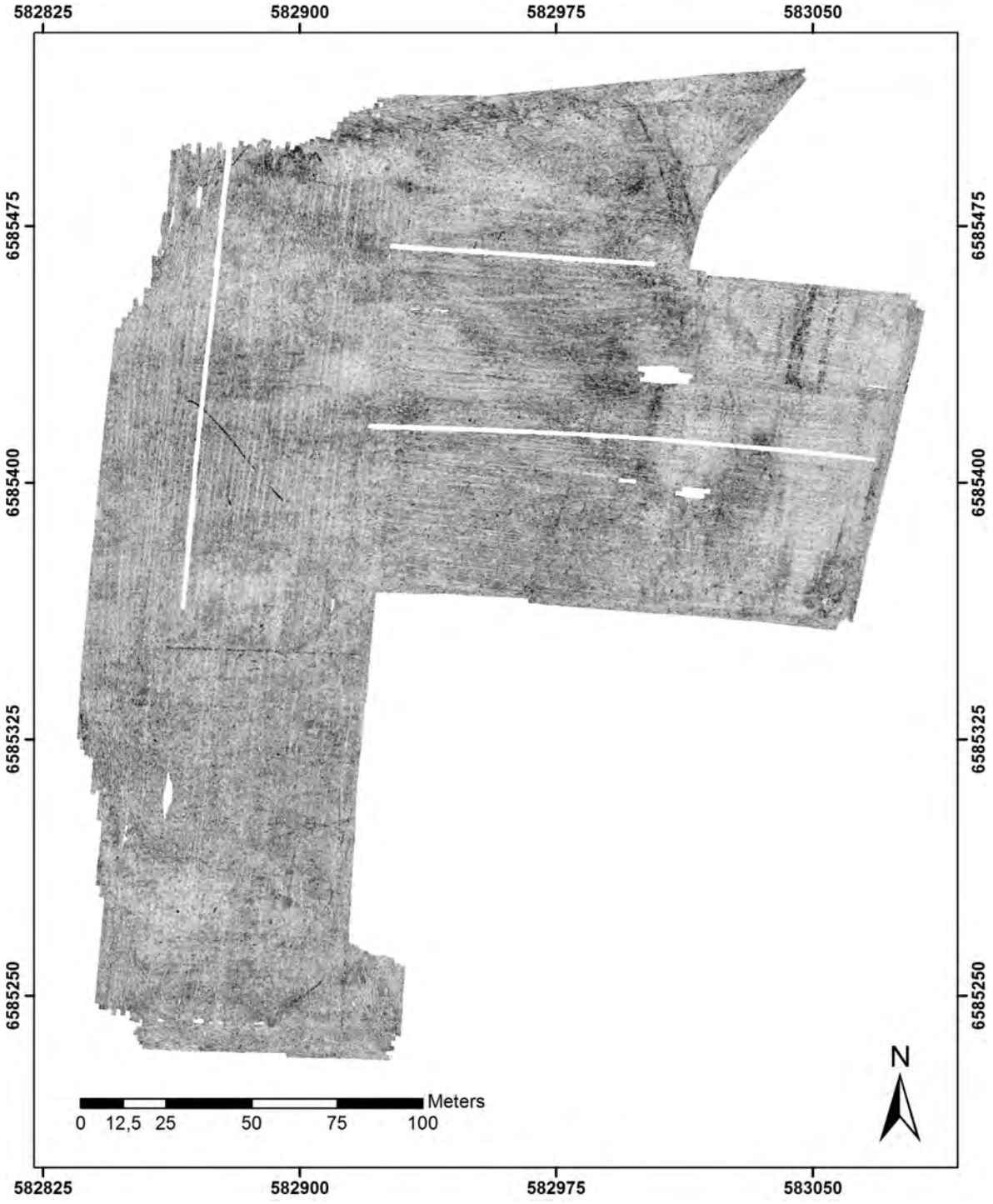

Figure 25: MIRA GPR depth-slice, circa 35 - 40 cm depth.

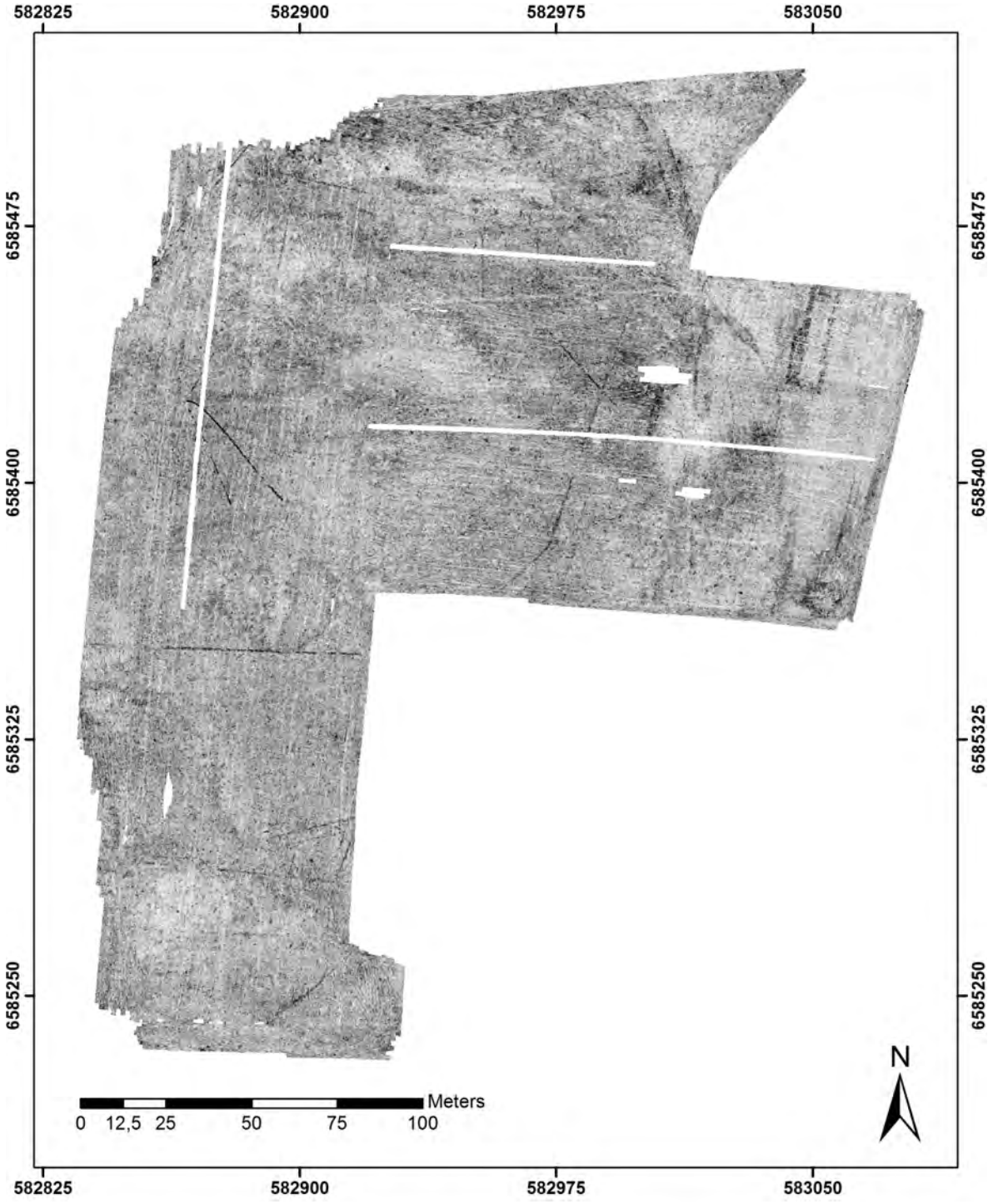

Figure 26: MIRA GPR depth-slice, circa 40 - 45 cm depth.

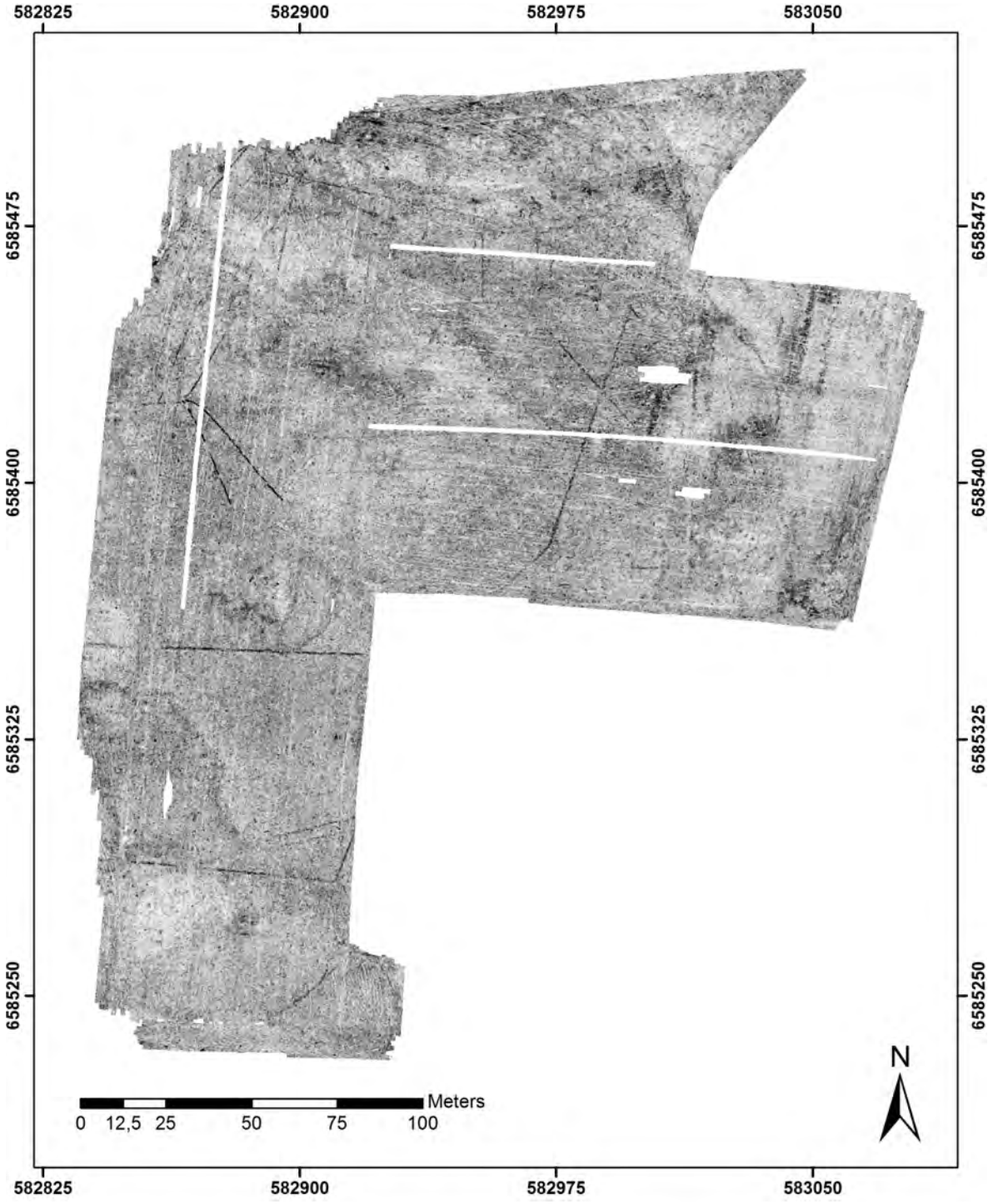

Figure 27: MIRA GPR depth-slice, circa 45 - 50 cm depth.

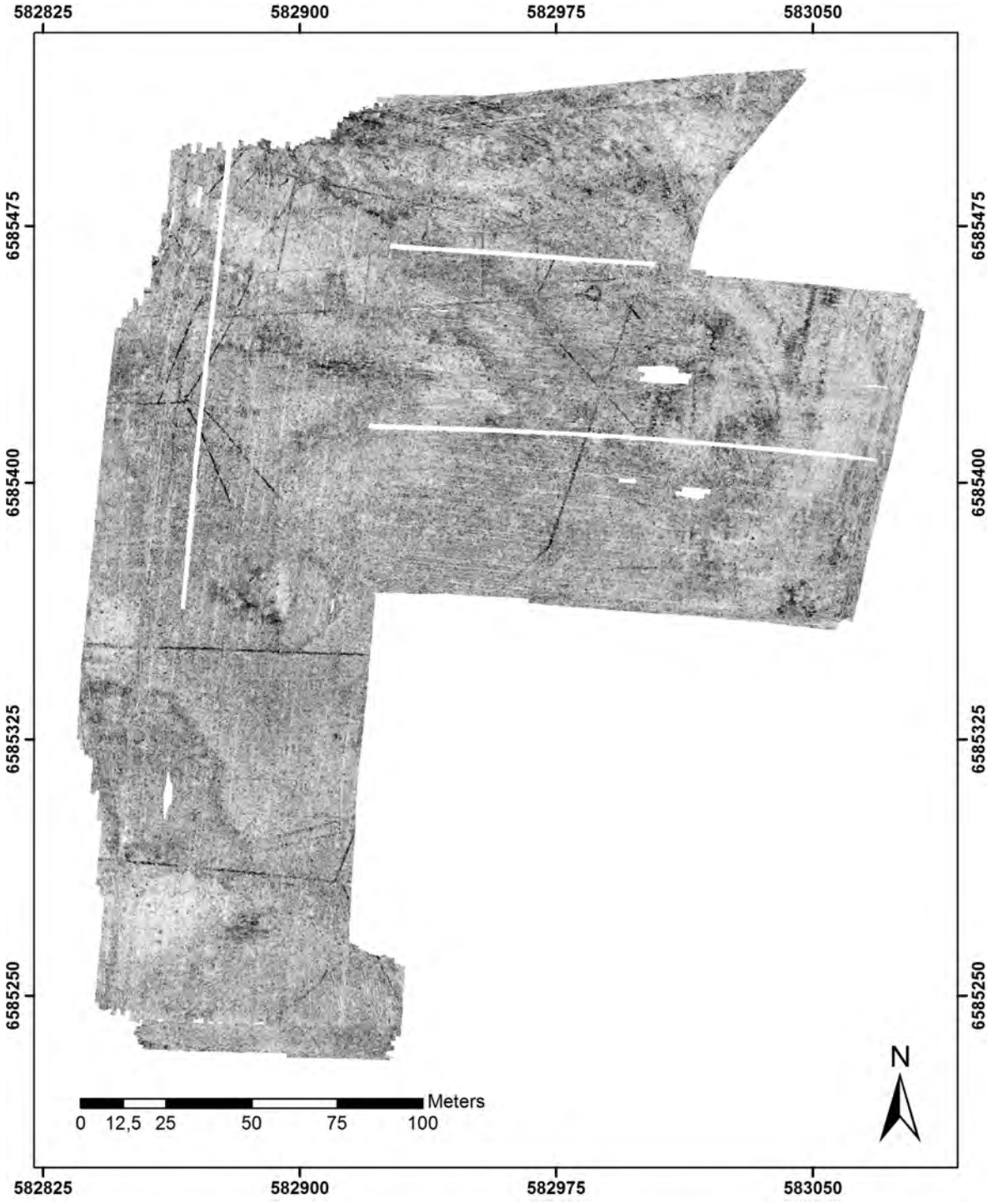

Figure 28: MIRA GPR depth-slice, circa 50 - 55 cm depth.

Figure 29: MIRA GPR depth-slice, circa 55 - 60 cm depth.

Figure 30: MIRA GPR depth-slice, circa 60 - 65 cm depth.

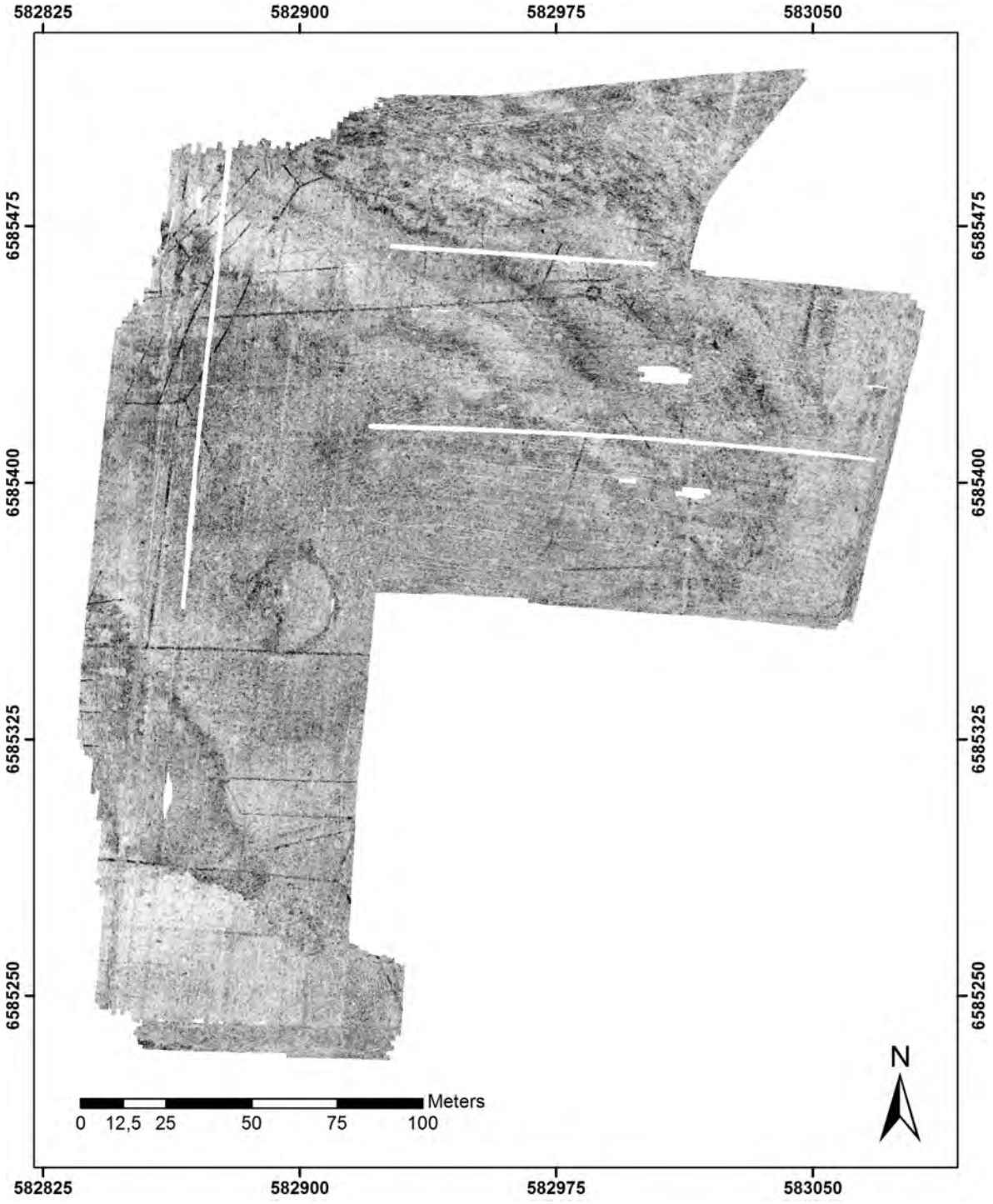

Figure 31: MIRA GPR depth-slice, circa 65 - 70 cm depth.

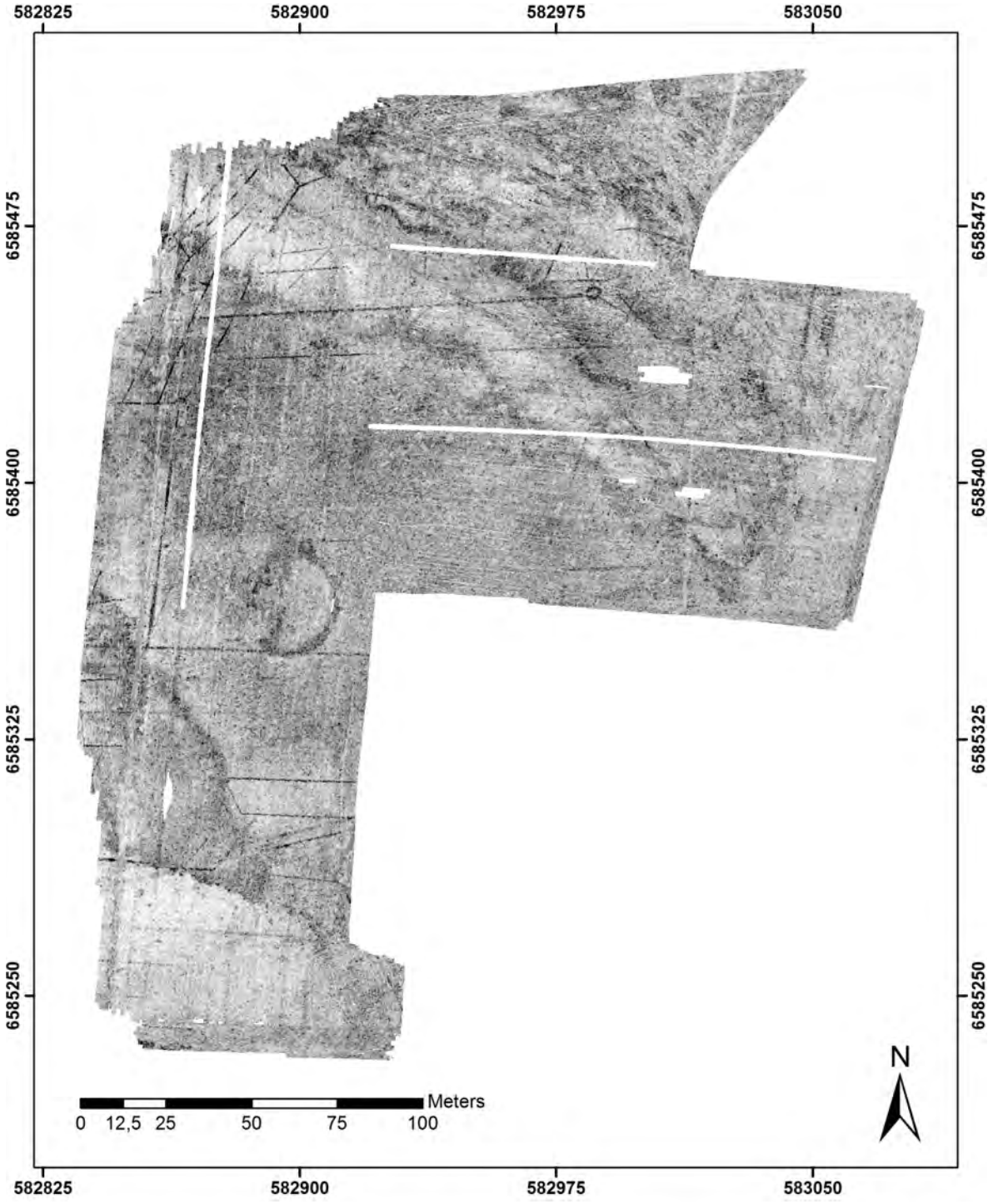

Figure 32: MIRA GPR depth-slice, circa 70 - 75 cm depth.

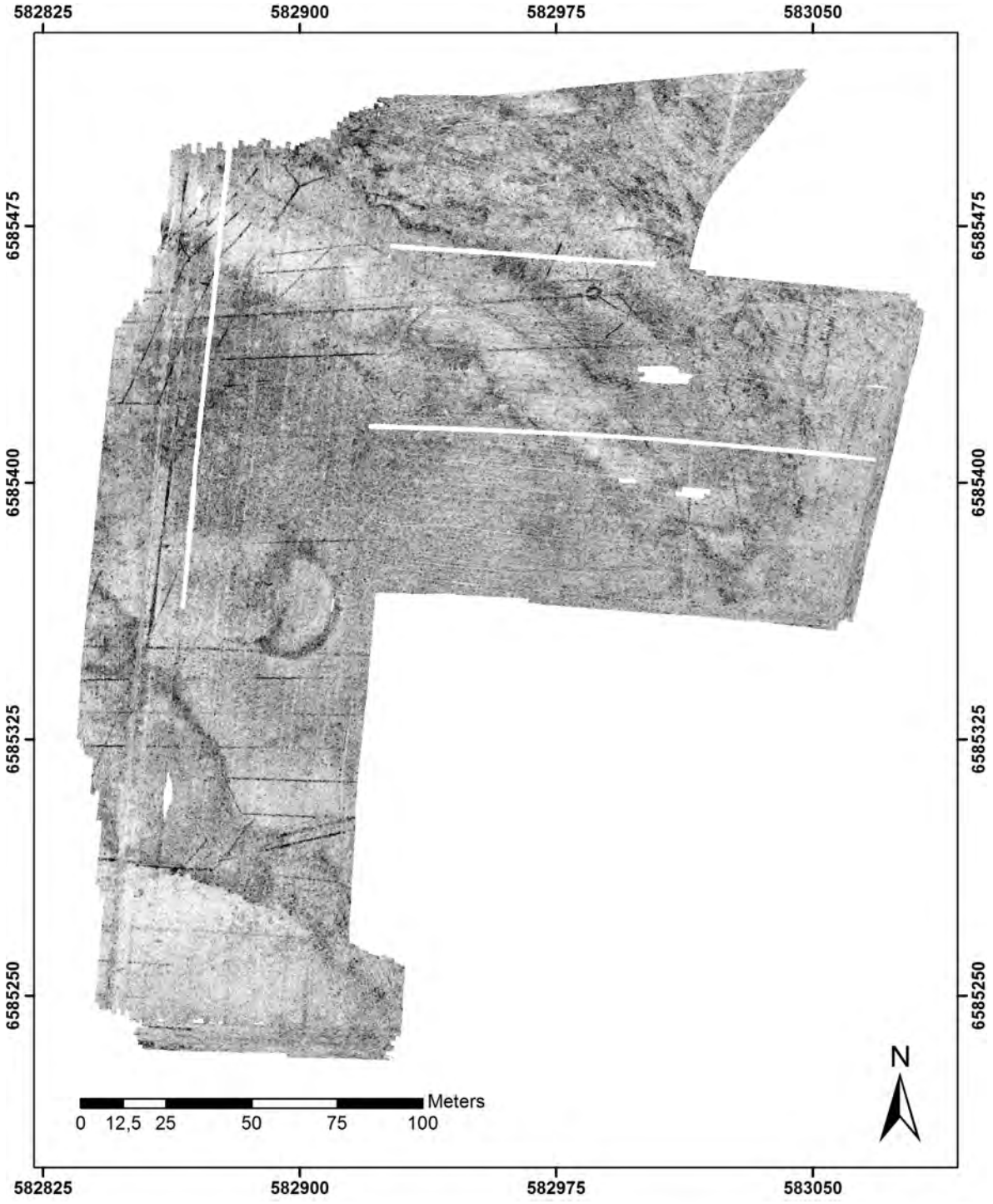

Figure 33: MIRA GPR depth-slice, circa 75 - 80 cm depth.

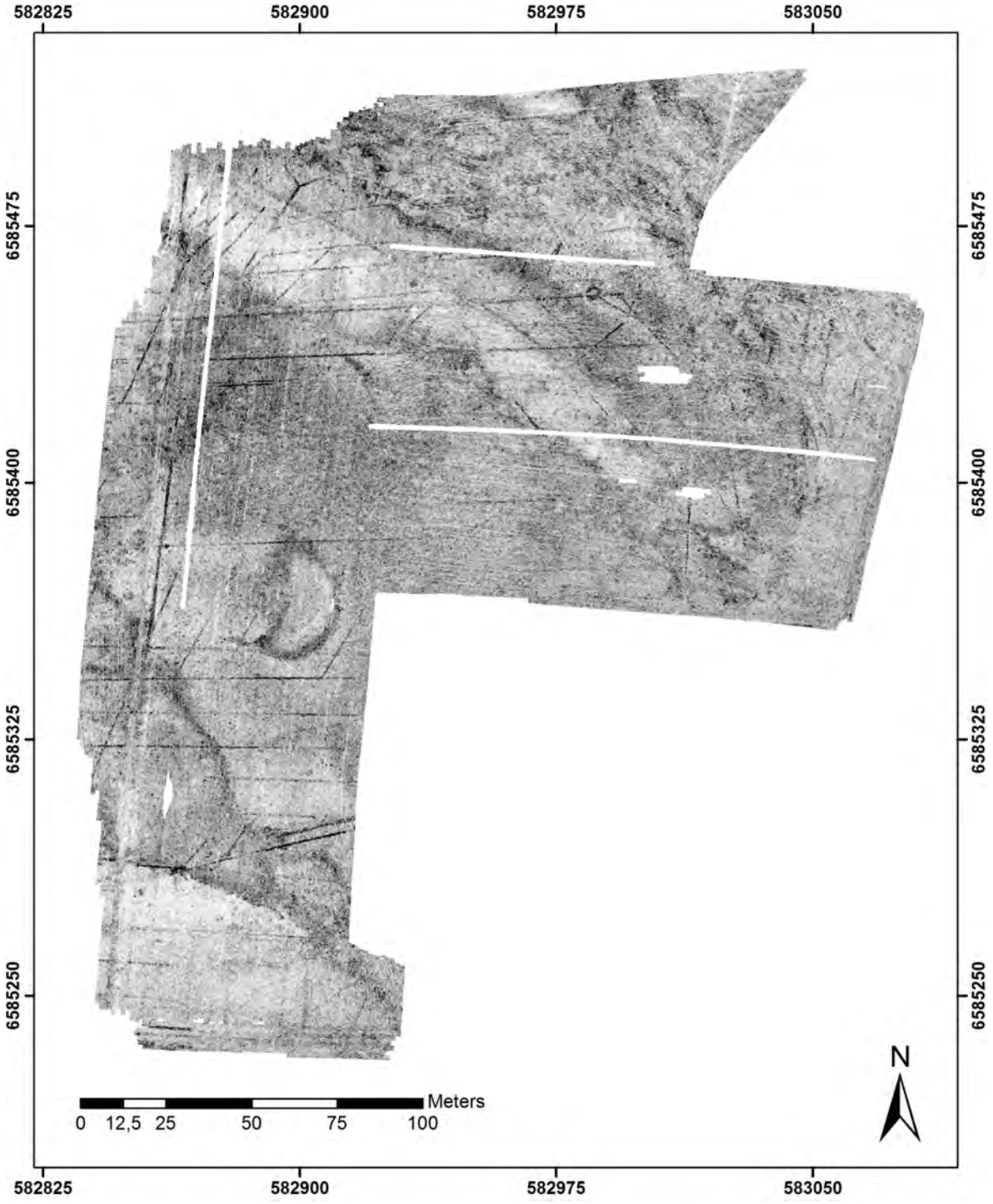

Figure 34: MIRA GPR depth-slice, circa 80 - 85 cm depth.

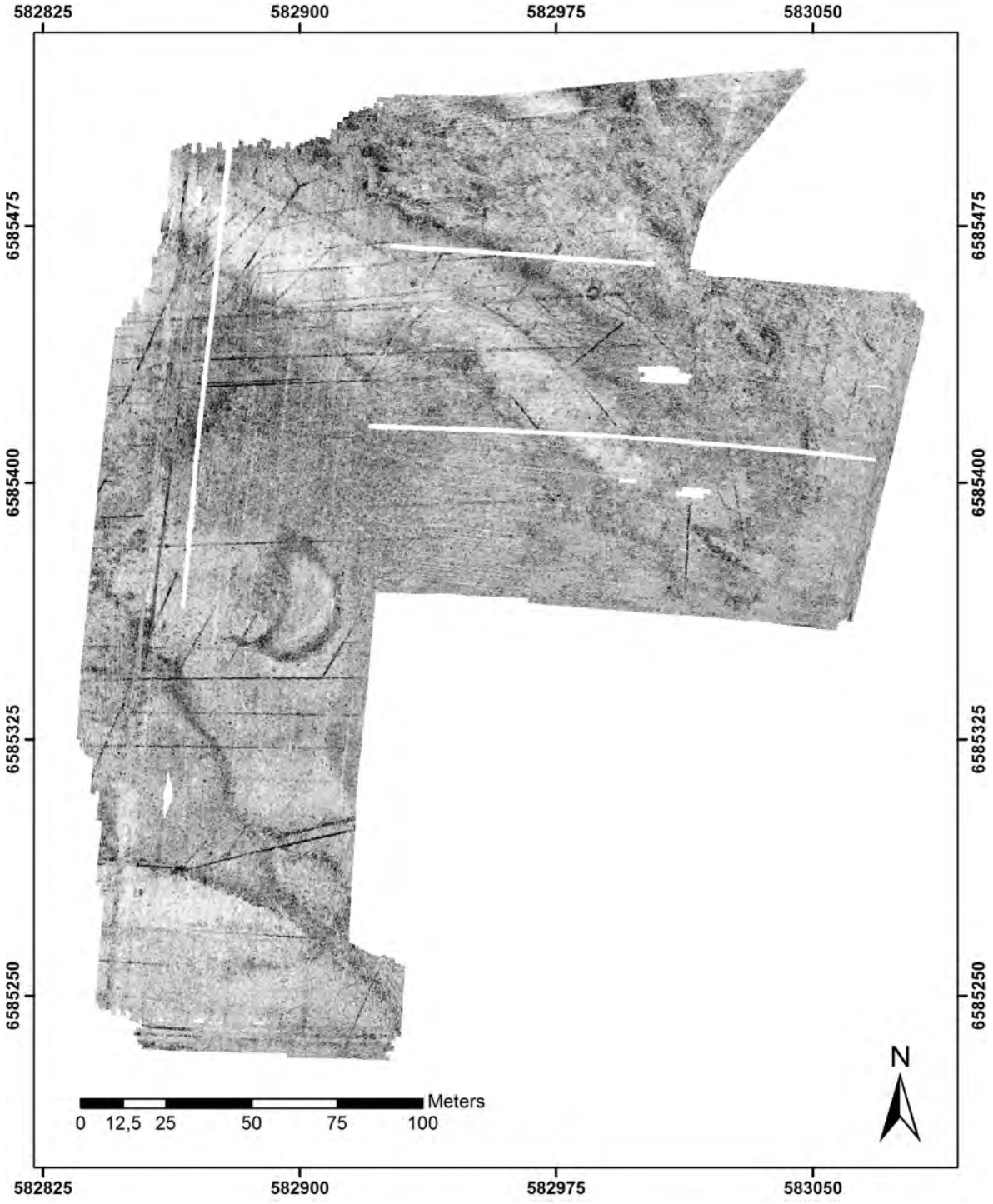

Figure 35: MIRA GPR depth-slice, circa 85 - 90 cm depth.

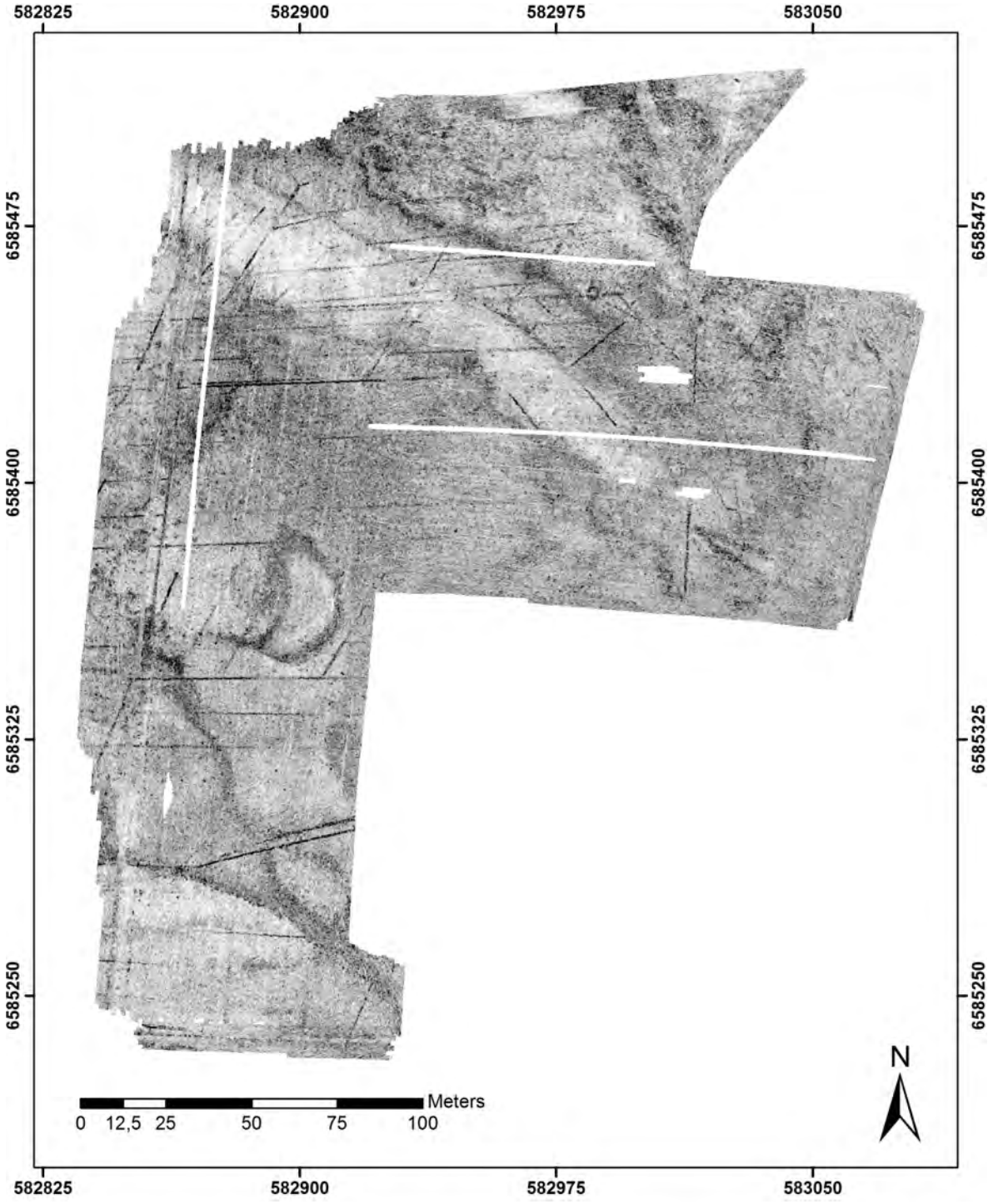

Figure 36: MIRA GPR depth-slice, circa 90 - 95 cm depth.

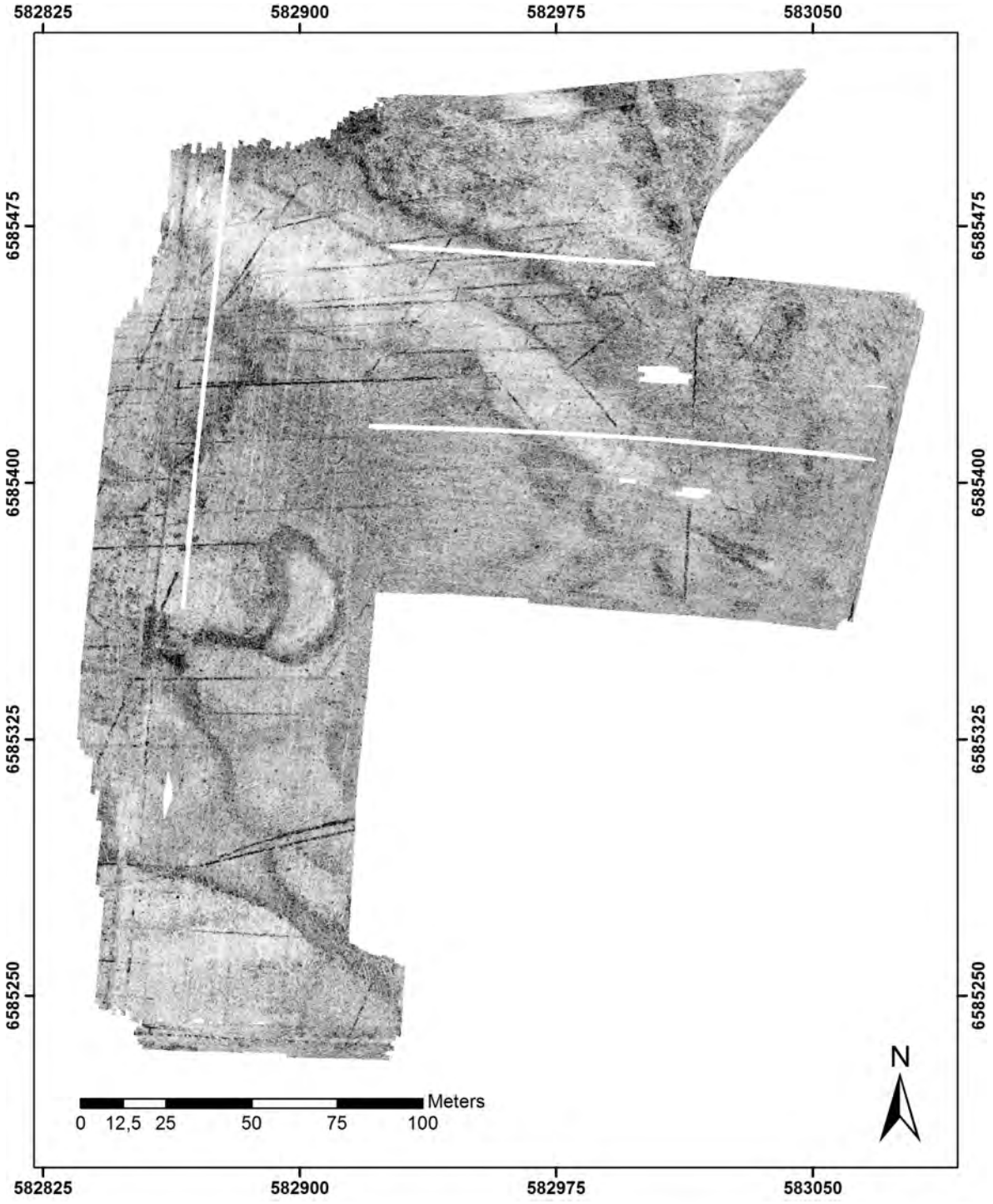

Figure 37: MIRA GPR depth-slice, circa 95 - 100 cm depth.

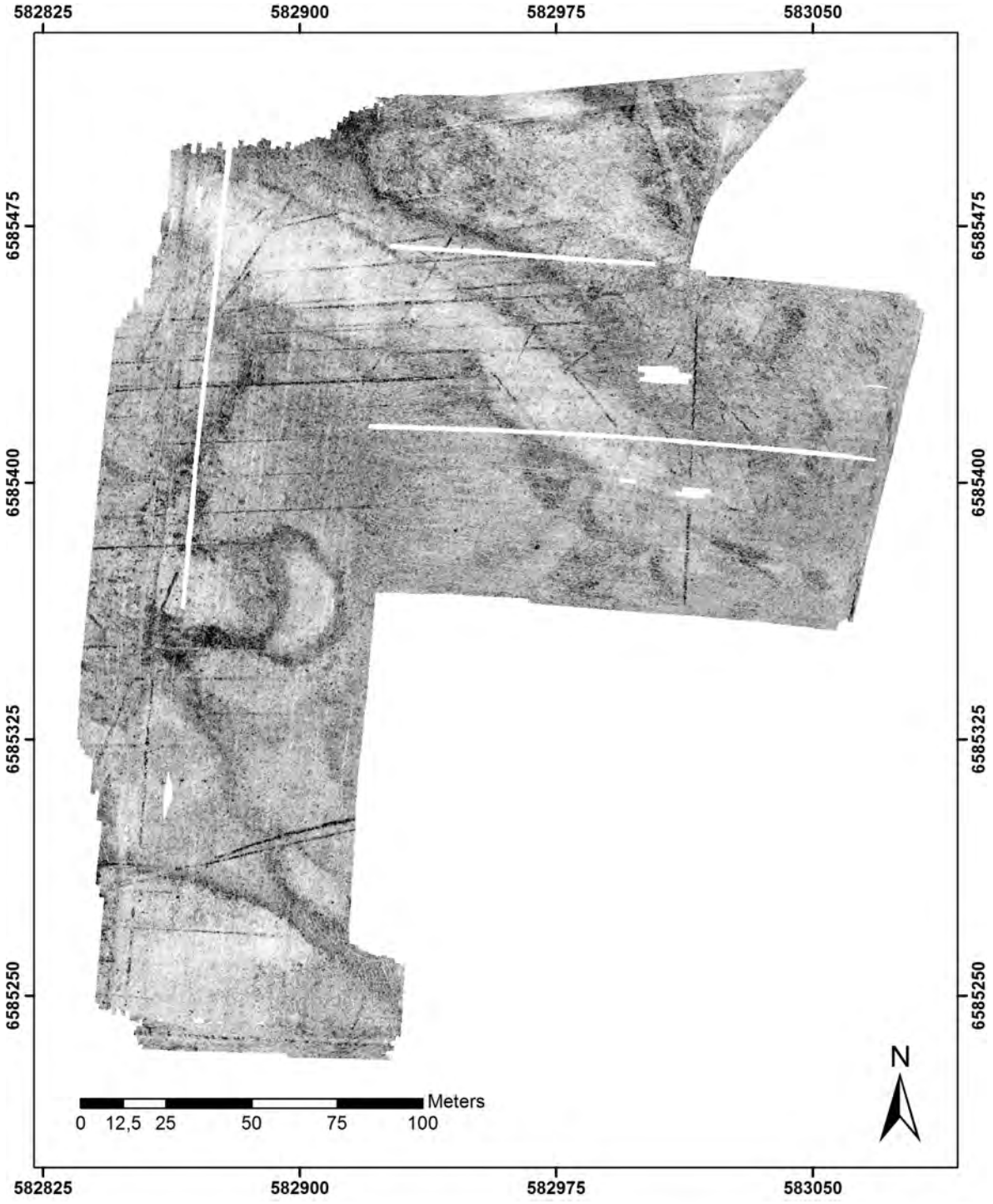

Figure 38: MIRA GPR depth-slice, circa 100 - 105 cm depth.

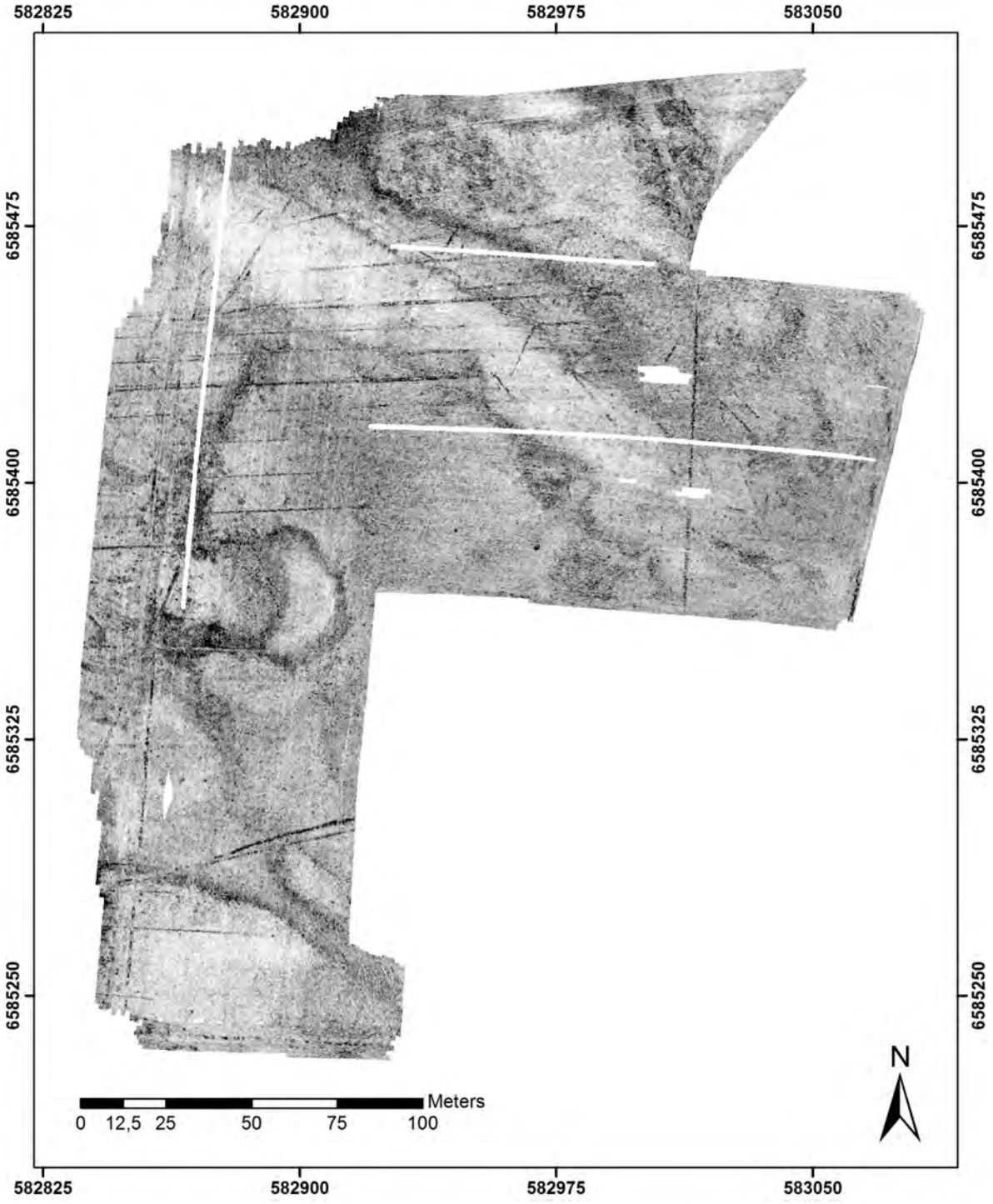

Figure 39: MIRA GPR depth-slice, circa 105 - 110 cm depth.

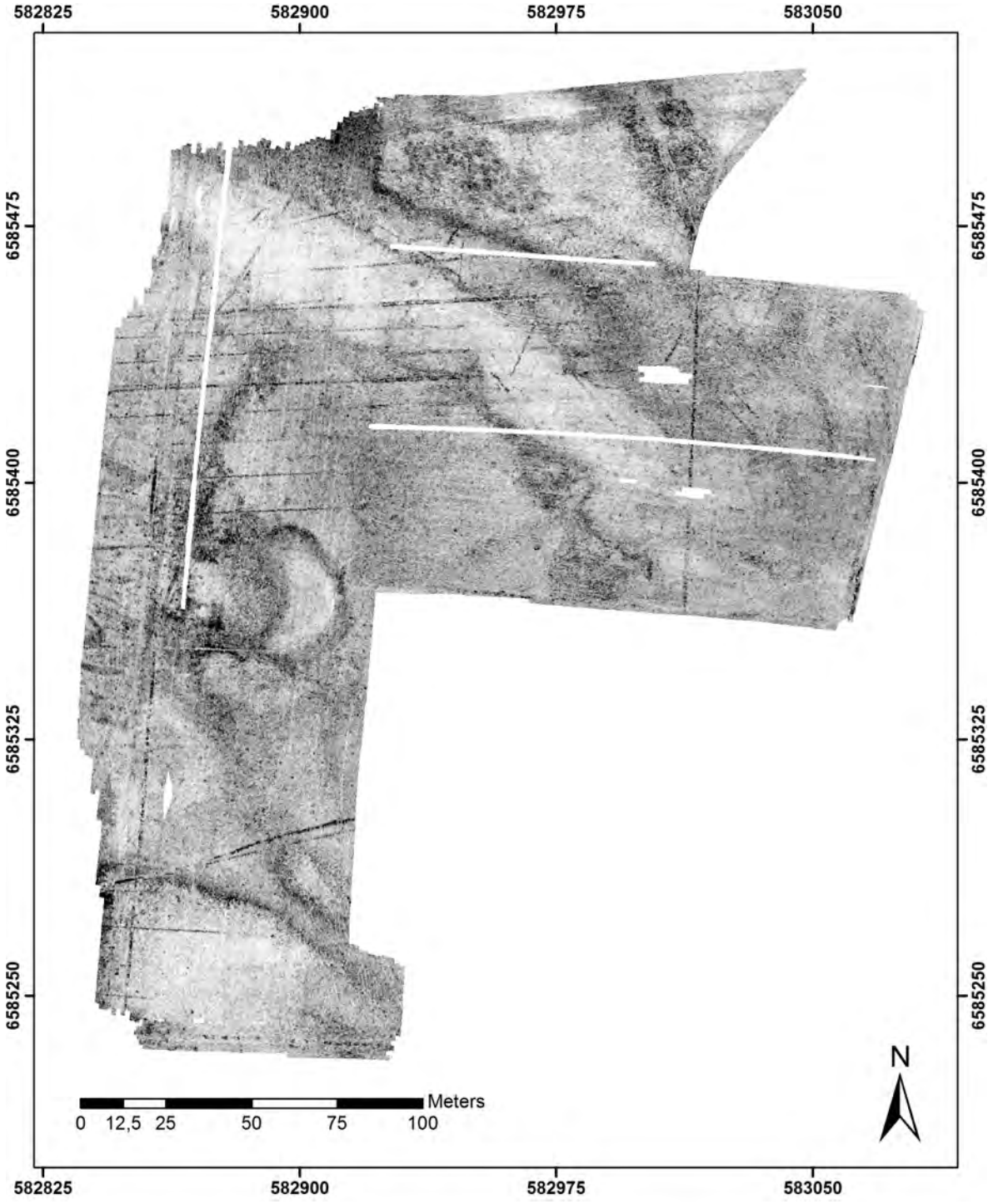

Figure 40: MIRA GPR depth-slice, circa 110 - 115 cm depth.

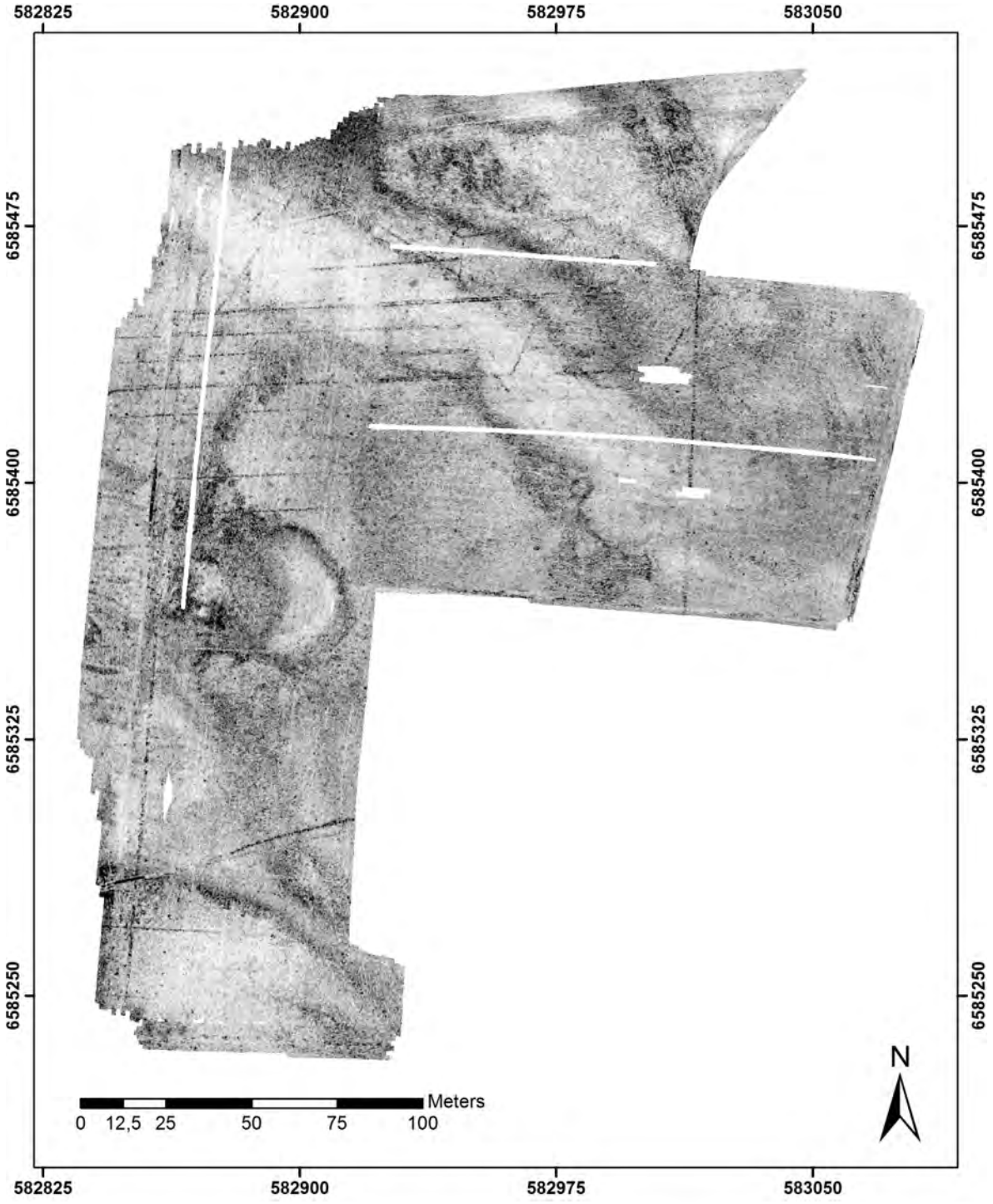

Figure 41: MIRA GPR depth-slice, circa 115 - 120 cm depth.

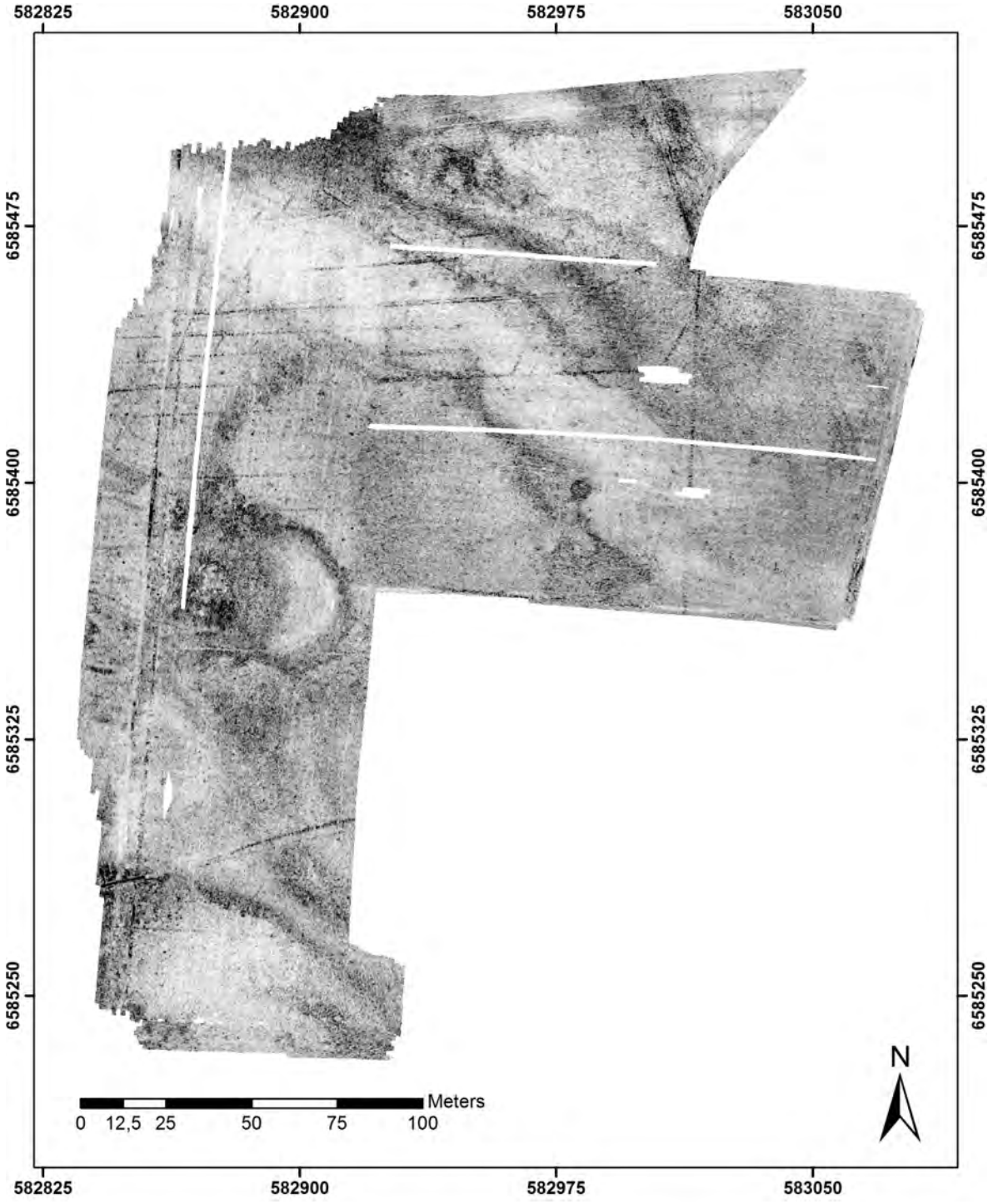

Figure 42: MIRA GPR depth-slice, circa 120 - 125 cm depth.

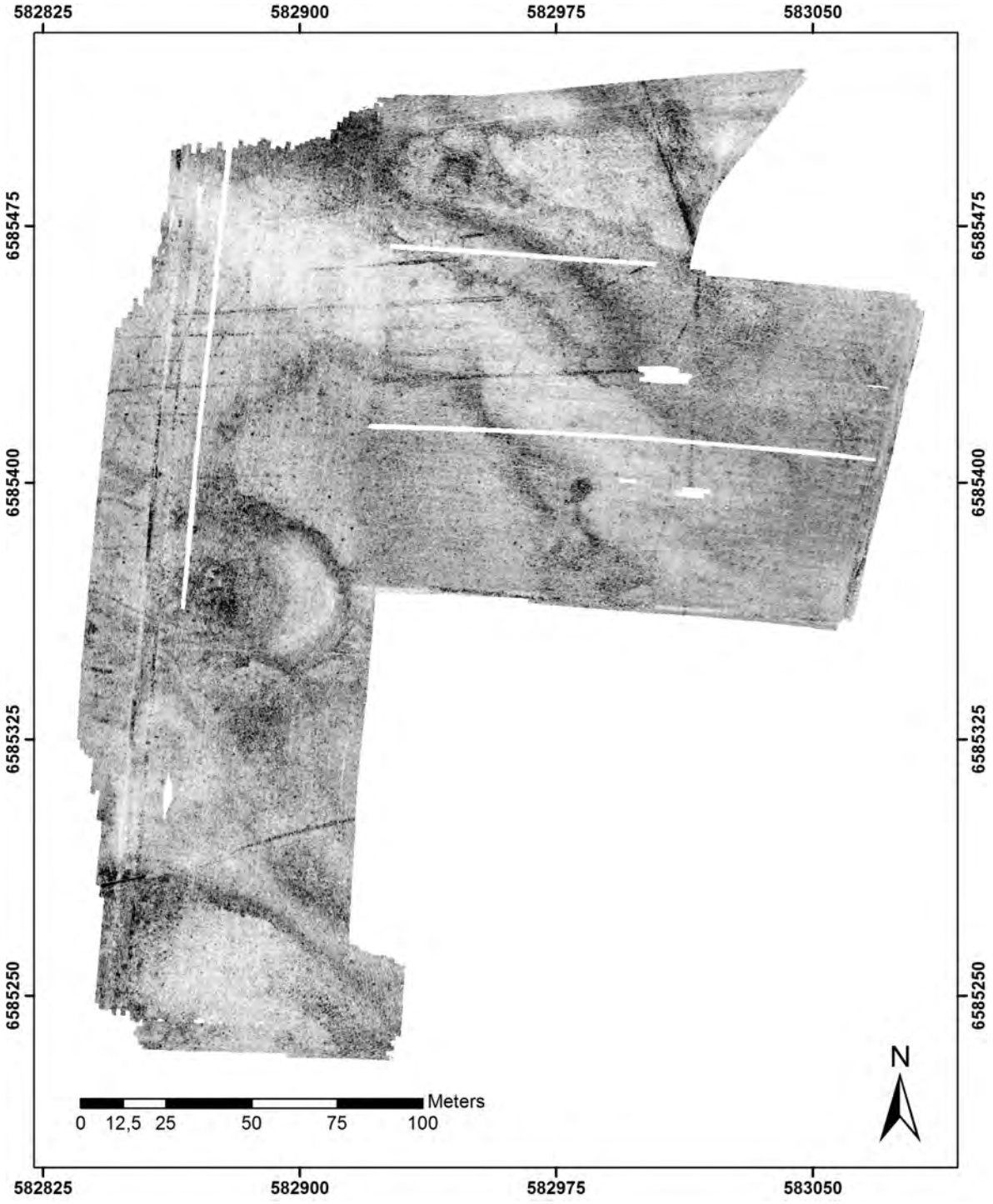

Figure 43: MIRA GPR depth-slice, circa 125 - 130 cm depth.

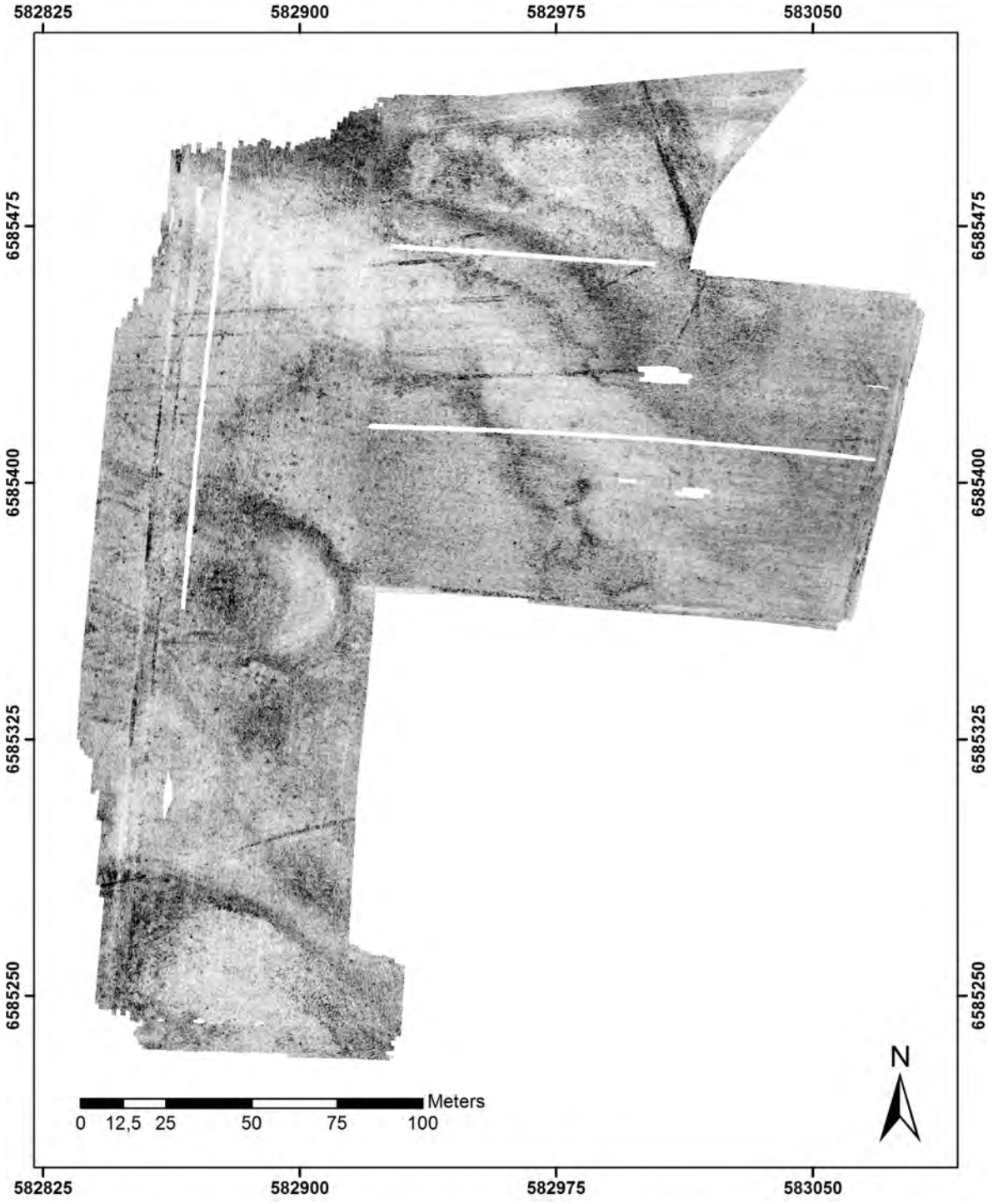

Figure 44: MIRA GPR depth-slice, circa 130 - 135 cm depth.

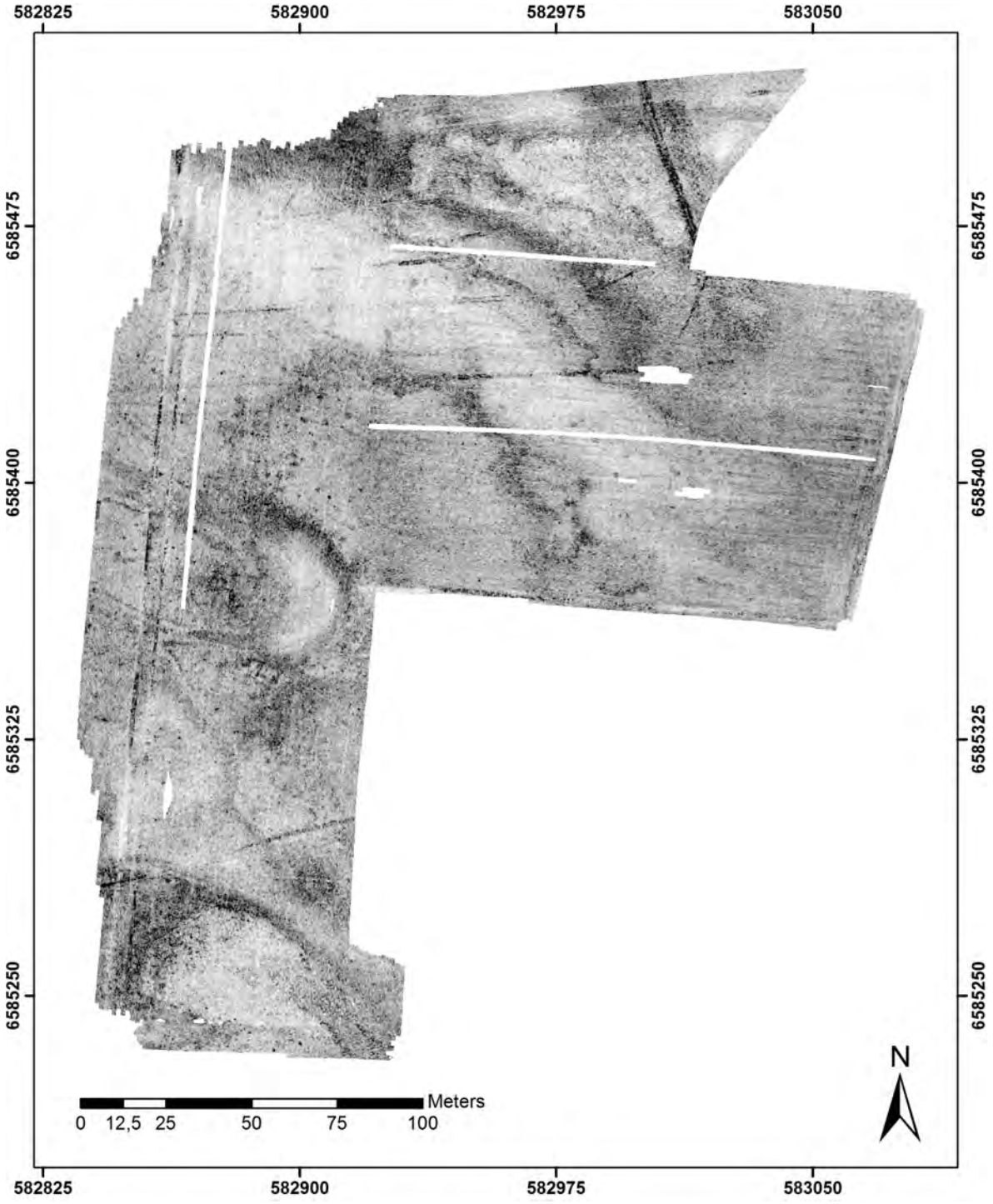

Figure 45: MIRA GPR depth-slice, circa 135 - 140 cm depth.

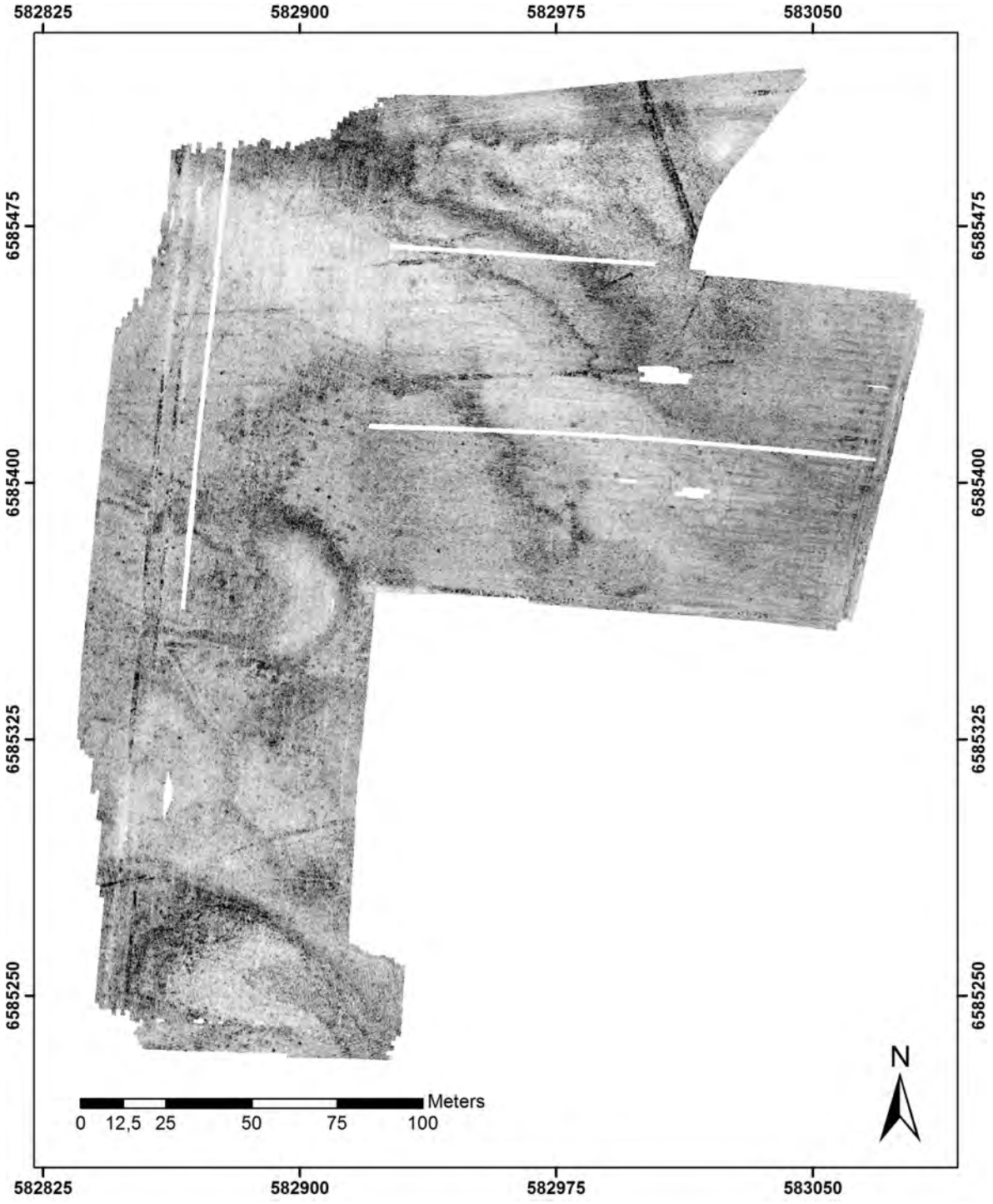

Figure 46: MIRA GPR depth-slice, circa 140 - 145 cm depth.

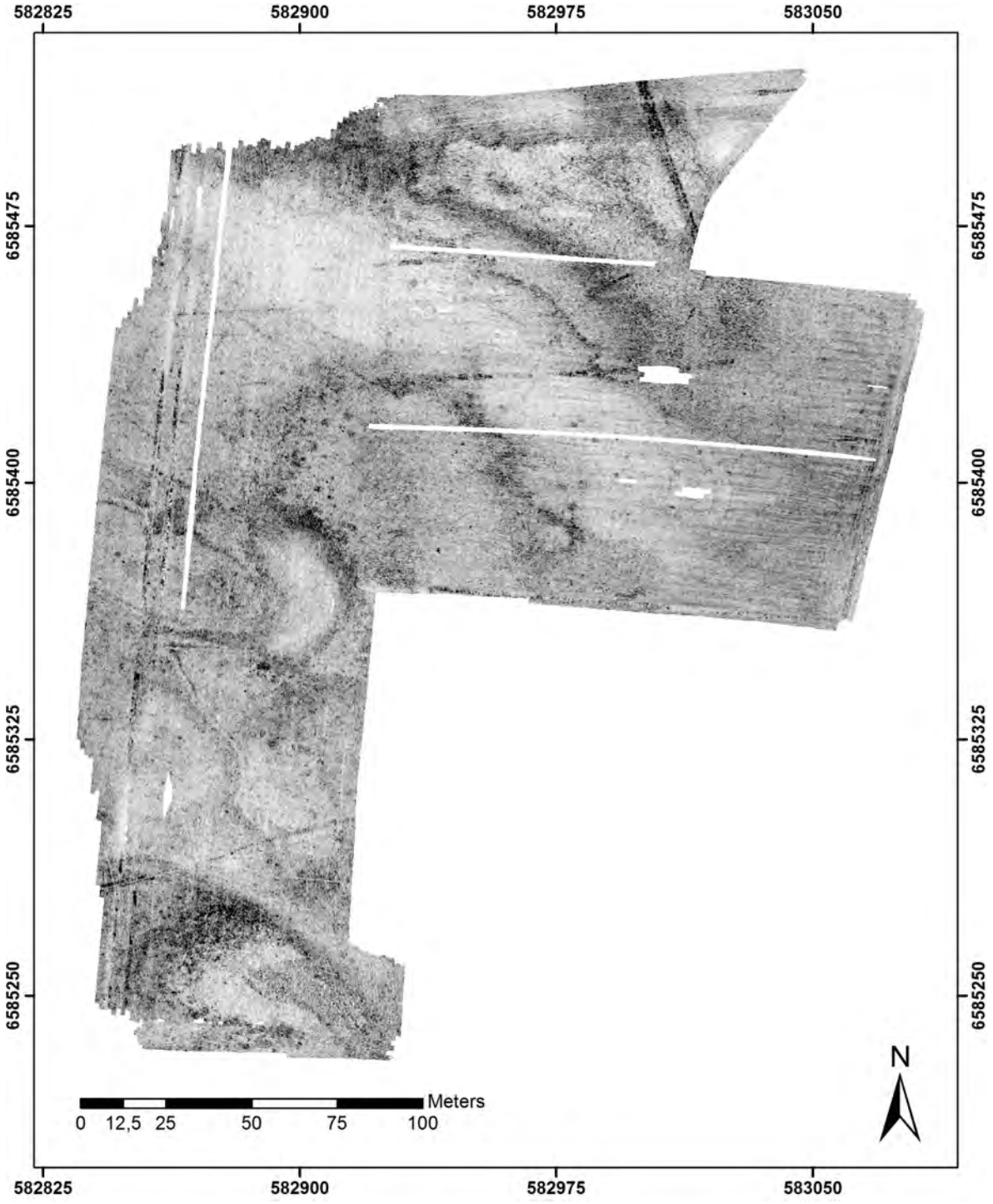

Figure 47: MIRA GPR depth-slice, circa 145 - 150 cm depth.

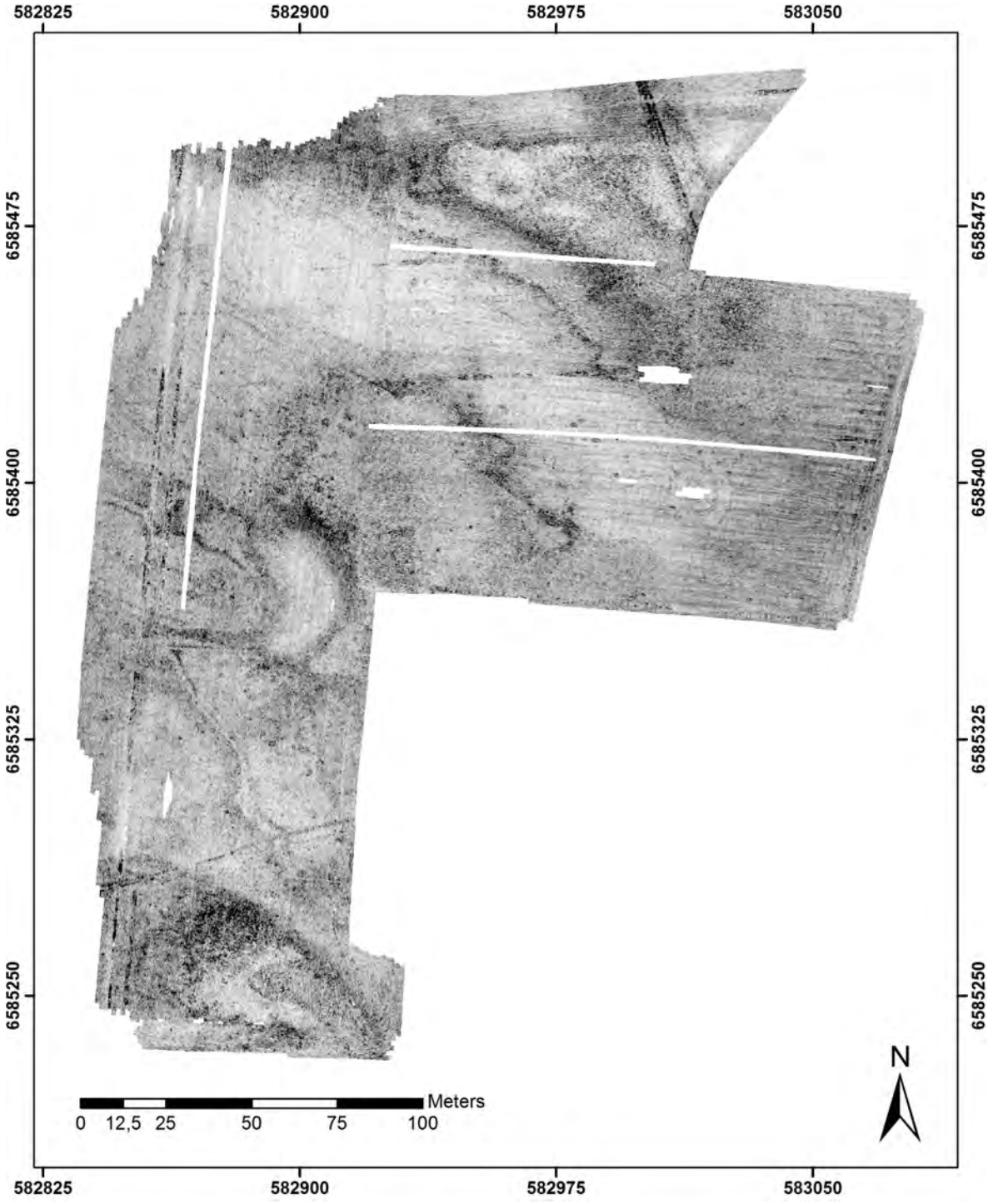

Figure 48: MIRA GPR depth-slice, circa 150 - 155 cm depth.

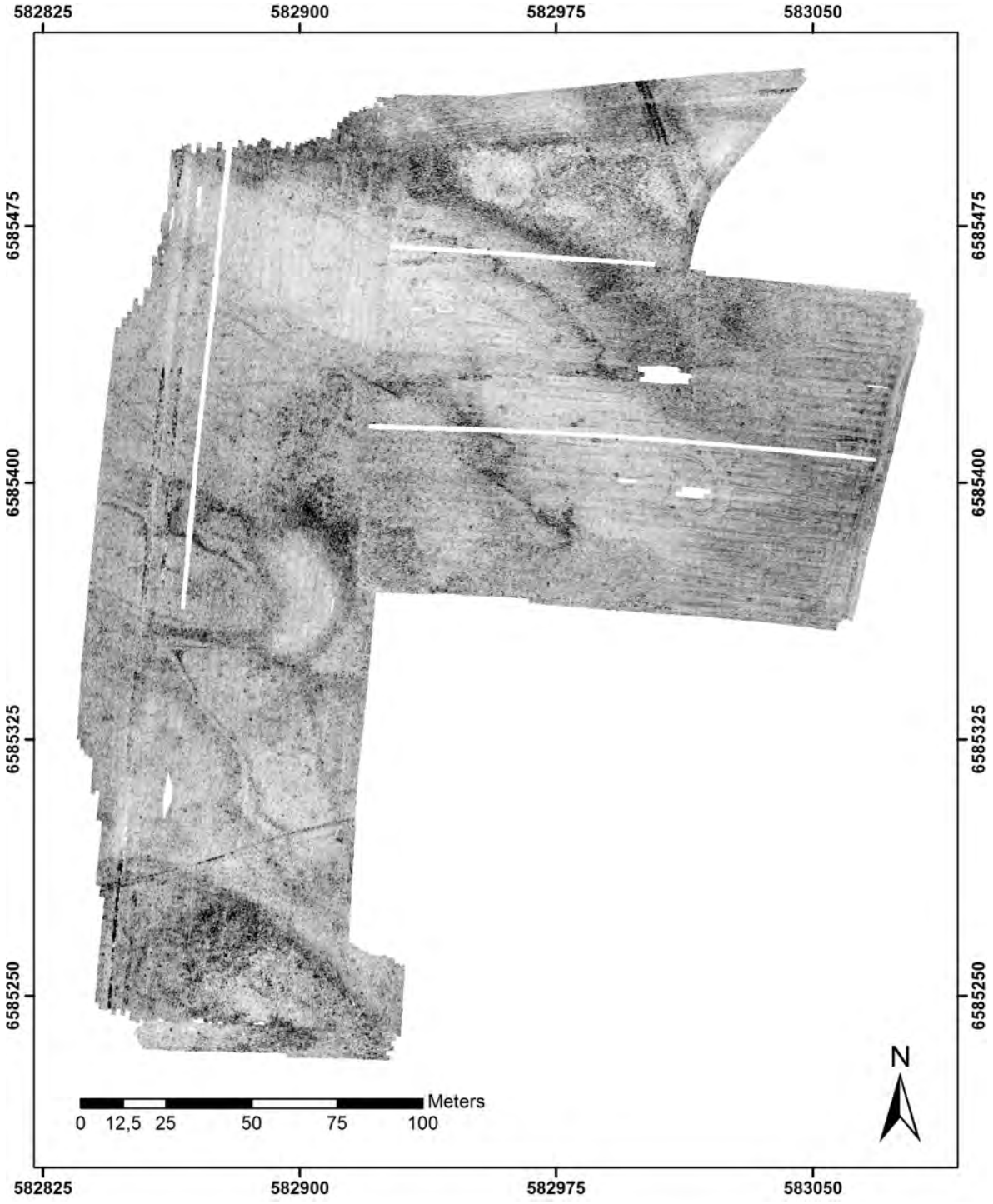

Figure 49: MIRA GPR depth-slice, circa 155 - 160 cm depth.

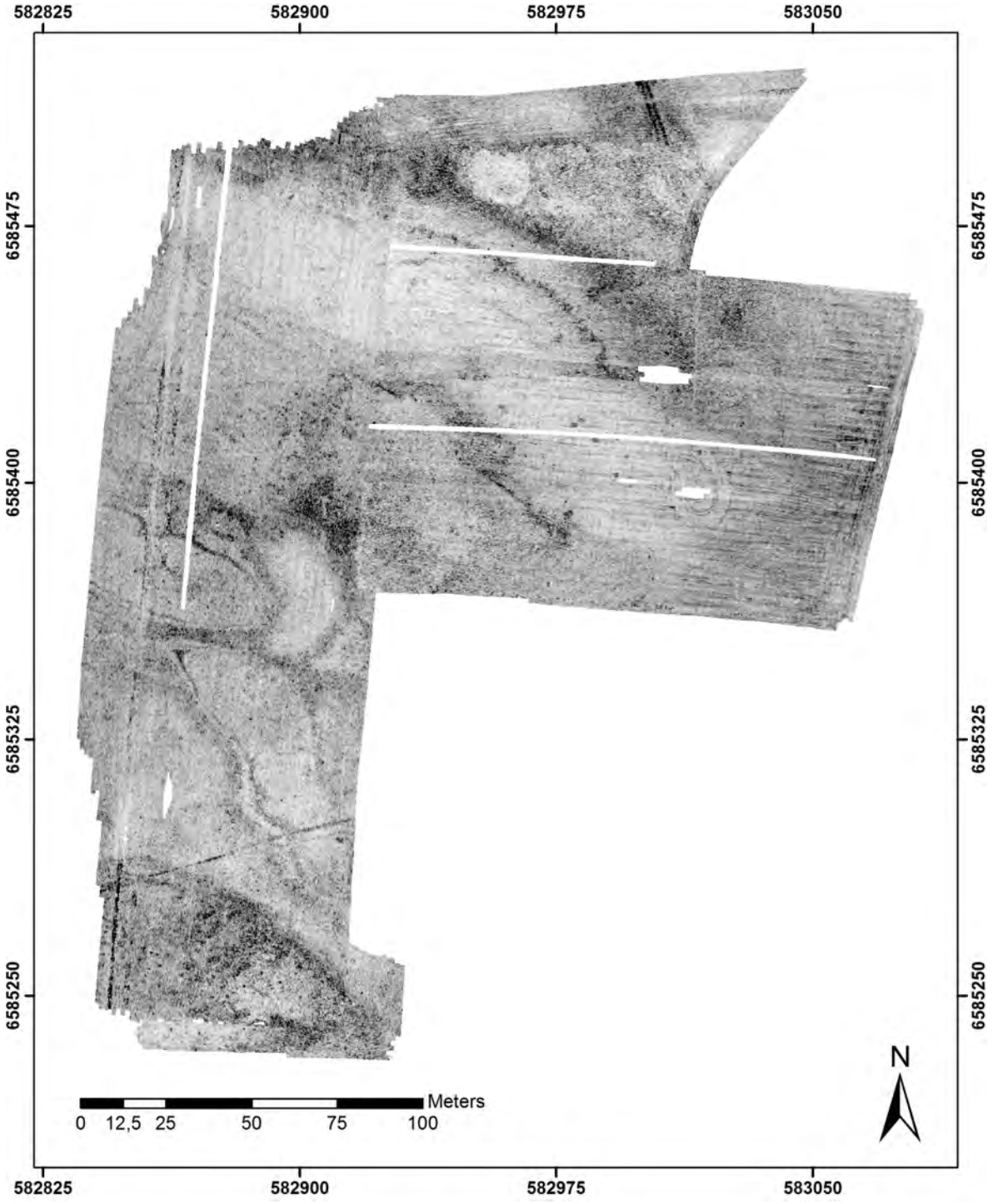

Figure 50: MIRA GPR depth-slice, circa 160 - 165 cm depth.

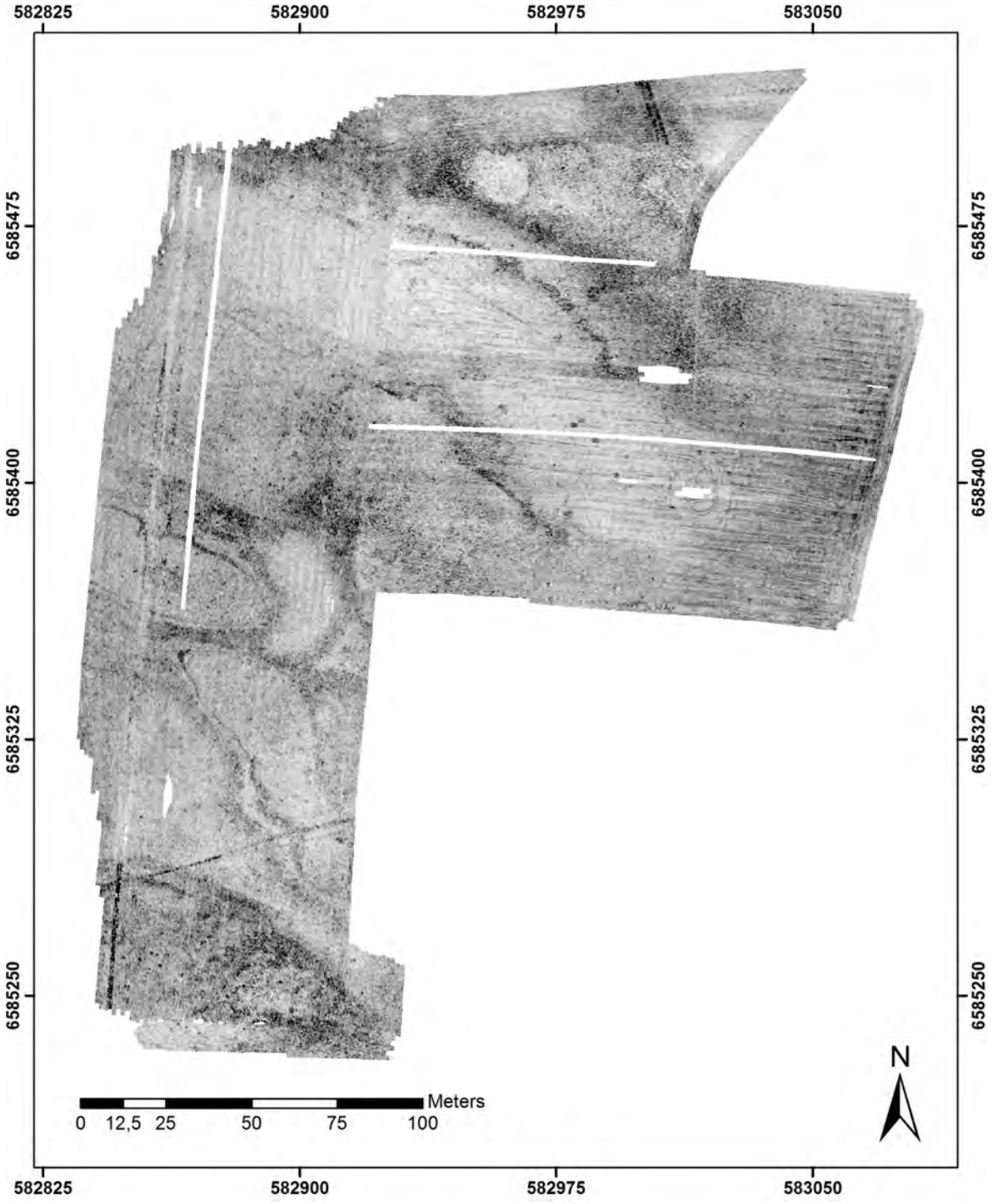

Figure 51: MIRA GPR depth-slice, circa 165 - 170 cm depth.

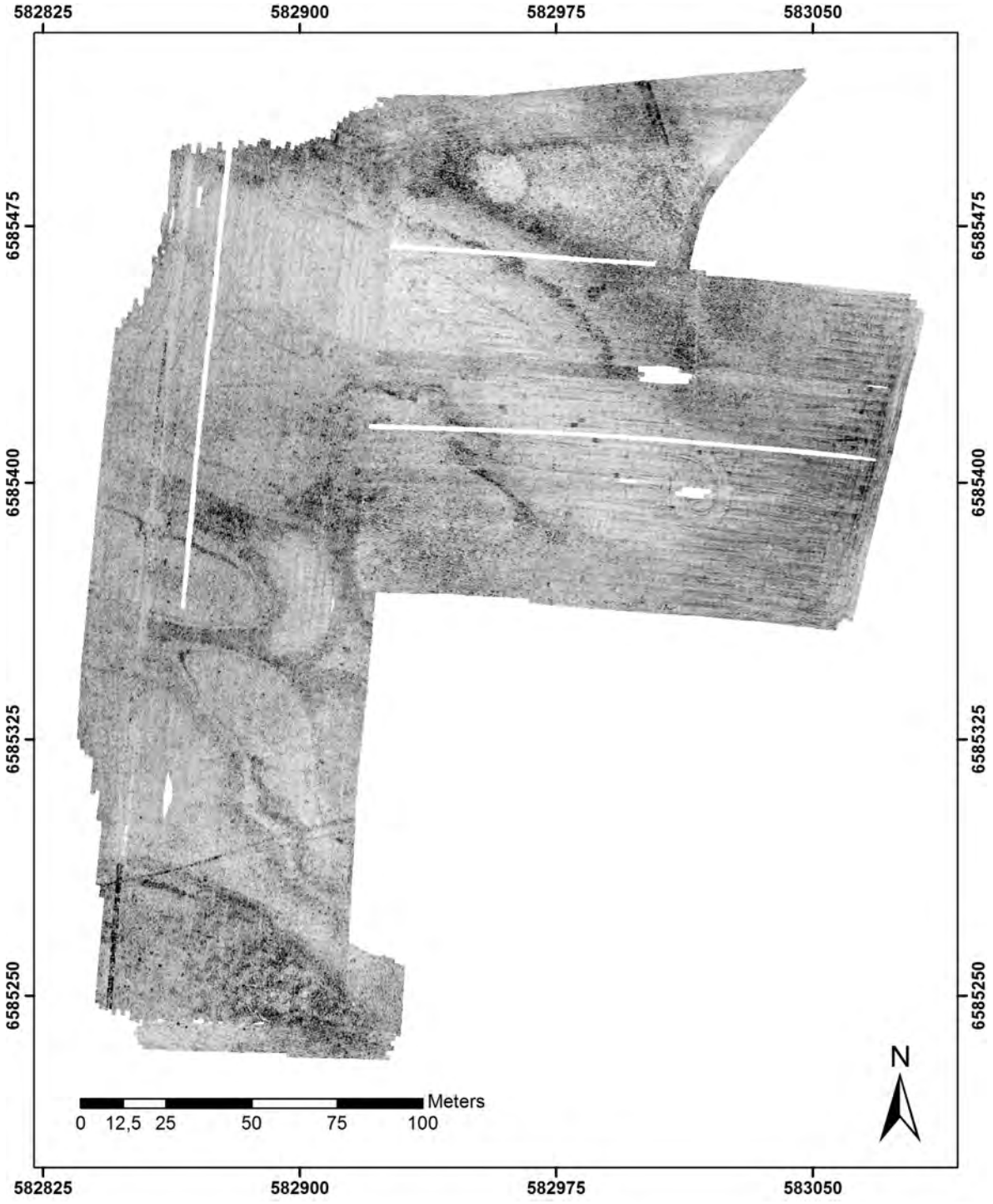

Figure 52: MIRA GPR depth-slice, circa 170 - 175 cm depth.

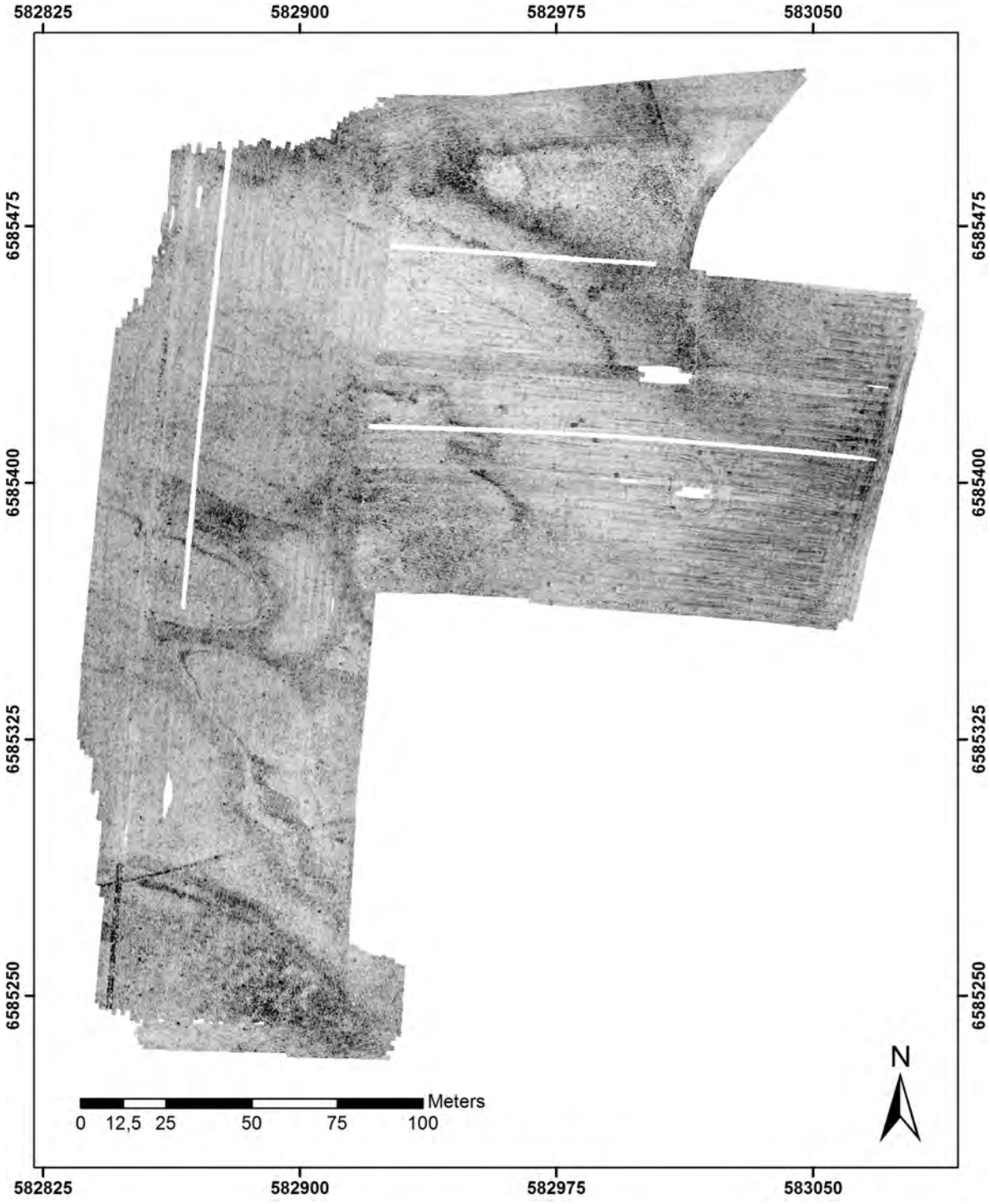

Figure 53: MIRA GPR depth-slice, circa 175 - 180 cm depth.

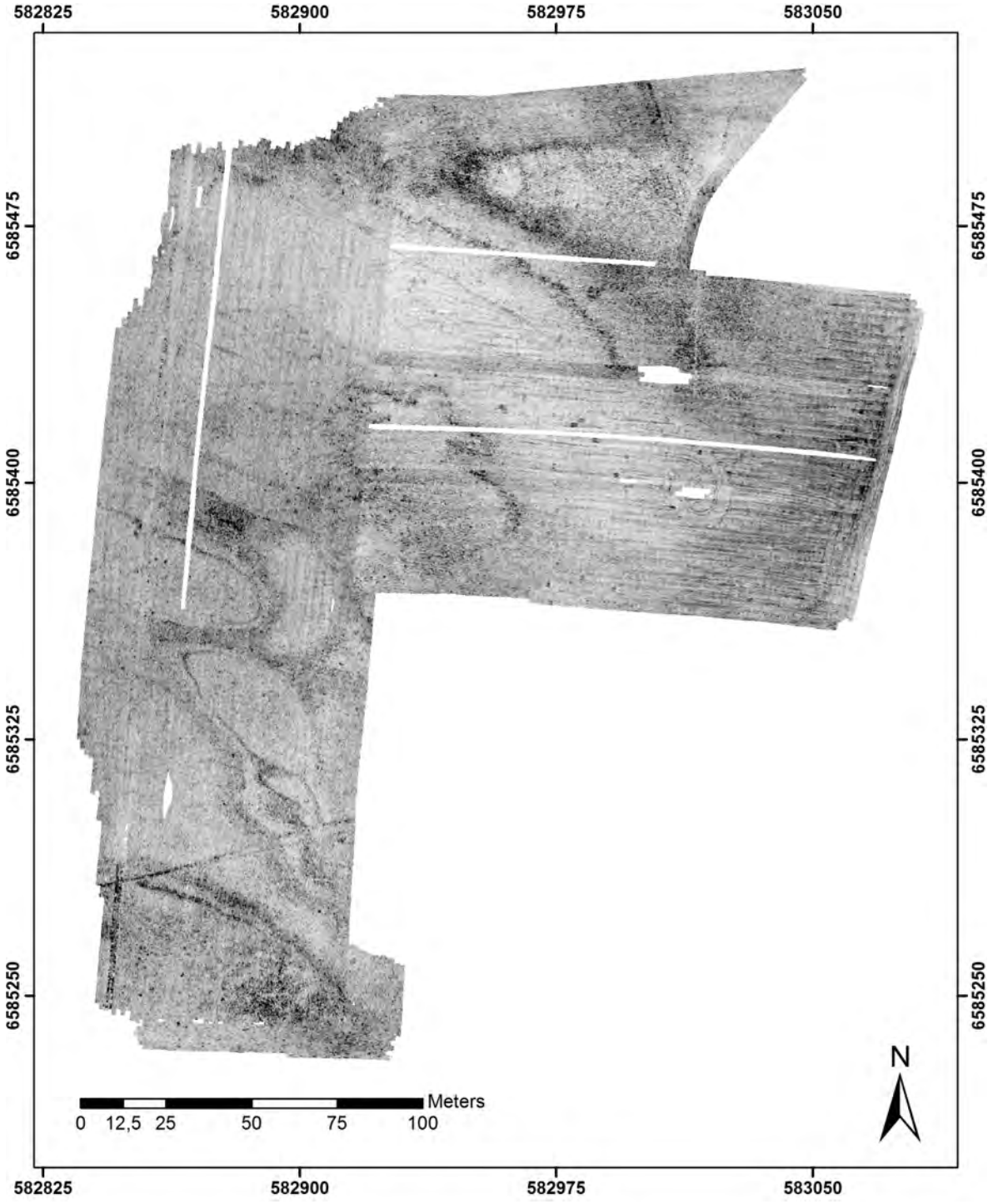

Figure 54: MIRA GPR depth-slice, circa 180 - 185 cm depth.

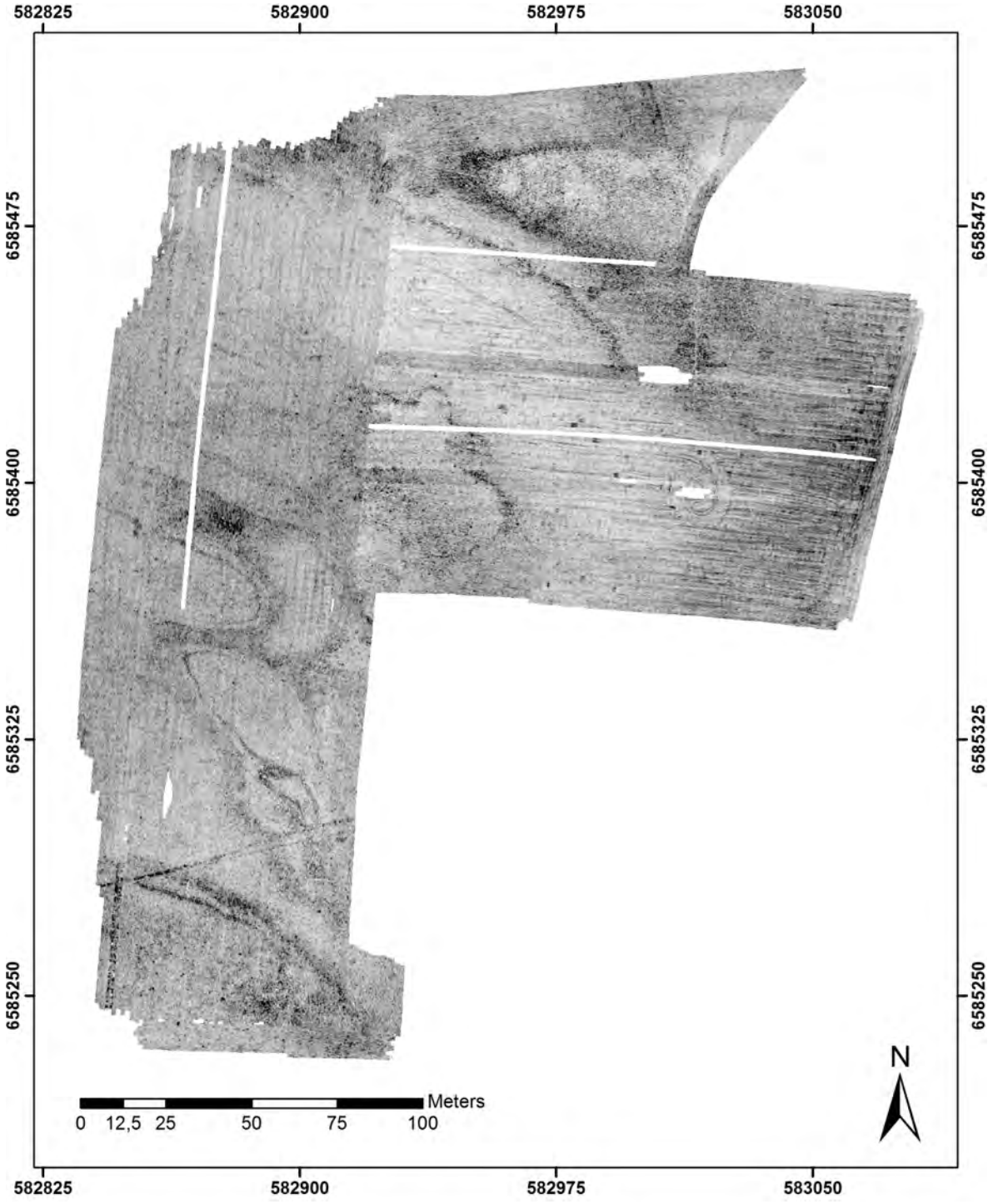

Figure 55: MIRA GPR depth-slice, circa 185 - 190 cm depth.

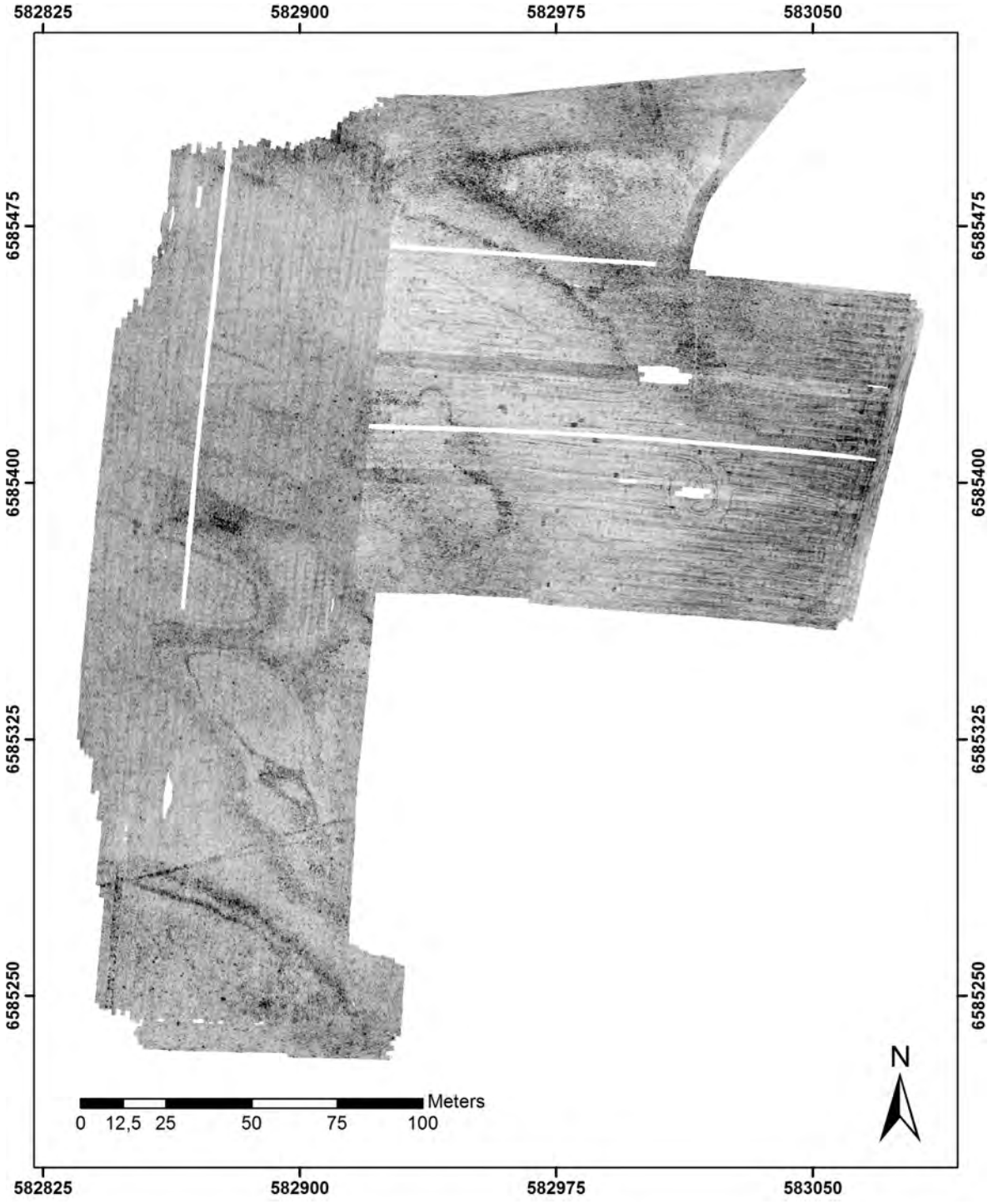

Figure 56: MIRA GPR depth-slice, circa 190 - 195 cm depth.

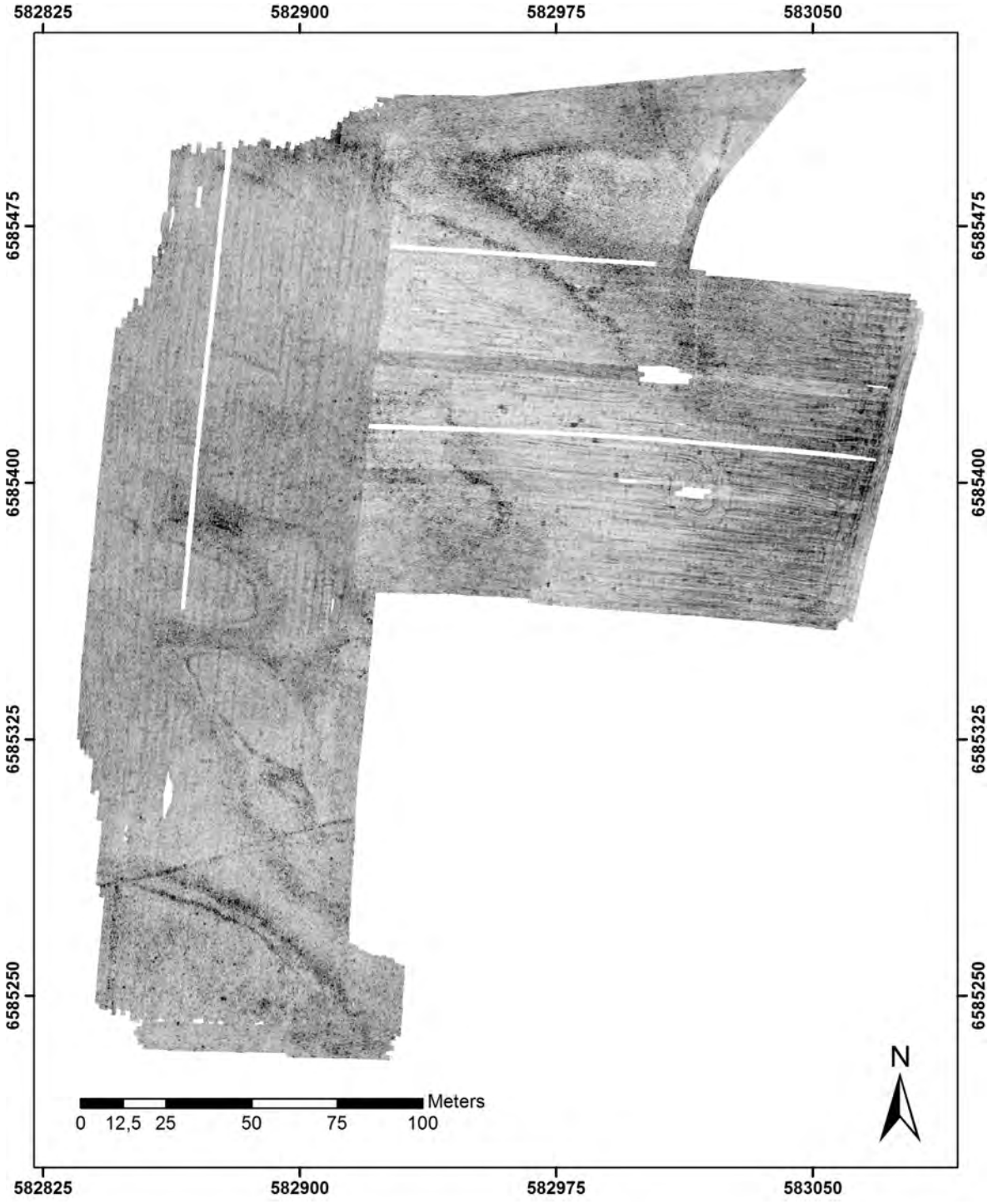

Figure 57: MIRA GPR depth-slice, circa 195 - 200 cm depth.

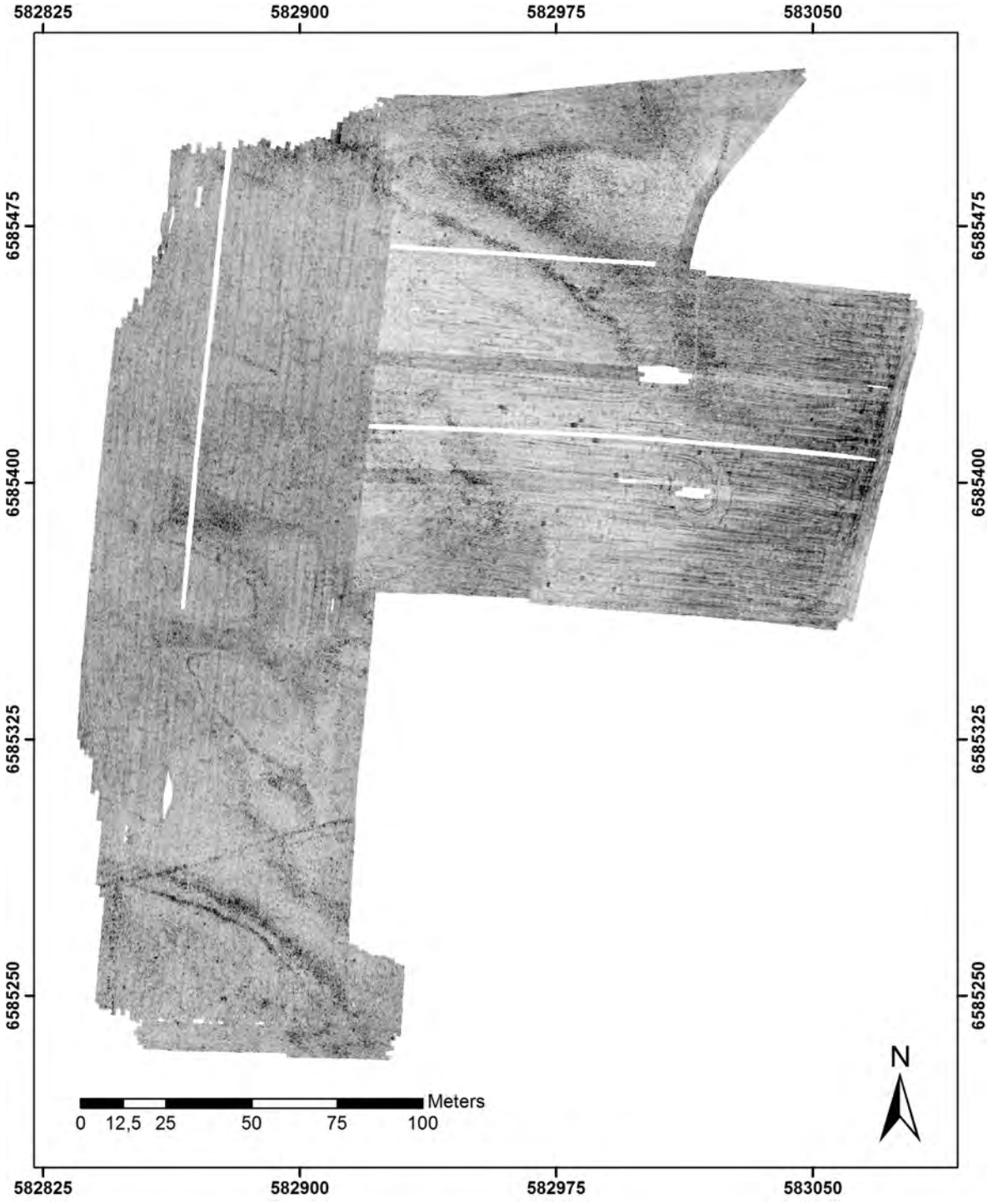

Figure 58: MIRA GPR depth-slice, circa 200 - 205 cm depth.

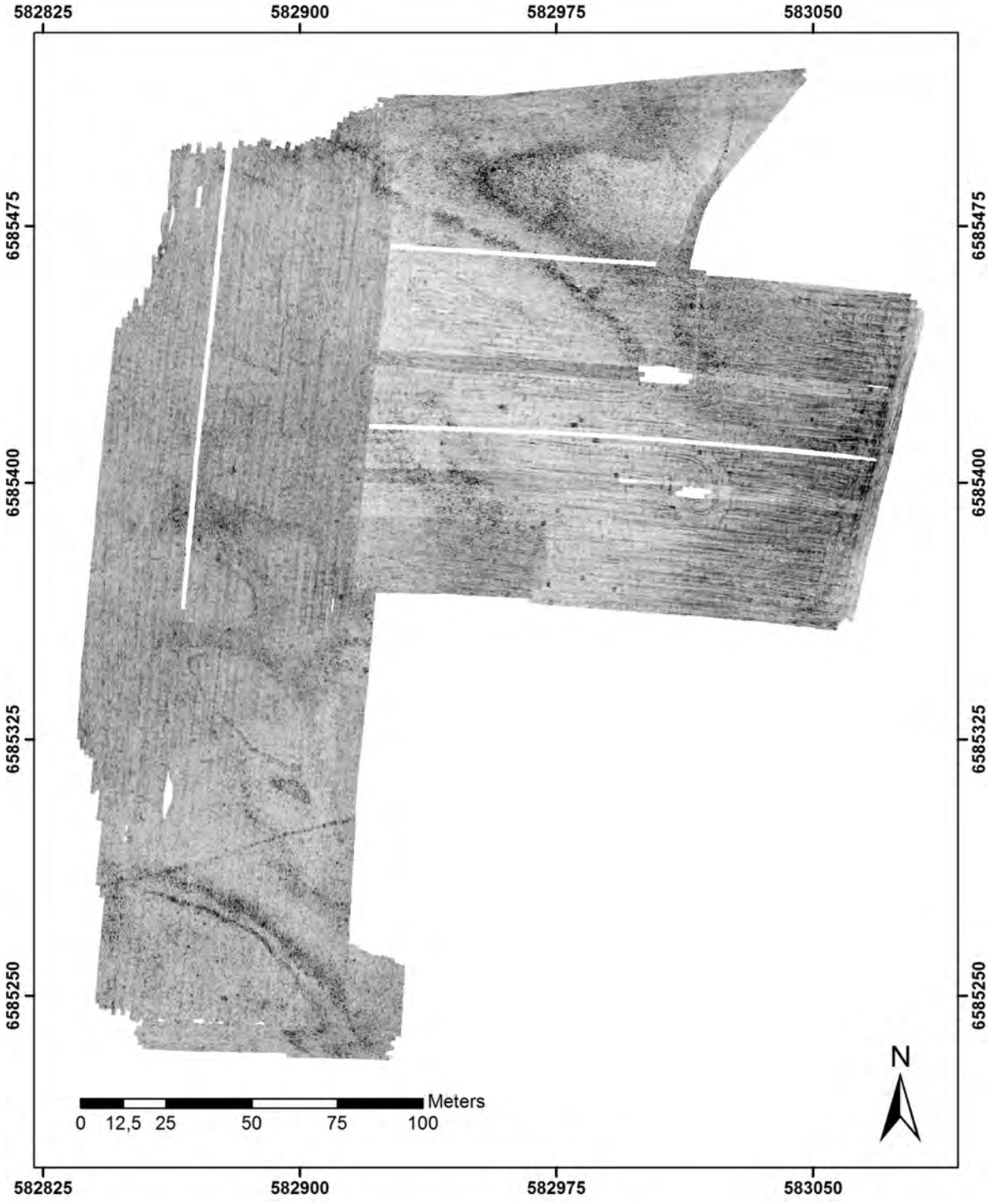

Figure 59: MIRA GPR depth-slice, circa 205 - 210 cm depth.

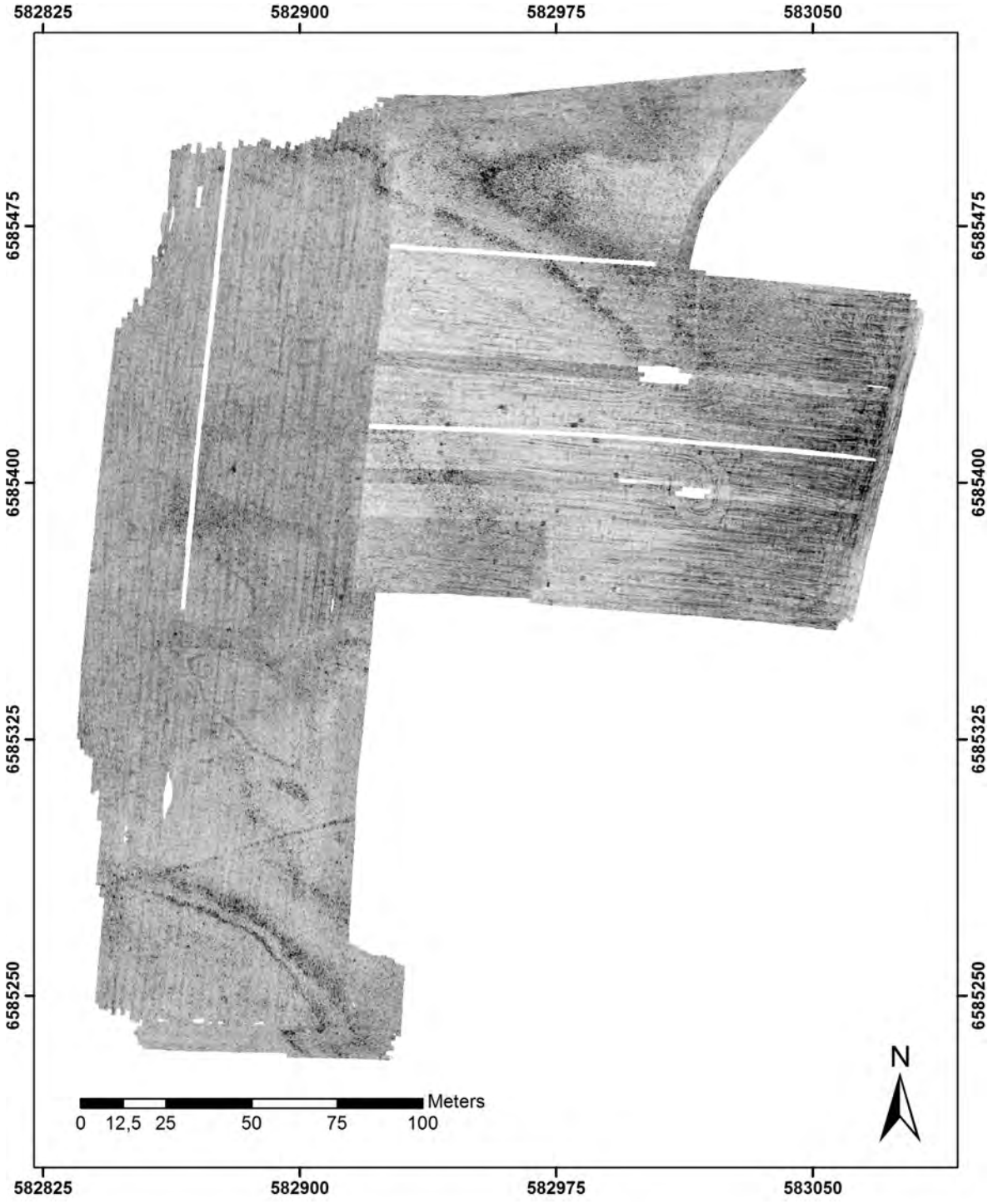

Figure 60: MIRA GPR depth-slice, circa 210 - 215 cm depth.

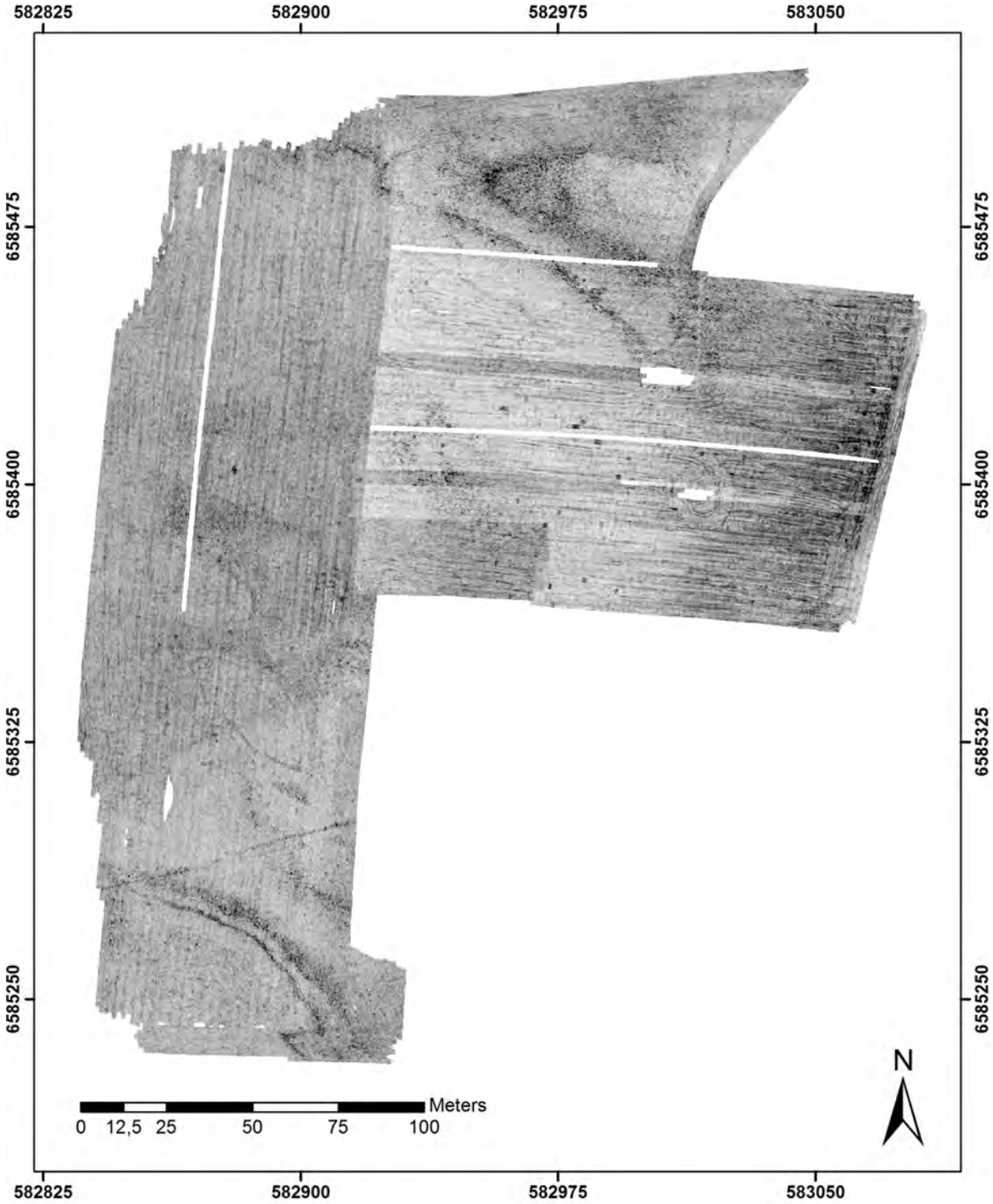

Figure 61: MIRA GPR depth-slice, circa 215 - 220 cm depth.